2005

Glutathione conjugation of a cocaine pyrolysis product AEME and related compounds

Alan Lewis Myers
West Virginia University

GLUTATHIONE CONJUGATION OF A COCAINE PYROLYSIS PRODUCT AEME AND RELATED COMPOUNDS

Alan Lewis Myers

A DISSERTATION

Submitted to
The School of Pharmacy
At
West Virginia University

In partial fulfillment of the requirements for
the degree of

Doctor of Philosophy
in Pharmaceutical Sciences

Patrick S. Callery, Ph.D., Chair
Peter M. Gannett, Ph.D.
Robert L. Haining, Ph.D.
Michael R. Miller, Ph.D.
Timothy S. Tracy, Ph.D.

Department of Basic Pharmaceutical Sciences

Morgantown, West Virginia
2005

Keywords: Cocaine, Pyrolysis Products, Glutathione, Glutathione Adducts, Anhydroecgonine Methyl Ester, Anhydroecgonine Ethyl Ester

Abstract

GLUTATHIONE CONJUGATION OF A COCAINE PYROLYSIS PRODUCT AEME AND RELATED COMPOUNDS

Alan Lewis Myers

Free-base ("crack") cocaine smoking continues to be a popular method of drug abuse in the United States. Pyrolysis of free-base cocaine readily occurs, forming primarily benzoic acid and anhydroecgonine methyl ester (AEME), which structurally contains an α,β-unsaturated carbonyl functional group. This electrophilic structure is suggestive of chemical reactivity with ubiquitously occurring cellular nucleophiles, such as glutathione. Glutathione adducts formed *in vivo* are metabolized to *N*-acetylcysteine derivatives by the enzymatically driven mercapturic acid pathway. AEME and its transesterification product in the presence of ethanol, anhydroecgonine ethyl ester (AEEE), were synthesized from cocaine hydrochloride. Glutathione (GSH) and mercapturic acid (NAC) conjugates of AEME were synthesized, and the stereochemistry of the AEME-NAC conjugate was structurally elucidated by NMR and mass spectrometry. Using Ellman's method to monitor glutathione depletion over time, AEME reacted with GSH at a slower rate (6.8×10^{-3} $mM^{-1}min^{-1}$) than equimolar concentrations of arecoline or ethacrynic acid (2.2×10^{-1} $mM^{-1}min^{-1}$ and 4.1×10^{-1} $mM^{-1}min^{-1}$, respectively). AEME also reduced the chemical formation of the DCNB-SG conjugate. In pooled human liver cytosol, the incubation of AEME with GSH at 37°C for 60 minutes at different pH levels was analyzed by LC-MS. We found unequivocal data suggesting enzymatic catalysis of AEME to AEME-SG in the presence of reduced GSH. However, AEME (10 mM) significantly reduced GST activity ($p < 0.005$) following a 20 hour incubation with HLC (1 mg). Additionally, AEME exhibited mixed-linear inhibition ($K_i = 334$ μM) towards cytosolic GST activity. A solid phase extraction (SPE) method was developed to extract cocaine and cocaine metabolites from urine. We identified approximately 50 ng/mL of AEEE by LC-MS in the urine of a known freebase cocaine/ethanol abuser, and additionally confirmed the structure of the metabolite by LC-MS/MS. This SPE method is useful in detecting AEME conjugates in biological fluids. We studied the cytotoxicity of pyrolysis products on A549 lung fibroblasts using trypan blue exclusion and flow cytometry. To summarize, our work suggests that AEME plays a potential role in the sequelae of abused cocaine related toxicities.

DEDICATED to my Mother, Father and Sister

for their encouragement and support…

Author's Acknowledgments

No story is ever complete without a comprehensive list of the many individuals who helped me during this grueling, sometimes emotional yet exciting journey of achieving a Ph.D. in the Pharmaceutical Sciences. Firstly, my advisor, Dr. Patrick S. Callery, offered many helpful suggestions, ideas and corrections to my research project over the past several years. His experience in research and education within the Pharmaceutical Sciences, taught through classroom lectures, individual discussions, laboratory meetings and personal stories, has provided me with a solid framework in pursuing a career in this exciting science. Also, his expert advice in applying mass spectrometry to our project was extremely beneficial. Special thanks to Dr. Peter M. Gannett for his assistance regarding the organic synthesis of compounds and NMR analyses. Dr. Timothy S. Tracy provided much needed assistance in HPLC analysis and AEME inhibition studies. Additional thanks go to Dr. Robert L. Haining and Dr. Michael R. Miller for assisting in the analysis of human liver cytosol incubations, for serving on my committee, and for supporting my research project.

At one time the weekly forensics group within BPS was an exciting scientific forum to participate in. Around the initiation of this group, my project was slowly developing. Thanks to the members of this group, including Diaa Shakleya, Padma Tirumalai and Madhu Sanga, who supported my project and directed my ideas.

I feel deep gratitude to fellow graduate students in the School of Pharmacy at WVU who traveled this path along with me and provided support, especially Brenda Schuler, Jonathan Daft, Tina Bland, Islam Younis and Jarod Kabulski. I am grateful for the assistance of two exceptional undergraduate forensic chemistry students, D'Anne Hoferka and Heather

Williams. I also owe thanks to Penny Dailey and Meena Sivaneri, as it has been a pleasure working with them over the past several years.

I am additionally grateful to the many teachers, professors and mentors throughout early grade school, middle school, high school, pharmacy school and graduate school who shared with me a portion of their knowledge and experience. Without them I could never compile a scientific research project into this extensive volume of written pages, figures, tables and diagrams.

Finally, I owe deep thanks to my Mom, Dad and Sister who supported my decision to pursue academic research and for tolerating me during the tough, grinding days and sometime weeks of repeated laboratory failures. I owe special thanks to Slawomir Lukomski, Ph.D., Joan C. Olson, Ph.D. and Rachel Wiechman in the WVU Department of Microbiology, Immunology & Cell Biology, School of Medicine for their assistance with the cell toxicity studies. Thank you all for your support!

Table of Contents

List of Figures

List of Tables

Chapter 1: Introduction

1.1.1 Cocaine

Cocaine (Fig 1.1) is a naturally occurring alkaloid with a concentration of approximately 1% within the leaves of the coca plant (*Erythroxylon coca*), a tree indigenous to mountainous regions of Peru and Bolivia (1). Use of the drug for recreational, medicinal and religious purposes has dated back thousands of years. Native Indians of South America are often recognized as the first known tribal group to chew the coca leaves for its mild stimulatory effects (2). During the late nineteenth century, cocaine hydrochloride was first isolated from coca leaves and the extraction of pure cocaine was then possible. The first cocaine epidemic to strike the United States, according to one author, occurred in the late 1880's (2). During this time, cocaine was widely used and touted as a panacea for many illnesses (2). Sigmund Freud, a prominent psychiatrist, recommended in his paper entitled *On Cocaine* that cocaine be used as a local anesthetic, an aphrodisiac and as a primary pharmacologic agent in treating depression, alcoholism and morphine addiction (2). Cocaine was available in a variety of products during this time, including patent medicines, tonics and soft drinks.

John Styth, an apothecary, formulated the syrup base for Coca-Cola in 1886 using a compounded mixture of coca plant extract with an extract from the African kola nut, also a stimulant (2). Later, Styth marketed the drink as a medicine. Inhalation of burning coca leaves or smoking coca evolved slowly and remained major modes of medicinal and recreational use around this time (3). In 1903 the dangers of cocaine were publicized and cocaine was removed from the Coca-Cola formulation (2). Federal legislation soon followed with the enactment of the Pure Food and Drug Act of 1906 and the Harrison Narcotic Act of 1914 (3). This legislation curtailed the distribution and use of coca leaves and coca products, listing cocaine as a narcotic (2). Although legislation made cocaine use legal solely through a physician's

prescription, cocaine use ironically diverged to intravenous and intranasal abuse since these forms were now readily available (3).

Cocaine HCl was typically smoked as a cigarette or in a pipe with marijuana, tobacco or other herbs (3). Achieving only mild effects from smoking the hydrochloride salt, users found smoking coca paste (crude extract containing free alkaloids) and later cocaine free-base (crack cocaine) to produce more pleasurable effects (3). In the early 1970's, cocaine abuse re-emerged, particularly among middle-class Americans, and reached epidemic status in the early 1980's (2). In 1985, one survey found that cocaine use peaked in U.S. society with approximately 5.8 million chronic cocaine users (2). This number decreased over the next decade as surveys from 1991 and 1994 revealed around 1.9 million and 1.4 million, respectively, cocaine users in society (2). Most of the sampled cocaine abusers were between 18-34 years old, while African-Americans had a slightly higher rate of abuse compared to whites, 1.3% to 0.5%, respectively (2).

Currently, cocaine use remains a serious concern in the United States with an estimated 1.5 million cocaine users age 12 and older (4) . One study of US middle and high schoolers from 1991-1998 revealed a slight increased trend in cocaine abuse among study subjects over the study period (4). Crack cocaine use also increased slightly, though not significantly, during the 1990's with roughly 500,000 crack users in 1994 compared to 604,000 users in 1997 (4).

1.1.2 Crack Cocaine

Crack cocaine is "smokeable cocaine" that derives its street name from the crackling sound heard when it is smoked (2). It is the free-base form of cocaine hydrochloride, a fine, white crystalline powder that is primarily abused by other routes, intranasally and

intravenously (2). Crack cocaine can be produced chemically from the hydrochloride salt by mixing with buffered ammonia, extracting with diethyl ether, and evaporating the organic solvent to produce crystals (2). Another more popular method today of creating crack in clandestine laboratories is to heat cocaine hydrochloride with sodium bicarbonate until a solid "rock" forms (2). Upon heating in a crack pipe or similar apparatus, the crystals liberate vaporized cocaine that is inhaled for pleasurable effects.

The popularity of crack cocaine abuse can be attributed to numerous factors, such as rapid euphoric effects (typical high occurs in less than 10 seconds) due to fast absorption within the extensive capillary network in the lungs, and a relatively inexpensive street value ($1-$3 per dose in 1996) (2). Despite an overall variable and low bioavailability (32 to 77%), non-decomposed cocaine in aerosolized form is highly available in human test subjects (5). Cocaine free-base has a lower melting point than its hydrochloride counterpart (95°C and 195°C, respectively), and the free-base is more volatile (3). Smoking of drugs is advantageous over intravenous use since purity of the drug is less important and the lessened inherent dangers of acquiring pathogenic blood borne diseases, such as HIV (6).

Overall, crack is a rapidly addicting form of cocaine that easily results in lethal overdose (3). Unfortunately, some of the underlying factors for this increased toxicity are still unclear, but may be attributed to lesser-known pyrolysis products, such as anhydroecgonine, anhydroecgonine methyl ester, and anhydroecgonine ethyl ester.

1.1.3 Cocaine Pharmacology

The following brief overview of cocaine pharmacology may explain, in part, the euphorigenic properties of the drug. Cocaine (Fig 1.1) is structurally similar to most local

anesthetics (i.e. lidocaine, procaine) with a tertiary amine structure derived from the amino-alcohol base ecgonine, which is methylated and esterified with benzoic acid to form cocaine (benzoylmethylecgonine) (7). Its overall tropane ring structure is similar to the potent muscarinic antagonist, atropine (Fig 1.1). Pharmacologically, cocaine blocks the re-uptake of important neurotransmitters, norepinephrine locally and dopamine within the central nervous system (7). Clinically, it provides nerve impulse blockade with concentrations as low as 0.02%, leading to local anesthesia and vasoconstriction that is useful in certain clinical settings, such as nasal surgery (1). However, the increased blockade of dopamine re-uptake leads to excitement, garrulousness and euphoria, a dreamy, pleasurable state sought by drug users.

The intensity of euphoric effects from cocaine is faster and greater when cocaine is smoked or injected in comparison to intranasal use (8). Smoked cocaine is readily absorbed through mucous membranes in the lung vasculature, reaching cerebral circulation within 6 to 8 seconds (9). By comparison, the intravenous route requires approximately 16 to 20 seconds to reach the cerebral vasculature, whereas nasal insufflation requires 3 to 5 minutes (9). The bioavailability by the nasal route averaged 80% (5). As previously mentioned, bioavailability after smoking cocaine varied (32-77%), but most undecomposed cocaine (ca. 44%) reaches the circulation unchanged (5). *In vitro* simulated smoking experiments of a 50 mg free-base cocaine dose, inhaled at 30 second intervals over 5 minutes, showed that the first 4 puffs contained 94% of the cocaine delivered, and no cocaine was obtained after the 6^{th} puff (10). Under optimal smoking conditions, smoking 50 mg free-base cocaine resulted in inhalation of approximately 16 mg cocaine (10). Also, 16 mg of cocaine induced effects similar to or slightly more intense and pleasurable than 20 mg of IV cocaine HCl (10). Overall, cocaine has pronounced, intense euphoric effects, yet they are ephemeral and rapidly dissipate, largely due

to the rapid hydrolysis of cocaine (short half-life) *in vivo* to primarily non-psychoactive metabolites.

1.1.4 Cocaine Metabolism

The metabolism of cocaine is extensively reviewed within the scientific literature and worthy of discussion in this proposal. Cocaine is primarily biotransformed through hydrolysis of the methyl and benzoyl esters to produce benozylecgonine (BE) and ecgonine methyl ester (EME), respectively (Figure 1.2) (11). Further hydrolysis of either moiety results in the formation of ecgonine (E) (11). Interestingly, hydrolysis of cocaine to BE or EME is catalyzed by different human esterases. Human carboxylesterase 1 (hCE-1), a microsomal serine hydrolase found in the liver, small intestine, kidney, lung, testes, heart and plasma, catalyzes the conversion of cocaine to BE (12). Both human carboxylesterase 2 (hCE-2) and serum butyrylcholinesterase hydrolyze the benozyl ester linkage on cocaine to EME (12). The non-enzyme mediated chemical hydrolysis of either ester group also occurs at physiological pH (13).

In the presence of ethanol, hCE-1 also catalyzes the transesterification reaction of cocaine to cocaethylene (CE), a toxic, pharmacologically active metabolite (12). Traces of CE (ethyl cocaine) were reported in the urine of cocaine users who co-abused ethanol (14,15). Jatlow and co-workers (16) found, in 4 out of 7 human postmortem samples from victims who abused both cocaine and ethanol, a higher concentration of cocaethylene than cocaine. Several studies state that cocaethylene is a more toxic compound than cocaine. Cocaethylene exhibits similar affinity for the dopamine re-uptake transporter as cocaine (16,17). The acute toxicity of cocaethylene was compared to cocaine in Swiss-Webster mice, and the LD_{50} of

cocaethylene was less than cocaine, 61 mg/kg and 64 mg/kg, respectively, suggesting it is more potent in inducing lethality (18). Additionally, cocaethylene has a slower clearance and longer elimination half-life than cocaine (19). Finally, the cocaine and alcohol combination can produce more intense feelings of 'high', and potentate the tendency towards violent thoughts and threats, which may result in an increase of violent behaviors (20)

Cocaine is susceptible to other metabolic pathways in addition to hydrolysis and transesterification. It is *N*-demethylated at the tertiary *N*-methyl group to produce norcocaine, a metabolite with similar pharmacologic activity as cocaine (11) and associated with cocaine related toxicities such as hepatotoxicity (21). This *N*-demethylation is catalyzed by the cytochrome P450 isoenzyme, P450 3A, in humans and mice (21,22). Norcocaine can be oxidized to *N*-hydroxynorcocaine by brain FAD-containing monooxygenases and further metabolized to norcocaine nitroxide by brain microsomes (23). Additionally, norcocaine can be hydrolyzed to benzoylnorecgonine. Cocaethylene is *N*-demethylated to norcocaethlylene or hydrolyzed to ecgonine ethyl ester (24). Ester hydrolysis of norcocaethylene and ecgonine ethyl ester also proceeds non-enzymatically at physiological pH (24). Cocaine or any other metabolite retaining the benzoyl functional group are theoretically subject to aromatic hydroxylation at the meta and para positions (25).

1.1.5 Cocaine Addiction Therapeutics

Approximately 16% of Americans have tried cocaine at least once, and 17% of those who try the drug will become addicted (26). With a significant amount of U.S. citizens suffering from cocaine addiction, the National Institute of Drug Abuse (NIDA) is funding three different cocaine vaccine trials that aim to help cocaine users overcome their habit (27). TA-

CD therapeutic vaccine, currently in phase I clinical trials, is comprised of a protein conjugate that couples succinylnorcocaine to a carrier protein (recombinant cholera toxin B) with aluminum hydroxide as an adjuvant (28). TA-CD (13, 82 or 709 μg) was well tolerated in 28 test subjects and induced cocaine-specific antibodies, warranting further clinical studies (28). Other vaccines with slightly different modes of action are being pursued at Scripps Research Institute (La Jolla, CA) and at the University of Cincinnati (27). Another vaccine being developed at Columbia University (New York) functions as a catalytic antibody (27). The researchers have synthesized a phosphonate monoester transition-state analog for benzoyl esterolysis that selectively attacks circulating cocaine molecules, degrading them to the non-toxic metabolites, benzoic acid and ecgonine methyl ester (29).

Attacking cocaine (or any drug of abuse) addiction by synthesizing novel vaccines and related pharmaceutical agents, in the author's opinion, has more clinical promise than simply synthesizing a cocaine analogue that has a greater affinity for the dopamine transporter. Still, many unanswered questions persist regarding the complexity of treating drug abuse, and additional data and research is needed to determine if these new therapeutic agents actively address the addiction.

1.1.6 Pyrolysis of Other Drugs of Abuse

The formation of pyrolysis products during the smoking of drugs of abuse is not unique to cocaine. Heroin (diacetylmorphine), phencyclidine (PCP) and methamphetamine (MA) are all heavily abused drugs in the US and susceptible to pyrolysis reactions during smoking (6,30,31). The pyrolysate of heroin hydrochloride contained the following principal products on HPLC analysis: 6- acetylmorphine, *N*-acetylnorheroin, *N*,6-diacetylnormorphine and heroin

itself (6). The tertiary benzylamine, PCP, undergoes an elimination reaction during pyrolysis to form primarily 1-phenylcyclohexene (PC) (32). The newly formed double bond on PC, conjugated with the phenyl ring system, is oxidized to an epoxide, and then hydrolyzed to a diol (6). The PC-epoxide may be a substrate for GST's, and the resulting PC-SG adduct is potentially a novel metabolite of smoked PCP use.

Methamphetamine, a CNS stimulant, mixed with tobacco produces a plethora of thermolytic products upon heating, such as phenylacetone, *N*-cyanomethylmethamphetamine, *trans*-β-methylstyrene, styrene, dimethylamphetamine and methamphetamine (30,31). *trans*-1-Phenyl-1-propene, a major thermal degradation product of methamphetamine hydrochloride, is a good substrate for CYP1A2, forming the epoxide, *trans*-1-phenylpropylene oxide (33). The epoxide, also a substrate for cytosolic GST's, is potentially a cytotoxic compound and forensic marker of smoked methamphetamine hydrochloride use (33).

1.2.1 Anhydroecgonine Methyl Ester (AEME), a Pyrolysis Product of Cocaine

Cook and Jeffcoat (32,34) first reported the thermal degradation of cocaine to methylecgonidine (AEME, andydroecgonine methyl ester). Briefly, [*N*-CD_3]-cocaine (25-200 mg) was heated in a pyrolysis apparatus, and then the pyrolysis products were collected, dissolved in acetonitrile, and analyzed by GC/MS (34). Also, the collected urine of a consented, test subject who inhaled about 50 mg free-base cocaine was compared to urine from test subjects administered the drug by intravenous or intranasal routes (34). A greater proportion of 'unknown' metabolites (likely AEME and derivatives) were discovered in the urine of smoked cocaine subjects (34).

Lowry (35) first identified methylecgonidine in the bile of a cocaine overdose patient. However, his discovery was likely an artifact for two primary reasons. Firstly, the decedent reportedly abused cocaine intravenously, a route of administration not known to produce significant amounts of methylecgonidine. Secondly, the investigators analyzed bile extractions from the patient using a GC/MS assay. Toennes and co-workers recently reported that artifact AEME is formed by thermolytic breakdown of cocaine in the heated GC injector port (36). Furthermore, Lowry (35) reported a mass chromatogram of bile extract with a low intensity AEME peak (7%) roughly proportional to that observed from the thermal degradation of cocaine (37 μg/L in the bile) in the heated GC injector port (36,37). Therefore, the earliest reports of the identification of AEME in humans following the suggestive NIDA report appeared in the literature during 1990 (38,39), and numerous studies thereafter (24,40,41).

Typically, a cocaine user places a lump of crack on a screen in a pipe and heats the material while inhaling (42). A significant rise in temperature causes cocaine to rapidly change state from solid to liquid to vapor (42). Pyrolytic degradation of cocaine commences at temperatures greater than 170ºC (42). For reference, the temperature of a glowing end of a tobacco cigarette reaches 800°C (34). As the cocaine travels away from the flame and cools, smoke forms consisting of cocaine base droplets and pyrolysis products, primarily benzoic acid and AEME (42). The vapor pressure of AEME is greater than cocaine free-base, so AEME coats the earlier condensing cocaine droplet during formation of the aerosol (42). AEME is faster to evaporate, lingering around the "crack" smoking atmosphere longer than cocaine particles, suggesting that AEME may have forensic smoke and indoor air quality implications (42).

Determining a standard AEME amount formed during crack smoking is difficult due to variability in temperature and formation (43). Cocaine is almost completely degraded at 800°C with only 16% of the pyrolysis product being intact cocaine (6). One pyrolysis project indicated that 68% cocaine free-base was converted to AEME when heated to 320°C under vacuum, conditions not achieved in a crack pipe (44). Another research group observed a maximum of 2% AEME formed after heating 10 mg cocaine free-base in a model crack pipe with a Bunsen burner at atmospheric pressure (42). When 30 mg of free-base was heated to ignition, a maximum of 5% AEME was recovered (42).

1.2.2 AEME Metabolism

In specific forensic cases, AEME has been detected in the urine (38), blood/plasma (36), saliva/perspiration (40), hair (40), brain and liver (45) of crack cocaine users. Although methylecgonidine has been identified in numerous matrices, fewer studies have reported its presence in blood or plasma samples (43). The maximal urinary AEME concentration reported in the literature is 6.34 μg/mL while the maximum reported concentration in blood or plasma is 0.11 μg/mL (43). Part of the explanation on why AEME is detected in blood/plasma at lower concentrations than other matrices is due to its metabolism.

The metabolism of AEME, in many ways, mirrors the metabolism of cocaine. AEME is primarily metabolized by butyrylcholine esterase to a more polar entity, AE (anhydroecgonine), which has an average longer half-life than AEME (116 min vs. 20 min, respectively), and also a forensic marker of smoked cocaine use (43). Although no studies have reported to date, AEME is likely a substrate for human carboxylesterase-1. Similar to cocaine, the chemical hydrolysis of AEME proceeds more rapidly with increasing pH. In one

study, AEME concentration was measured over time in phosphate buffer at pH 10 and 7.4 (46). After 7 days, the AEME concentration decreased by more than 96% at pH 10, while after 30 days, the AEME concentration decreased only 50% at pH 7.4 (46).

In addition to hydrolysis, AEME is oxidized to AEME *N*-oxide (AEMENO), a metabolic pathway also seen with cocaine and norcocaine (23). AEMENO was detected by LC-MS after incubation of AEME (20 µg) with rat liver microsomes (47). The *N*-oxide was also identified in the urine of known crack cocaine users (47). The esterase-mediated transesterification of cocaine to cocaethylene in the presence of ethanol is well documented (48-50). In fact, this transesterification reaction has been documented with several other pharmaceutical agents, including meperidine (51), methylphenidate (51-53), and acitretin (54,55) (Figure 1.3). In rat liver microsomes, AEME (5 mM) was combined with ethanol (250 mM), generating AEEE (anhydroecgonine ethyl ester, ethylecgonidine, EEG) (Figure 1.4) (56). This transesterification reaction was blocked by NaF (200 mM), a non-specific esterase inhibitor (56).

In an analogous fashion to AEME, artifactual AEEE or AE may be generated in the heated GC injector port by the thermal breakup of cocaethylene or cocaine metabolites, confounding GC-MS analysis. Recently, the artifactual production of AE from cocaine metabolites, benzoylecgonine, ecgonine or *m*-hydroxybenzoylecgonine, was reported, suggesting it is not a good marker for smoked cocaine use (37). The identification of AEEE as a metabolite of cocaine and ethanol co-abuse has been *suggested* earlier by Isenschmid (57), but actual reports of AEEE in human subjects are non existent, to our recent knowledge, in peer-reviewed scientific reports.

1.2.3 AEME and AEEE Pharmacology

AEME has unique pharmacological properties from cocaine in which it reportedly has no significant euphoric or reinforcing features in test subjects (58). Containing a chemical structure (Fig 1.5) similar to the muscarinic agonists, arecoline and anatoxin A, AEME was originally hypothesized to exhibit cholinergic agonist activity (38). Most later pharmacological studies on AEME reported results supporting this hypothesis (59-61). In contrast, AEME was shown to relax airway smooth muscle in guinea pigs and antagonized bronchoconstriction induced by acetylcholine (58). A recent, well-published report found that AEME acts as a muscarinic agonist *in vivo* when tested in awake sheep. AEME administered intravenously (0.1-3.0 mg/kg) produced significant hypotension and tachycardia in sheep, and these effects were antagonized by pretreatment with the peripherally acting muscarinic antagonist, atropine methyl bromide (15 μg/kg) (43).

Pharmacological studies conflict on the chemical actions of AEME's transesterification product, AEEE. An intravenous dose of 3 mg AEEE was administered to rabbits, producing similar cardiovascular effects as AEME, such as hypotension and increased heart rate (60). Another study reported that AEEE exhibited only weak activity at muscarinic subtypes (m1-m5) and showed no receptor selectivity (62). The pharmacology of AE (ecgonidine), a hydrolysis product of AEME or AEEE, is currently unknown (43) The exact role of cocaine pyrolysis products (AEME, AEEE, AE) in the sequelae of cocaine related toxicity continues to be studied.

Chemically, AEME is an alkaline, bicyclic compound containing an electrophilic α,β-unsaturated carbonyl moiety. Based on previous literature reports of other compounds with a similar α,β-unsaturated carbonyl functional moiety, such as ethacrynic acid (63), arecoline

(64), methyl cinnamate (65) and morphinone (Fig 1.6) (66), AEME is susceptible to nucleophilic attack by thiol-containing compounds, like glutathione and cysteine. The driving chemical reaction behind glutathione conjugation to such electrophilic compounds is a 1,4-Michael addition reaction, also known as the Michael reaction.

1.3 The Michael Reaction

In 1887 Arthur Michael reported that olefins conjugated with electron-withdrawing groups (Z) are susceptible to nucleophilic attack (67). Although actually first reported by Claisen, Michael received widespread credit for the reaction known by his name, the Michael Reaction (68). Structures of model 'Michael reaction acceptors' include CH_2=CH-Z, R-CH=CH-Z (including quinones) and R-C≡C-Z (acetylenes) (67). In general, the unsaturated compound in the Michael condensation is referred to as the acceptor (or electrophile), while the active hydrogen compound is the addendum (or nucleophile) (69). The nucleophilic compound attacks the electrophilic compound to form a conjugate or adduct.

The demonstrated order of reactivity of olefins conjugated with electron withdrawing group (Z) with the standard nucleophiles (pyrrolidine or morpholine) is: Z= $CONR_2$ < $CONH_2$ < CO_2R < CN < COR < CO < COAr < NO_2 (67). Reactions were followed to at least 75% completion and overall, were second order (first order in each of the reactants) (67). For instance, at 30°C, morpholine (80M) reacted with methyl acrylate (100M; Z=$COOCH_3$) to produce a 2^{nd} order rate constant of 103 L/mol·sec , whereas the reaction of morpholine (0.128 M) with acrolein (0.128M; Z=CHO) or methyl vinyl ketone (0.128M; Z=$COCH_3$) produced larger rate constants of 11,360 and 13,000, respectively (67).

We speculate that the acrolein or methyl vinyl ketone conjugate carbanion, formed after nucleophile addition, is more stable than the methyl acrylate carbanion counterpart, leading to greater product generation. Greater stabilization of a carbanion bearing an aldehyde or ketone substituent versus a methyl ester group was documented previously (70). Additionally, the methyl vinyl ketone conjugate anion, versus the acrolein conjugate anion, demonstrates possible enhanced stabilization due to polarization by the additional methyl group (71).

Michael reactions are reversible, regenerating the original olefin, by the same alkaline catalyst that favors condensation (72). In general, lower temperatures favor condensation while elevated temperatures increase retrogression (72). Preferably, the *in vitro* reaction is carried out for only several hours, as increased reaction time re-generates greater concentrations of the original reactants (LeRoy Salerni, Ph.D., Butler University; unpublished data). The retro-Michael reaction can be retarded, in part, by using an excess of one of the reactants, causing a shift in equilibrium towards conjugate formation (72). Retrogression is more likely to occur when the condensation is slow (72). One of the factors that slows condensation is the presence of a large number of substituents at the α,β double bond (72). For example, the reaction rate at room temperature for pyrrolidine (80M) mixed with acrylamide (100 M; Z= $CONH_2$) is 83.5 L/mol·sec, while the reaction is markedly decreased (0.541) with p-nitrostyrene [100 M; Z=C_6H_4·NO_2-*p*] (67).

A competing 1,2-addition (to the C=O or C≡N) sometimes predominates over the 1,4-addition (73). However, the 1,2-addition mainly occurs in aldehydes (73). In addition, 1,2-adducts are often substantially less stable than the 1,4 adducts, and if the Z group (from the electrophile) is not a sufficiently good leaving group, the initial 1,2-adducts can reform the starting nucleophile and acceptor (74).

The Michael Reaction shows stereospecificity. When the substrate contains suitably different R groups, two new chiral centers are generated (73). The product, therefore, can exist as two pairs of enantiomers (73). In a distereoselective process one of the two pairs is predominantly formed as a racemic mixture (73). Many examples have been reported in the literature (74). In this research project, the stereochemistry following nucleophile addition to AEME is partially elucidated.

A key player in a biologically occurring Michael reaction is the cellular nucleophile, glutathione (GSH), which is reviewed next.

1.4 Glutathione (GSH) Conjugation

GSH was initially called "philothion" and was first isolated in 1888, but its structure was elucidated 40 years later (75). GSH is a ubiquitous tripeptide (L-γ-glutamyl-L-cysteinylglycine) that is usually the most prevalent intracellular thiol (76). The intracellular concentrations of GSH range between 0.1-10 mM and varies among tissues (76). Regarding tissue distribution, the highest concentrations of GSH are found in the liver, spleen and kidneys while lower concentrations are present among the heart, lungs and blood (77). GSH is oxidized at the thiol group of the cysteine residue to the disulfide product, GSSG, which was measured at 10-15% of the total GSH concentration in rat blood plasma (78). Interestingly, this oxidation reaction is more active in rat kidney cells in comparison to rat liver cells (78).

GSH functions directly or indirectly in many important biological processes, including the synthesis of proteins and DNA, transport, enzyme activity, metabolism and protection of cells (78). The GSH function pertinent to this discussion involves the conjugation of the nucleophilic thiol-group of GSH to electrophilic xenobiotics, precluding the toxic reaction of

these substances, in most cases, with biological macromolecules (75). For example, the commonly used analgesic agent acetaminophen (Tylenol®) is enzymatically *N*-oxidized to a reactive, electrophilic quinoneimine metabolite (NAPQI), which reacts with GSH to form a less toxic glutathione conjugate (79). At therapeutic doses, acetaminophen is non-toxic to normally functioning livers, but in excessive doses it causes severe liver necrosis, arising from metabolite induced glutathione depletion that allows the reactive quinone to covalently bind macromolecules in the liver (79).

In less common instances, glutathione conjugation can lead to the formation of a bioactive substance (75). Ethacrynic acid, a loop diuretic, reacts with GSH to form an ethacrynic acid-SG adduct, which was found to be a potent inhibitor of rat and human glutathione-*S*-transferases (80,81). Other chemicals biotransformed to bioactive GSH-conjugates include dihalomethanes and isocyanates (75). For example, the GSH conjugation of the dihaloalkane, dichloromethane, initially yields *S*-chloromethyl-GSH (82). This intermediate is converted nonenzymatically to *S*-hydroxymethyl-GSH (a hemimercaptal of formaldehyde and GSH), which eliminates formaldehyde and glutathione (82). Dichloromethane-GSH metabolism has been linked to the development of tumors in animals (82).

Some thiol adducts of α,β-unsaturated aldehydes, such as 1:2 crotonaldehyde-cysteine, exhibit biologic activity similar to the parent chemical (75). One explanation for this phenomenon suggests that the retro reaction leads to adduct dissociation at the target site and regeneration of the toxic, parent compound (83). Another study demonstrated that the reaction of 4-hydroxy-pentenal with sulfhydryl groups of proteins is reversible by an excess of GSH or other protein thiol groups (84). Using ethacrynic acid (EA), Ploemen and co-workers (85)

studied the retro Michael cleavage of the EA-SG conjugate by the addition of an excess of *N*-acetylcysteine or the enzyme GST P1-1 (pi). Their findings suggest that EA may be transferred from one low molecular weight compound to another or to a reactive cysteine in proteins, such as cysteine 47 of GST P1-1 (85).

1.5 The Mercapturic Acid Pathway

The mercapturic acid pathway is a multi-step enzyme-mediated process that initially forms a glutathione adduct and then prepares it for elimination in the body (Fig 1.7). Several of the significant steps will be reviewed here.

1.5.1 Glutathione *S*-Transferases (GST's)

GSH conjugation to xenobiotics is the first step in the mercapturic acid pathway. In 1960, researchers first concluded that GSH conjugation is catalyzed by rat liver cytosol (86). During the mid 1970's, four different glutathione transferases were isolated from rat liver cytosol (75). These enzymes, which have evolved together with GSH in aerobic organisms, are abundant and widely distributed in most forms of life (87). Today, there are currently eight identified human soluble/cytosolic glutathione *S*-transferase (GST) isoforms that comprise the major GST supergene family (88): alpha (A), mu (M), theta (T), pi (P), zeta (Z), sigma (S), kappa (K), and omega (O). Kappa GST, although soluble, is mitochondrial and not found in the cytoplasm (89). Allelic variants have been discovered in all of the isoforms except kappa, sigma and omega (88). The other superfamily of GST's are microsomal proteins termed MAPEG and primarily involved in the metabolism of arachidonic acid (89).

Overall, the GST family of isoenzymes represent around 1% of total cellular protein (90). In the human liver, the cytosolic GST's are more concentrated and comprise on average about 4-5% of total cytosolic protein (91,92). In general, different organs express different concentrations of soluble GST isoforms (89). For instance, the kidneys express alpha, pi, mu, theta and omega isoforms, the lungs contain predominantly pi, and the developed liver expresses alpha, kappa, mu, theta and omega (89). Many tumor cells over express total cytosolic GST activity, leading to resistance of chemotherapeutic drugs by chemical detoxification through elevated GSH conjugation (93). Several reports have found total cytosolic protein concentration ranging from 4-40 μg of GST/mg of cytosolic protein in tumors and tumor cell lines (93). Potent inhibitors of GST's, such as ethacrynic acid, have been utilized in clinical studies to potentially enhance the cytotoxic effects of anti-tumor drug regimens (90).

Although they may serve as intracellular carrier proteins for ligand transport (87), the GST's primarily catalyze conjugation reactions toward a diverse range of substrates (i.e. epoxides, lactones, quinones and esters) that are potentially hazardous to cells (92). Substrates share, however, the common feature of being mostly hydrophobic and bearing an electrophilic center (92). Each cytosolic enzyme has two active sites per dimer that behave independently of each other (92). The active site contains at least two binding regions: specific hydrophilic GSH binding site (G site) and less specific hydrophobic substrate binding site (H site) (92). Interestingly, a tyrosine residue within the active site is one of the few known residues conserved among the known GST sequences, suggesting an important role in the catalytic mechanism (92). Current understanding of the mechanism by one author implies that the thiolate anion of enzyme-bound GSH is stabilized at neutral pH through hydrogen bonding

with the hydroxyl group of the tyrosine residue (75). On the other hand, another hypothesis suggests that a basic amino acid residue, such as arginine or histidine, converts GSH to the active $^{-}$SG moiety (94). Site-directed mutagenesis studies revealed that replacement of arginine residues in GST-α with other amino acids results in decreased activity (94).

1.5.2 Metabolism of GSH Conjugates

GSH conjugates, whether enzymatically or non-enzymatically formed, are rarely excreted unchanged in the urine since they contain a high molecular weight and amphiphilic structure (79). Although they can be eliminated in the bile, most conjugates are metabolized further to mercapturic acid derivatives for elimination in the urine. The first step in the catabolism of GSH-conjugates is mediated by the enzyme, γ-glutamyltransferase (GGT), which hydrolyzes or transfers the γ-glutamyl group to an appropriate receptor (75). GGT is a ubiquitous enzyme present in serum and all cells except muscle cells (95).

The products of GGT catalysis, cysteinylglycine S-conjugates, are degraded to cysteine S-conjugates by the enzymes, cysteinylglycine dipeptidase (dipeptidase) or aminopeptidase-M (75). Dipeptidase is a zinc metalloproteinase which has been identified in the kidneys of humans (96). Aminopeptidase-M is also a zinc-containing metallopeptidase and is widely distributed in mammalian tissue within the central nervous system, kidney and intestinal microvilli (75). Although aminopeptidase-M is more abundant than cysteinylglycine dipeptidase, dipeptidase plays a larger role in the metabolism of GSH conjugates (75).

Cysteine S-conjugates are *N*-acetylated by cysteine S-conjugate N-acetyltransferase to *N*-acetylcysteine derivatives, also termed mercapturic acid derivatives or mercapturates (75). This acetyltransferase has been isolated from rat kidney microsomes and appears to function

within the proximal renal tubule cells (97). Additional metabolic pathways of GSH conjugates not discussed within this review in more depth include oxidation and cleavage of cysteine-S-conjugates followed by glucoronidation, sulfation or methylation (75).

1.5.3 GSH Conjugate Transport

Transport of GSH conjugates out of the cell is a critically important cellular function since accumulation of conjugates within the cell can lead to inhibition of GST's and GSH reductase (98). There are at least three different transport systems with different substrate and transport characteristics (75). The GS-X pump, or multi-specific organic anion transporter, is ATP-dependent and distributed among different organs and cell types in the body (98). The diverse range of substrates for the GS-X pump includes metabolites of anticancer drugs, glucuronide conjugates, sulfate conjugates, leukotrienes and prostaglandins (98).

Another transport system is Na^+-dependent and transports GSH, GSH conjugates, γ-glutamyl derivatives and probenecid (75). This system is found in the basolateral membranes of the kidneys and intestine (75). The third transport system is Na^+ -independent and found in the brush borders of intestinal cells and liver cells (75). It may exchange GSH conjugates or organic anions with GSH (75). Catabolites of GSH conjugates are possibly transported by carriers that also transport amino acids and dipeptides (75). Well known organic anion transporters in the liver and kidney transport mercapturic acid derivatives (75).

1.6 Examples of Michael Acceptors in the Literature

The pharmaceutical science literature is crowded with numerous examples of drugs and metabolites that conjugate with GSH. For this discussion, three pertinent compounds are reviewed: morphinone, arecoline and ethacrynic acid (Fig 1.6).

1.6.1 Morphinone

Morphinone (MO), containing an α,β-unsaturated ketone, is the oxidation product of the opiate analgesic morphine in the presence of morphine dehydrogenase (66). MO reacts readily with the thiol containing compounds 2-mercaptoethanol, cysteine and glutathione by a 1,4 Michael addition reaction (99). The *in vitro* reaction of MO with GSH obeyed second order kinetics ($k = 13.5\ Lmole^{-1}min^{-1}$) while the reaction with cysteine was too rapid to determine the rate constant (99). Ishida and co-workers (66) synthesized and purified an authentic MO-GSH adduct for analytical comparison to the MO-GSH metabolite extracted from test animals. Briefly, morphine (25 mg/kg) and GSH (100 mg/kg) were injected at different sites into guinea pigs and the bile was subsequently collected for 8 hours (66). MO-GSH was purified from the bile after extensive chromatography, and the structure of the metabolite was analyzed by FABMS ($MH^+ = 591$) and NMR spectrometry. Interestingly, two-dimensional NMR spectrometry (COSY and HETCOR) confirmed that the GSH residue preferentially attacks C-8 from the upper (less sterically hindered) side of the molecule, forming the 8*S* isomer (66). A similar stereochemical picture is observed with the related metabolite codeinone-GSH, an oxidation product of codeine, which has been detected in the bile of codeine-treated guinea pigs (100).

An extension of these studies measured the enzymatic rate of GSH conjugation to MO (101). Enzymatic formation of MO-GSH was determined in an incubation mixture containing 1 mM MO, 1 mM GSH, enzyme (0.5 mg protein purified on a Sephadex G-25 column from the cytosol of guinea pig liver), and 0.1 M sodium phosphate buffer (pH 6.5) to a final solution volume of 2 mL (101). Reactions were carried at 25°C for 2 minutes. MO-GSH was formed in both native and boiled cytosol preparations containing MO and GSH (101). Interestingly, the enzymatic rate proceeds at an optimum pH of 6.0, whereas the non-enzymatic rate increases with increasing pH (101). In addition, the enzymatic reaction was greater at lower concentrations of GSH, with an optimal rate achieved with 1 mM GSH (101). This observation of enhanced rate at lower GSH concentrations has also been reported with GSH addition to the acetaminophen metabolite, NAPQI (102).

1.6.2 Arecoline

Arecoline (arecaidine methyl ester) is the major alkaloid of betel nuts, fruits of *Areca catechu,* a tall palm cultivated in India, southestern Asia, the East Indies and East Africa (103). A common masticatory mixture (betel) composed of the nut, shell lime and leaves of *Piper betle* (a climbing species of pepper) is chewed to release euphoretic chemicals (104). Natives of India and the East Indies have consumed this mixture for its stimulatory properties since antiquity (104). Arecoline has been used therapeutically in veterinary medicine as a vermicide and taeniacide (104). Pharmacologically, it binds to muscarinic and nicotinic receptors (104).

Currently, there are an estimated 600 million betel quid (BQ) chewers in the world, and BQ chewing is a major etiologic factor of oral cancer (105). Briefly, arecoline was found to deplete cellular glutathione levels, one of several key factors leading to the disruption of the

normal cell cycle control of oral mucosal fibroblasts and keratinocytes (105). Boyland and co-workers (64) were among the first researchers to show that arecoline is hydrolyzed to arecaidine in rats, and both substances are eventually converted to mercapturic acid derivatives. Arecoline (12.5 nM) or arecaidine (12.5 nM) plus GSH (5 nM) when incubated for 40 minutes, with or without liver preparations, (mouse, rat, hamster, duck or whole rat) at pH 6.8, formed the corresponding GSH conjugate (64). However, the presence of liver preparations did not affect the rate of reaction (64).

Another study reported that arecoline 20 and 40 mg/kg administered intraperitoneally to swiss albino mice of either sex for 10 or 30 days significantly enhanced cystosolic GST activity in both sexes at 10 and 30 days (106). In addition, arecoline 40 mg/kg significantly reduced acid soluble sulfhydryl content in liver tissue in both sexes after 10 and 30 days (106). But a later study from a different research group showed that arecoline (25-200 μg/mL) incubated for 24 hours with human buccal mucosal fibroblasts significantly reduced GST activity towards the common GST substrate, CDNB (1-chloro-2,4-dinitrobenzene), at all tested arecoline concentrations (107). Chang's study suggests that arecoline is a GST inhibitor (107).

1.6.3 Ethacrynic Acid (EA)

EA (Fig 1.6) is a potent, short-acting loop diuretic that inhibits the Na^+-K^+-$2Cl^-$ symport in the thick ascending limb of the loop of Henle within the renal tubules (108). Chemically, it is a phenoxyacetic acid derivative that contains a reactive electrophilic α,β-unsaturated ketone moiety. In one of the earliest reports on the metabolism of ethacrynic acid, ^{35}S-GSH was administered intravenously to rats one hour before ^{14}C-EA at a dose of 5 or 50 mg/kg (63). The radioactive EA-GSH adduct was identified in the bile within 10 minutes

following administration (63). After 30 minutes, the major metabolite identified in the bile was the EA-mercapturate (63).

The chemical synthesis of the EA-SG adduct resulted in approximately equal amounts (46:54) of diastereoisomers (*R* or *S* about C-9) based on NMR analysis (109). GSTP1-1 (pi), mutant GSTP1-1 (C47S) and GSTA1-1 (alpha) all stereospecifically catalyze the formation of one of the diastereomers, whereas GSTA1-2 and GSTA2-2 showed no stereospecificity (109). Three-dimensional crystal structures of GSTA1-1 and GSTP1-1 in complex with an EA-SG diastereoisomer are deposited in the Brookhaven PDB databank (109). Interestingly, the PDB file of the complexed GSTA1-1 shows the *R*-isomer, while the GSTP1-1 complex PDB file contains the *S*-file (109). Currently, the correct diastereometric structure (*R* or *S* about C-9) of the enzyme catalyzed product is unknown.

EA is a potent reversible inhibitor of rat and human glutathione S-transferases with reported I_{50} (μM) values for alpha, mu and pi class GST's of 4.6-6.0, 0.3-1.9 and 3.3-4.8, respectively (81). The EA-SG conjugate displayed a stronger inhibition for alpha and mu GST's with I_{50} (μM) values around 0.8-2.8 and 0.1-1.2, respectively (81). The conjugate, however, showed a weaker inhibition of the pi class with a measured inhibitory value of 11.3 μM (81). EA also inhibits rat and human pi-class GST's through covalent binding to a cysteine residue on the enzyme (81). Time course labeling of GST pi was followed by incubating ^{14}C-EA (6.25 μM) with 1.25 μM enzyme, resulting in 65-93% inhibition of GST catalytic activity towards CDNB (81). GST pi class isoforms (1μM) inactivated by 10 μM EA (> 90% loss) regained full catalytic activity by incubation with an excess of glutathione (1 mM) over 125 hours (81).

Finally, one study compared the rates of formation of the EA-SG adduct in enzymatic and non-enzymatic preparations (110). EA (4 mM) was incubated at 25°C with GSH (2.5 mM) in phosphate buffer (pH 6.0, 6.5 and 7) with or without GST-π (22 μg/mL) (110). Small aliquots (100 μL) were analyzed by injection onto a HPLC column over various time intervals from 1 to 150 minutes (110). Enzyme accelerated the initial rate of EA-SG formation by approximately 2.8 and 1.1 fold at pH 6.5 and 7.4, respectively (110). Initially, the enzymatically mediated reaction was faster for 10 minutes, but the two rates were comparable thereafter until the final time point of 150 minutes (110). In addition, the non-enzymatic rate showed a positive correlation with increasing pH, as an approximately 2.5 fold greater rate was reported at pH 7.4 than at pH 6.5 (110).

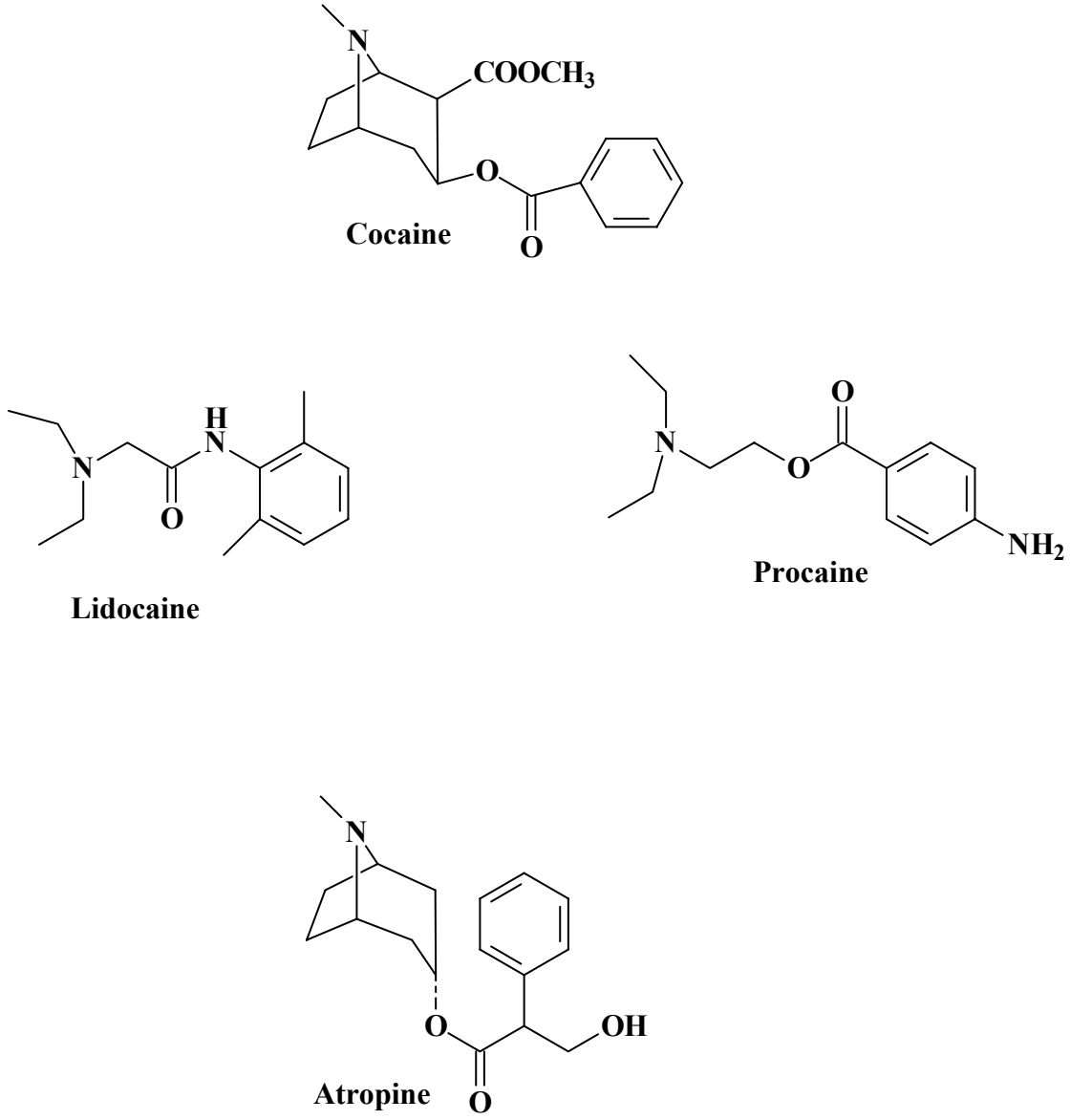

Figure 1.1: Chemical structures of cocaine and chemically related derivatives.

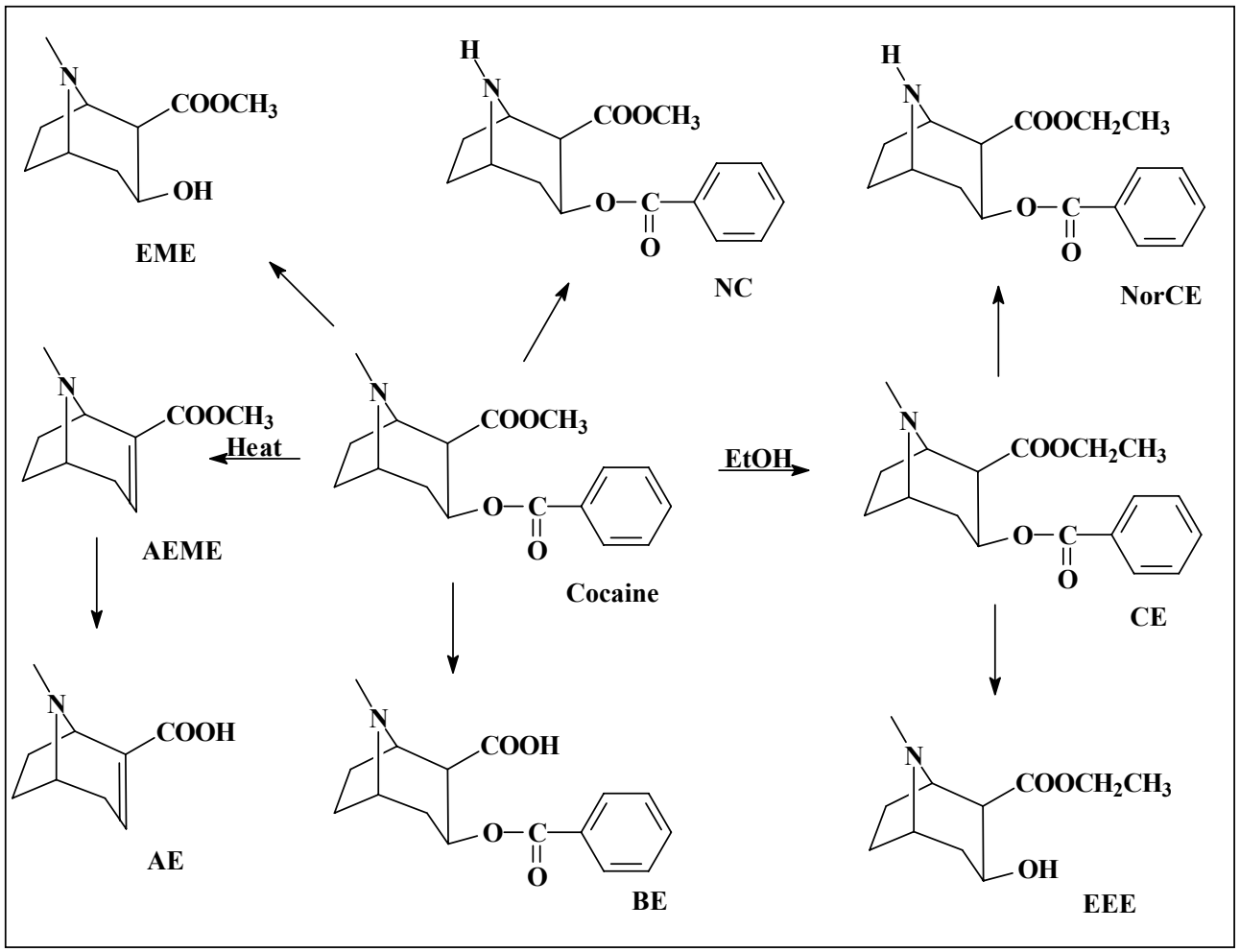

Figure 1.2: Schematic showing the major pathways of cocaine metabolism.

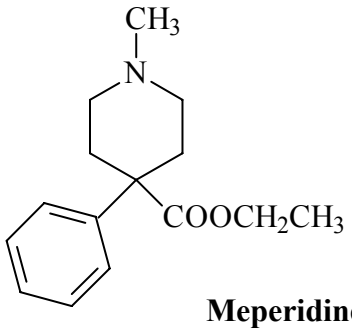

Meperidine

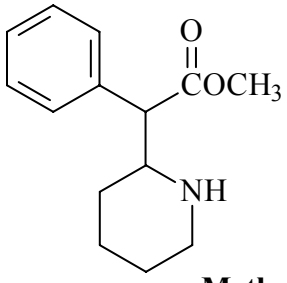

Methylphenidate

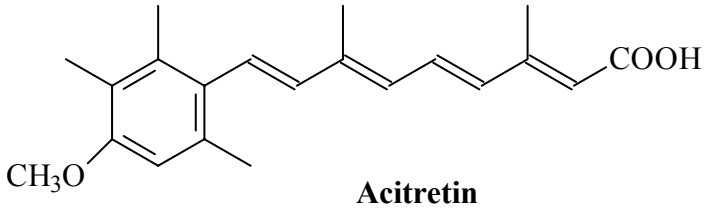

Acitretin

Figure 1.3: Chemical structures of pharmacologic agents that undergo transesterification (or esterification) reactions in the presence of ethanol.

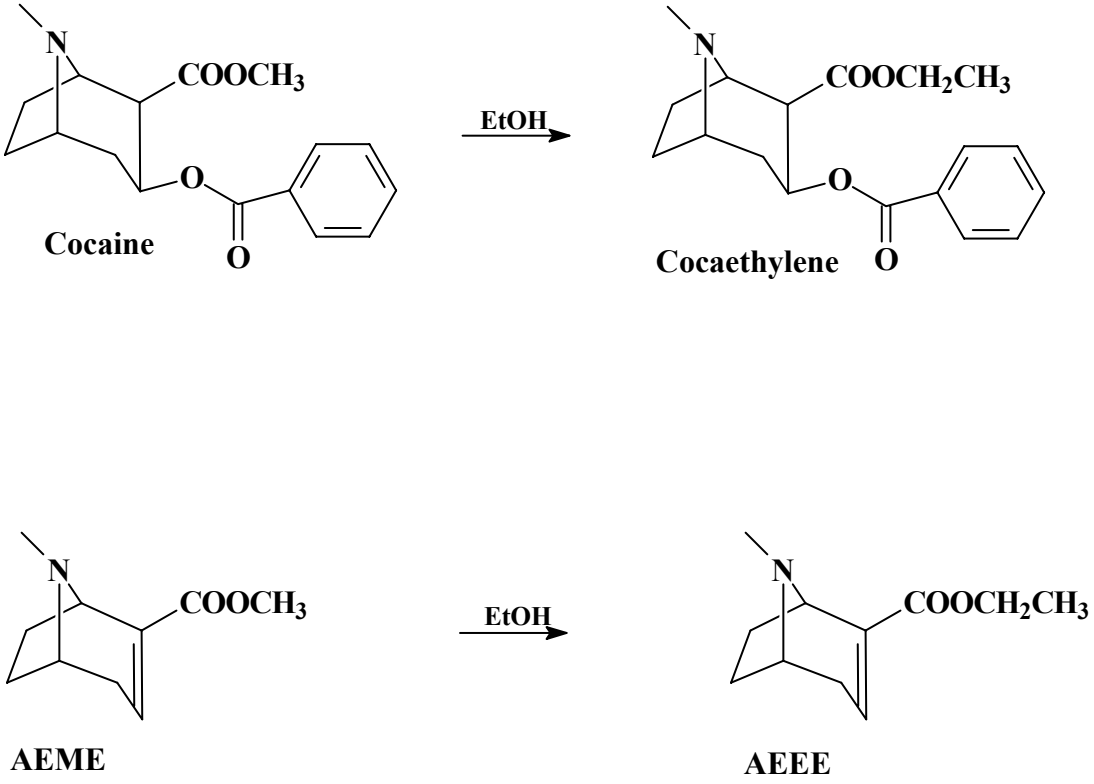

Figure 1.4: Schematic showing the transesterification of cocaine to cocaethylene and AEME to AEEE in the presence of ethanol.

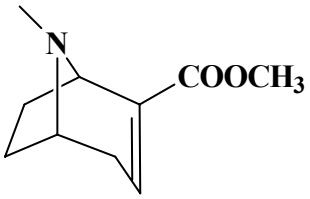

AEME

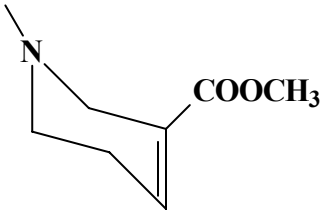

Arecoline

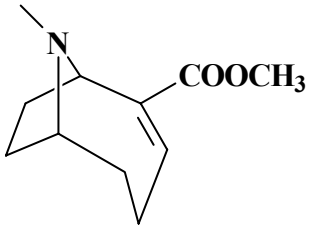

Anatoxin

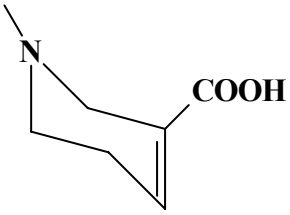

Arecaidine

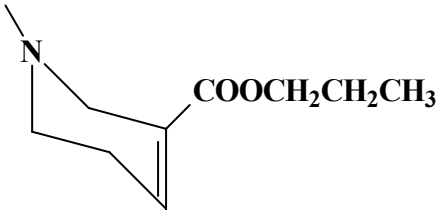

Arecaidine Propyl Ester

Fig. 1.5: Chemical structures of AEME and related compounds.

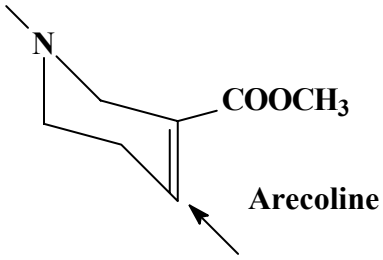

Arecoline

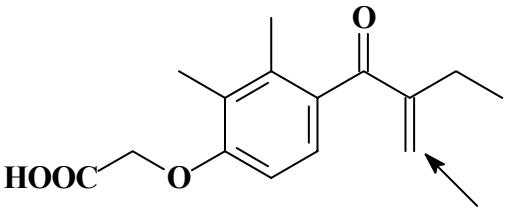

Ethacrynic Acid (EA)

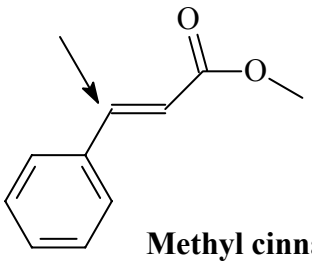

Methyl cinnamate

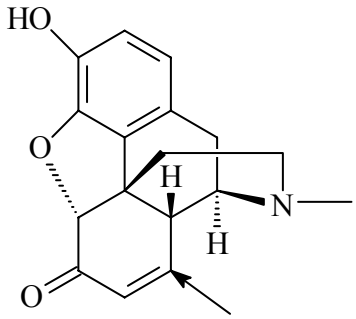

Morphinone

Figure 1.6: Chemical structures of compounds containing an α,β-unsaturated carbonyl functional group. Arrows indicate point of attack by nucleophilic agents.

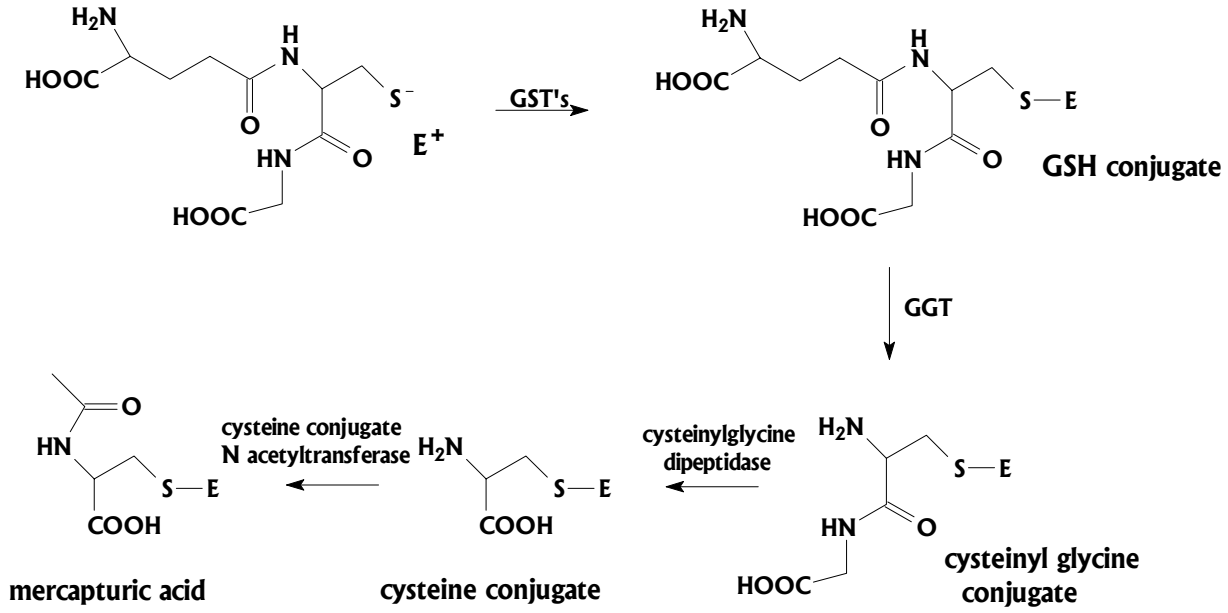

Figure 1.7: Overview of the mercapturic acid pathway. $\mathbf{E}^+$ represents a generic substitution for an electrophilic agent.

1.7 Research Objectives

Since smoking free-base cocaine results in the formation of electrophilic, potentially reactive compounds, these toxic metabolites may play a role in cocaine associated toxicity. In addition, some of these metabolites may be additional human markers of smoked cocaine use. The main research objectives are the following:

1. To synthesize mercapturic acid and glutathione conjugates of arecoline and related derivatives.
2. To synthesize mercapturic acid and glutathione adducts of AEME and related compounds.
3. To analyze the stereochemistry of the AEME mercapturate (C-2 and C-3) following NAC addition to AEME.
4. To investigate the chemical kinetics of glutathione addition to AEME and other known Michael acceptor compounds.
5. To demonstrate the reduction of chemically generated DCNB-SG conjugate in the presence of AEME, arecoline or EA.
6. To monitor the degradation of selected glutathione conjugates over time at physiological pH.
7. To determine if AEME is a substrate for cytosolic glutathione S-transferases contained within pooled human liver cytosol.
8. To establish if AEME inhibits cytosolic GST activity.
9. To quantify the relative concentration of AEEE in a urine sample from a known cocaine/ethanol abuser.

10. To identify AEME-NAC in a urine sample from a known free-base cocaine user.
11. To assess the cytotoxicity of AEME, AEEE, AE and cocaine against A549 lung fibroblasts using a trypan blue exclusion assay and flow cytometry.

Chapter 2: Experimental Methods

2.1 Materials and Methods

Chemicals: Anhydroecgonine methyl ester and anhydroecgonine HCl were purchased from Cerilliant Corp. (Austin, TX) and used in earlier synthetic and analytical studies. AEME fumarate was graciously supplied by F. Ivy Carroll, Ph.D. (National Institute on Drug Abuse, Division of Neuroscience and Behavioral Research, Research Triangle Park, NC) and used in some synthetic procedures. Glutathione (GSH), NAC (*N*-acetylcysteine), DTNB ((5,5'-dithio-bis (2-nitrobenzoic acid)); Ellman's reagent), DCNB (3,4-dichloronitrobenzene), CDNB (1-chloro-2,4-dinitrobenzene), THAM® (tris-hydroxymethyl aminomethane), ammonium acetate, potassium phosphate, potassium carbonate, sodium bicarbonate, sodium sulfate, cocaine HCl, fumaric acid, arecoline HBr, DMSO (dimethyl sulfoxide), DMSO-d_6, CD_3OD, CD_3Cl, and D_2O were all purchased from Sigma-Aldrich Chemical Co. (St. Louis, MO). A 5 mM solution of Ellman's reagent in phosphate buffer (pH 7.4) was prepared for UV analysis.

Methanol, chloroform, acetonitrile, benzene, diethyl ether, acetone, 1-propanol, 2-propanol, methylene chloride, ammonium hydroxide (21%), glacial acetic acid and sulfuric acid were obtained from Fisher Co. (Pittsburgh, PA). Concentrated HCl (37%) was obtained from Acros Organics (New Jersey, USA). Absolute ethyl alcohol (200 proof) was obtained from Aaper Chemical Co. (Shelbyville, KY). Distilled water was generated from a Barnstead Nanopure system (Dubuque, IA).

HPLC grade solvents were used for HPLC analyses, laboratory or HPLC grade solvents were utilized for synthetic procedures, and optima grade solvents were used for MS, LC-MS, LC-MS/MS analyses. SPE elution mixture consisted of optima grade solvents and optima grade ammonium hydroxide.

Pooled human liver cytosol (20 mg/mL protein content) and single donor human liver cytosol (HK27; 20 mg/mL) were obtained from Gentest (BD Biosciences; Woburn, MA) and stored at -80°C until use. A549 lung fibroblast cells were obtained from the American Type Culture Collection (ATCC; Manassa, VA). Hank's Balanced Salt Solution was purchased from Mediatech, Inc. (Herndon, VA). Kaughn's modification of F12 (HyQ Ham's/F-12 media containing 1.00 mM L-glutamine) and trypsin containing 0.25% EDTA were purchased from Hyclone (Logan, Utah). Trypan blue (0.4% in PBS) was purchased from Mediatech, Inc. (Herndon, VA). Propidium iodide (PI) was purchased from Sigma-Aldrich (St. Louis, MO). A549 cells, salt solution, media, trypsin/EDTA, trypan blue and PI were generously donated from the laboratory of Slawomir Lukomski, Ph.D. (Deparment of Microbiology, Immunology and Cell Biology, West Virginia University).

Urine Samples: Urine samples collected from several multiple drug overdose/suicide victims at the Office of the Chief Medical Examiner (OCME) in Charleston, WV were stored at -80°C in a vacuum-sealed container until future use. Urine samples were completely thawed before use by placing in a laminar airflow hood (Labconco; Kansas City, MO) at room temperature for several hours.

Instrumentation: All melting points were determined on a Thomas-Hoover melting point apparatus. Samples were evaporated to dryness using solely or a combination of the following systems: Rotavapor-R (Büchi, Flawil, Switzerland) rotavap system connected to a vacuum pump (Duo Seal, General Electric); Savant Speed Vac SVC 100 (GMI; Ramsey, MN); or standard vacuum dessicator connected to a vacuum pump. Incubations were conducted at

37°C in a Precision (Winchester, VA) shaking water bath incubator. Experiments measuring UV/VIS absorbance of analytes utilized a Beckman DU 640 spectrophotometer (Beckman Coulter; Fullerton, CA). NMR data was recorded on a Varian Gemini 2000, 300 MHz broadband spectrometer or Varian Inova 600 spectrometer (Varian; Palo Alto, CA).

GC-MS analysis of the metabolites was conducted on an Agilent (Palo Alto, CA) 5973 Electron-Impact gas chromatograph/ mass spectrometer. Samples were analyzed on a Supelco Equity 1 (St. Louis, MO) capillary column with an oven temperature of 90°C held for 1 minute and then programmed at 20°C/min to 280°C, with a total run time of 12.50 minutes. Helium was the carrier gas, and the injection volume was 2 μL per injection.

One LC-MS system was as follows. Reversed phase LC analysis of compounds was performed with a Waters 2695 (Milford, MA) separation module and a Waters 996 Photodiode Array Detector with UV scanning from 200 to 400 nm. This HPLC system was coupled to a Waters Micromass ZMD mass spectrometer programmed to utilize electrospray ionization in a positive ion mode. Source conditions: capillary 3.35 kV; sample cone 20 V; extraction cone 8 V; source block temperature of 100°C and desolvation gas temperature of 300°C; and desolvation gas flow and cone gas flow (both N_2) were 250 L/hr and 95 L/hr, respectively.

A stand-alone LC system (Waters) similar to the HPLC described above was utilized in some experiments. Types and conditions of analytical columns and solvent systems will be described in more detail under the experiments to follow.

Multistage mass spectrometry LC-MS/MS: Shimadzu (Columbia, MD) LC-10AD_{vp} LC system (equipped with a SPD-10A UV/VIS detector, SIL-10AD_{vp} auto injector and DGU-14A degasser) coupled to a Thermoquest LCQ DECA (San Jose, CA) ion trap mass spectrometer was used for MS, MS/MS and MS^3 analyses. The electrospray source (ESI)

included: positive ion detection; sheath N_2 gas flow rate 80 (arbitrary units); spray voltage 2.5 kV; capillary temperature 240°C; capillary voltage 7.00 V; and tube lens offset 15.0 V.

The microscope used for determining cell viability was an Axiostar Plus microscope (Zeiss; Thornwood, NY) with an AxioCam for capturing cell images. Flow cytometry was performed with a FACSCalibur (Becton Dickinson; Franklin Lakes, NJ) flow cytometer with a 15 milliwatt 488 nm argon laser; and it was operated by Dr. Cynthia Cunningham of the Flow Cytometry Core Facility at WVU.

2.1.1 Synthesis of 4-(*N*-Acetylcystein-*S*-yl)Arecoline

The synthesis of the arecoline mercapturic acid (arecoline-NAC) was modified from a previously reported method (64). Arecoline hydrobromide was dissolved in 15.0 mL distilled water, alkalinized with K_2CO_3 (ca. 4 g) to pH 10.0, extracted several times with methylene chloride (50 mL), and dried for 20 minutes over sodium sulfate. The combined, dried organic layers were vacuum filtered and evaporated *in vacuo* to a yellowish oil containing arecoline free-base. Arecoline free-base (0.619 g, 3.99 mmole) was combined with *N*-acetylcysteine (NAC; 4.14 mmole) and dissolved in 25 mL absolute ethanol. The solution was stirred for 3 hours at room temperature under N_2 and then evaporated to dryness. The gummy clear residue was dissolved in 15 mL warm ethanol, cooled to below room temperature, and precipitated by the dropwise addition of diethyl ether. The white precipitate was dissolved in a minimal amount of warm 1-propanol, transferred to a sublimation apparatus, reduced to dryness, and sublimed under reduced pressure to yield soft, white crystals: yield= 44%; m.p. 115-120°C; ESI-MS (MH^+= 319, MS/MS= 190, 156, MS^3 of 190 = 156; ^1H NMR spectrometry (DMSO-d_6): disappearance of the olefinic proton (H-4) at 7.01 ppm.

2.1.2 Synthesis of 4-(Glutathion-*S*-yl)Arecoline

The synthesis of the arecoline-SG conjugate was modified from the aforementioned synthesis of the arecoline mercapturate. Briefly, arecoline HBr (0.5 g) was alkalinized, extracted into organic phase, dried over sodium sulfate and the volatile components evaporated *in vacuo*. Arecoline free-base (240 mg, 1.55 mmole) was combined with reduced glutathione (1.7 mmole) and dissolved in 30 mL of 50% ethanol. The solution was stirred under N_2 for 4 hours at room temperature, and then extracted twice with diethyl ether (40 mL). The combined aqueous layers were concentrated under vacuum and dried under reduced pressure. The soft, glassy residue was precipitated from a water/acetone mixture. Arecoline-SG was analyzed as follows: m.p. 160-165°C; ESI-MS (MH^+= 464; MS/MS= 335; MS^3 of 335= 302, 190, 188, 156); one single spot on TLC (R_f = 0.42 on SiO_2 plates eluting with propanol/10% ammonium hydroxide 67:33; developed under iodine vapor); HPLC (t_R = 3.05 minutes using a mobile phase of methanol/water (70:30), at 1.0 mL/min, UV detection at λ= 215 nm, separated by a Phenomenex Bondclone C18, 10μ, 300x3.90 mm analytical column).

2.1.3 Synthesis of Arecaidine Propyl Ester

Arecaidine propyl ester (Fig. 1.5) was initially proposed as an internal standard for future experiments. Even though those experiments were not conducted, this synthesis was useful as a practice method for the synthesis of AEME from cocaine. Here, the brief details of this synthesis follow. Arecoline HBr was converted to its free-base (588 mg, 3.79 mmole), dissolved in 20 mL of 6M HCl solution and refluxed at 110°C for 17 hours. Following refluxing, the mixture was evaporated to dryness as a white powder and precipitated from a combination of 80% ethanol and diethyl ether. The precipitate was stored at 0°C overnight,

vacuum filtered and dried further under vacuum to a fine, white powder. Arecaidine (1.7 mmole) was dissolved in 20 mL 1-propanol and 0.4 mL concentrated HCl and refluxed overnight. The resultant solution was cooled to room temperature, evaporated under vacuum to a yellowish, gummy oil and dried further in a dessicator: yield= 94%; m.p. 129-131°C; ESI-MS (MH^+= 142; MS/MS= 123, 105, 96); one single spot on TLC (R_f= 0.800 eluting on silica plates using a solvent system consisting of chloroform:methanol:ammonium hydroxide, 80:18:2).

2.1.4 Synthesis of 4-(Glutathion-*S*-yl)Arecaidine Propyl Ester

Briefly, arecaidine propyl ester HCl (10 mg, 54.6 μmole) and reduced glutathione (34 mg, 110 μmole) were dissolved in 1 mL ammonium acetate buffer (0.1 M, pH= 7.4) and stirred under N_2 at room temperature for 3 hours. The resultant mixture was evaporated *in vacuo* overnight, precipitated in warm 1-propanol and further cooled at 0°C overnight. The product was analyzed by ESI-MS (MH^+= 492; MS/MS= 363; MS^3 of 363= 184, 216, 303).

2.2.1 Synthesis of Anhydroecgonine Methyl Ester (AEME)

AE and AEME were synthesized by a modification of several literature methods (111-113).

Anhydroecgonine (AE): 670 mg cocaine HCl (1.97 mmol) was dissolved in 15 mL concentrated HCl and refluxed under N_2 at 110°C for 24 hours. After cooling, the aqueous solution was extracted thrice with ethyl ether (30 mL) to remove benzoic acid. The resulting aqueous layer was evaporated *in vacuo* and the resultant residue was dried by azeotroping with toluene (30 mL). A mixture (60:40) of anhydroecgonine hydrochloride was obtained by

precipitation of the residue from an acetone/water mixture. Product (1.0 g, 5.3 mmole) had m.p. 235-240°C (lit.[114] m.p. 239-243°C); ESI-MS (MH^+= 168; MS/MS= 150, 137, 122, 93, 82); and ^{1}H NMR (DMSO-d_6): δ 4.32 ppm, 4.38 ppm (H-1); 6.78, 6.88 (H-3); 3.00, 2.8 (H-4_{axial}); 2.39 (H-4_{eq}); 3.95, 4.07 (H-5); 1.79, 2.24 (H-6_{axial}); 2.30, 2.26 (H-6_{eq}); 2.34, 2.36 (H-7_{axial}); 2.0, 2.04 (H-7_{eq}); 2.73, 2.65 (N-CH_3).

Anhydroecgonine Methyl Ester (AEME): AE HCl (889 mg, 4.37 mmole) was dissolved in 13 mL methanol and 0.05 mL of sulfuric acid and refluxed under N_2 for 22 hours. Upon cooling, the organic layer was evaporated *in vacuo*, dissolved in 20 mL distilled H_2O and alkalinized to pH 9.6 with several drops of concentrated NH_4OH. The basic, aqueous layer was extracted several times with methylene chloride (35 mL), and then the organic layers were collected, dried over sodium sulfate, vacuum filtered, and evaporated *in vacuo*. A crop of impure AEME free-base (209 mg, 1.15 mmole) was combined with fumaric acid (67 mg, 0.58 mmole) and dissolved in 1 mL boiling methanol. The solution was allowed to boil for several minutes, cooled slightly in an ice bath and precipitated by the dropwise addition of ethyl ether (15 mL) to form a white precipitate, which was cooled overnight at 5°C. After decantion of the ether layer, the precipitate was washed with cold acetone (30 mL), re-dissolved in boiling methanol, vacuum filtered through a 0.45 μm filter and evaporated to dryness. AEME fumarate (133 mg, 0.45 mmole) was analyzed by the following: m.p. 175-177°C (lit.[115] m.p. 178-180°C); one single spot on TLC (R_f= 0.375 eluting on silica plates with glass backing, solvent system consisted of 2-propanol:10% NH_4OH, 67:33); ESI-MS (MH^+= 182, MS/MS= 168, 164, 151, 150, 122, 118, 107, 105, 91, 82); ^{1}H NMR (DMSO-d_6): δ 3.87 ppm (H-1); 6.80 (H-3); 2.01, 2.65 (H-$4_{ax\ \&\ eq}$); 3.41 (H-5); 1.56, 2.12 (H-6); 1.80, 2.12 (H-7); 2.37 (N-CH_3); 3.68 (O-CH_3);

6.56 (fumarate H's); ^{13}C NMR (DMSO-d_6): δ 58.2 ppm (C-1); 132 (C-2); 136.3 (C-3); 31.2 (C-4); 56.9 (C-5); 28.7 (C-6); 33.2 (C-7); 35.5 (N-CH_3); 51.6 (O-CH_3); 166.8 (C=O). Proton and carbon shift assignments were assisted by one-dimensional (^{1}H, ^{13}C) and two-dimensional (COSY, HETCOR) experiments, and previously reported ^{1}H and ^{13}C NMR spectra of AEME (62,111).

2.2.2 Synthesis of 3-(*N*-Acetylcystein-*S*-yl)Anhydroecgonine Methyl Ester

AEME (250 mg, 1.38 mmole), prepared in the previous section (2.2.1), was combined with *N*-acetylcysteine (324 mg, 2.00 mmole) in 20 mL ammonium acetate buffer (0.01M, pH 7.8) and stirred under N_2 in an ice bath for 24 hours. After evaporation under reduced pressure, the solution was washed with cold acetone (10 mL) and further dried under vacuum. The residue was alkalinized and extracted several times with methylene chloride to remove free AEME. AEME-NAC was purified by preparative HPLC, using a Econosphere C18, 10μ (250mm X 10mm) preparatory column (Alltech; Deerfield, IL), flow rate of 2.5 mL/min, UV detection at 220 nm, and a mobile phase consisting of acetonitrile:water (50:50) with the pH adjusted to 7.38 with a mixture of ammonium hydroxide/acetic acid. Fractions collected from the LC peak eluting at 5 minutes were stored in 0.1% formic acid to increase stability. Product was analyzed by several methods, including HPLC (t_R = 5.0 minutes); ESI-MS (MH^+= 345; MS/MS= 327, 313, 216, 182; MS^3 of 216= 182); and ^{1}H NMR (D_2O): δ 4.15, 4.28 (H-1); 3.40, 3.73 (H-2); 3.56, 3.60 (H-3); 2.59, 2.62 (H-4); 3.96, 4.03 (H-5); 2.20-2.60 (H-6); 2.20-2.60 (H-7); 2.84, 2.86 (N-CH_3); 3.80, 3.84 (O-CH_3); 3.00 & 3.16, 3.04 & 3.21 (β-CH_2); 4.35, 4.47 (α-CH); 2.08 (acetyl methyl).

A detailed NMR analysis of this compound included one-dimensional (^{1}H, ^{13}C, cycleNOE) and two-dimensional (COSY, HETCOR) experiments. The ^{1}H NMR of authentic *N*-acetylcysteine and cocaine HCl assisted in the proton assignments above, and are reported here:

***N*-Acetylcysteine:** ^{1}H NMR (DMSO-d_6): δ 1.85 ppm (CH_3); 2.40 (SH); 2.71, 2.81 (β-CH_2); 4.35 (α-CH); 8.15 (NH).

Cocaine HCl: ^{1}H NMR (DMSO-d_6/ $CDCl_3$): δ 4.25 (H-1); 3.53 (H-2); 5.48 (H-3); 2.3, 2.40 (H-4); 3.96 (H-5); 2.1, 2.3 (H-6); 2.13, 2.42 (H-7); 2.82 (N-CH_3); 3.63 (O-CH_3); 7.87 (C_6H_5-H_a); 7.63 (C_6H_5-H_b); 7.49 (C_6H_5-H_c). ^{13}C NMR (DMSO-d_6/ $CDCl_3$); δ 62.8 ppm (C-1); 47.8 (C-2); 63.7 (C-3); 32.3 (C-4); 62.4 (C-5); 22.2 (C-6); 23.8 (C-7); 38.8 (N-CH_3); 52.2 (O-CH_3); 129 (C_6H_5-C_a); 128.3 (C_6H_5-C_b); 133.2 (C_6H_5-C_c). Carbon shift assignments were also assisted by a one-dimensional DEPT experiment (spectrum not shown) and previous NMR data on cocaine and isomers reported by Carroll and co-workers (116).

2.2.3 Synthesis of 3-(Glutathion-*S*-yl)Anhydroecgonine Methyl Ester

AEME free-base (10 mg, 0.055 mmole) was mixed with GSH (24 mg, 0.078 mmole) in 2 mL of ammonium acetate buffer (0.063 M, pH= 7.8) and stirred under N_2 for 19 hours. The mixture was evaporated to dryness, the residue was dissolved in methanol (1 mg/mL) and a 5 µL aliquot was injected onto a HPLC system (Waters) with the following conditions: flow rate= 1.0 mL/min; UV detection at 220 nm; column= Zorbax SB-C8, 5µ (4.6mm X 250 mm) analytical column (Agilent; Palo Alto, CA). A chromatographic peak at 2.50 minutes was collected and directly injected onto the ESI-MS: MH^{+}=489; MS/MS= 360, 182; MS^{3} of 360 = 182.

2.2.4 Synthesis of 3-(Glutathion-*S*-yl)Anhydroecgonine

AE HCl (0.50 μmole in methanol) was combined with reduced glutathione (0.25 μmole) and ammonium acetate buffer (0.1 M, pH= 7.4) to a final volume of 1.0 mL. This mixture was stirred under N_2 for 4 hours at room temperature and dried under vacuum to a gummy residue. An aliquot (10 μg/mL in methanol) of the residue was injected directly onto an ion trap ESI-MS: MH^+= 475; MS/MS= 346, 290, 168; MS^3 of 168= 150, 137, 122, 119, 93, 91, 82.

2.2.5 Synthesis of Anhydroecgonine Ethyl Ester (AEEE, EEG, ethylecgonidine)

Anhydroecgonine (AE) was synthesized from cocaine HCl as previously described. AE HCl (139 mg, 0.68 mmole) was dissolved in 10 mL absolute ethanol, 5 mL benzene and 0.75 mL H_2SO_4. The mixture was refluxed for three hours and cooled, following which 10 mL of absolute ethanol were added, and the mixture was refluxed for an additional 2 hours. Upon cooling, the organic layer was evaporated *in vacuo*, the residue was dissolved in 8 mL distilled H_2O and alkalinized with several drops of concentrated NH_4OH to about pH 10. The basic, aqueous layer was extracted several times with methylene chloride (30 mL), and then the combined organic layers were dried over sodium sulfate, vacuum filtered and evaporated *in vacuo* overnight. AEEE free-base (54 mg, 0.28 mmole) was combined with fumaric acid (0.28 mmole) and dissolved in 1 mL of hot ethanol. The solution was cooled to room temperature, precipitated slowly by the dropwise addition of ethyl ether (5 mL), cooled overnight at 0°C, vacuum filtered and evaporated *in vacuo* to give AEEE fumarate (81.2 mg, 0.26 mmole): m.p 138-141°C (lit.[115] m.p. 144-146°C); GC-MS (**195**, 166, 138, 122, 94, 82); ESI-MS (MH^+= 196; MS/MS= 168, 150, 122, 108, 91; MS^3 of 150= 132, 122, 109, 96, 93, 82); ^1H NMR

(DMSO-d_6): δ 3.84 ppm (H-1); 6.78 (H-3); 2.0, 2.65 (H-4); 3.39 (H-5); 1.54, 2.10 (H-6); 1.78, 2.10 (H-7); 4.13 (O-$\mathbf{CH_2}CH_3$); 1.22 (O-$CH_2\mathbf{CH_3}$); 2.36 (N-CH_3).

Proton chemical shift assignments were greatly assisted by the previously reported detailed NMR analysis of the related congener, AEME. A small sample of AEEE fumarate (20 mg) was shipped to the OCME of WV to serve as a reference standard in the identification of this potential transesterification product in the urine of known crack cocaine/ethanol users.

2.3 Synthesis of the EA-SG Conjugate

The synthesis of the ethacrynic acid-SG (EA-SG) adduct was altered from a literature synthesis (80). EA (100 mg, 0.33 mmole) and GSH (100 mg, 0.33 mmole) were dissolved in 15 mL of a 50:50 mixture of absolute ethanol:water (solution was initially sparged by bubbling N_2 through the solution for 15 minutes). Next, approximately 12 drops from a saturated solution of sodium bicarbonate (pH 8.1) were added to the solution and the reaction was stirred under N_2 at room temperature for 72 hours. Upon reacting, the solution was evaporated *in vacuo* to a yellowish colored residue, dissolved in 2 mL of saturated $NaHCO_3$ solution, and precipitated by the drop wise addition of 1% H_3PO_4 until persistent cloudiness. Precipitate growth was maximized by storing at 0°C overnight. Next, the aqueous layer was decanted, and then the filtrate was washed with cold methylene chloride (45 mL). The filtrate was dissolved in warm methanol, vacuum filtered through a 0.45 μm filter, and evaporated *in vacuo* to obtain to obtain EA-SG (371 mg, 0.61 mmole). EA-SG was analyzed by LC followed by direct injection ESI-MS analysis as follows: HPLC conditions: UV=220 nm; flow rate= 1.0 mL/min; analytical column= Zorbax ODS, 5μ, 4.6 X 150mm; mobile phase contained methanol:water (40:60). A small aliquot (0.5 mg/mL in methanol:water, 50:50) was injected

(10.0 μL) onto the HPLC and a chromatographic peak at 2.5 minutes was collected and directly injected onto the ion trap: yield= 54%; m.p. 123°-125°C ; ESI-MS: MH^+= 610; MS/MS=535, 481, 463, 335; NMR (CD_3OD): δ 7.09 ppm (H-4); 7.58 (H-5); 3.21 (H-9); 1.32 (H-10); 1.61, 1.79 (H-11); 0.910 (H-12); 5.00 (H-14); 4.58 (Cys_α C-H); 2.79, 3.00 (Cys_β CH_2); 3.93 (Gly_α CH_2); 2.60 (Glu_γ CH_2); 2.18, 2.25 (Glu_β CH_2); 4.08 (Glu_α CH).

The ^1H NMR (D_2O) of commercially available reduced glutathione, which assisted in the proton assignments of EA-SG, is reported here:

GSH: δ 2.20 (Glu β-CH_2); 2.59 (Glu γ-CH_2); 2.97 (Cys β-CH_2); 3.86 (Glu α-CH); 4.0 (Gly α-CH_2); 4.59 (Cys α-CH).

2.4 Reaction of GSH with Michael Acceptor Compounds

Glutathione depletion over time was monitored by Ellman's method (117). Ethacrynic acid (10 mM), arecoline (10 mM), AEME (10 mM) or acetaminophen (10 mM) were combined with reduced GSH (10 mM) and stirred under N_2 at room temperature for 4 hours. Prior to reaction, the GSH solution was sparged under a strong stream of N_2 to retard oxidation to the disulfide, GSSG. In order to quantify the relative amount of GSH in solution over time, a small aliquot (20 μL) of solution was transferred into a 1.5 mL UV cuvette, then an excess of Ellman's Reagent (40 μL) and phosphate buffer (940 μL; pH 7.4; 100 mM) were added, and the absorbance at 412 nm was measured for three consecutive readings. Mean absorbance measurements at each time point were converted to GSH concentrations by calculation from a seven point standard curve (r^2= 1.0), computed from a regression analysis (Sigma Plot 2001, version 7.0) on a range of GSH concentrations from 0.008 mM to 0.5 mM. Second order decay curves plotted for GSH concentrations versus time (2 to 240 minutes) for each

compound (Enzyme Kinetics, Sigma Plot) were acquired. In addition, the relative 2nd order rate constants (k_1) were derived from the slope of the line plotting GSH^{-1} versus time for ethacrynic acid, arecoline, AEME and acetaminophen. The approximate half-life was calculated using the following equation:

$$t_{1/2} = [k \cdot C_0]^{-1}, \text{ where } k = \text{slope and } C_0 = [GSH]_{initial}$$

2.5 Chemical Formation of the DCNB-SG Conjugate

The formation of the 3,4-dichloronitrobenzene-SG adduct (DCNB + GSH → DCNB-SG) was monitored separately in the presence of AEME (10 mM), arecoline (10 mM) or EA (10 mM). AEME free-base, arecoline free-base and EA were dissolved in DMSO; DCNB was dissolved in a mixture of methanol:water (70:30); and GSH was dissolved in THAM® buffer (0.1 M, pH 7.4). Control solutions contained an equal amount of DMSO (181 μL) alone. In a UV cuvette, DCNB (7 mM), GSH (3 mM) and reactive compounds (or DMSO alone) were briefly mixed by inversion, and the absorbance was measured at 345 nm every minute for 20 minutes. A background UV recording was performed on all compounds mixed briefly in the cuvette and used as the zero time point reading. Mean absorbance recordings over 20 minutes (n=3) were plotted versus time and the corresponding line plots were generated by SigmaPlot 2001. Statistical analyses comparing the mean absorbance recordings versus control at 20 minutes alone were performed with a one-tailed, student's *t*-test.

2.6 Degradation of Selected Glutathione Conjugates in Solution

Chemically synthesized arecoline-SG and AEME-SG were monitored for the retro-Michael release of GSH into solution by a modification of Ellman's method (117). Solutions

of AEME-SG (1 mg/mL), arecoline-SG (1 mg/mL) or glutathione (1 mg/mL) were prepared in THAM® buffer (0.1 M, pH= 7.4) to a total volume of 5 mL. Reactions were stirred at 25°C under a gentle stream of N_2. Small aliquots (20 μL) were carefully withdrawn from solution at designated time intervals and reacted with Ellman's reagent, as described above (section 2.4), to obtain absorbance readings at 412 nm. Complete time trials (2 to 240 minutes), performed on each compound, were repeated three times and the mean absorbance for each time interval was calculated.

To confirm the presence of conjugates in solution, small aliquots (20 μg/mL) of solution at approximately 5 minutes and 24 hours were directly injected onto the ESI-MS and monitored for the presence of adduct ions and original reactant ions. Line plots depicting GSH concentrations versus time were generated for arecoline-SG and AEME-SG. Kinetic constants describing the relative rate of degradation, calculated from the data, were consistent with a first-order rate of degradation.

2.7 EA plus GSH in Human Liver Cytosol

A method to measure GSH conjugate formation and substrate depletion by cytosolic GST's contained within human liver cytosol was derived from the following experimentation with the known GST substrate, EA. First, a standard curve for detecting EA on HPLC was generated. HPLC conditions: UV detection (λ= 220 nm); Zorbax SB-C8 analytical column (4.6x150mm, 5μ); flow= 0.5 mL/min; mobile phase consisting of methanol:water (40:60); k' = 5.0 minutes. A six point linear standard curve was generated (r^2= 1.0) for EA from 0.69 mg/mL to 0.02 mg/mL injected onto column (5 μL). EA (1 mM or 0.5 mm in methylene chloride) was combined with GSH (2 mM in buffer), pooled human liver cytosol (1 mg) and

ammonium acetate buffer (total solution volume= 1 mL). Control solutions omitted EA, GSH or cytosol. Total amount of methylene chloride was maintained at < 2% total organic volume. Vials containing cytosol were pre-incubated for 5 minutes at 37°C and the reaction was initiated by the addition of EA. Total incubation time was 4 minutes, following which the enzyme was quenched by the addition of ice cold methanol (100 μL). Next, vials were centrifuged at 10,000 rpm for 5 minutes (Eppendorf Mini Spin; Westbury, NY), and a small aliquot (5 μL) was injected onto the HPLC. The area under the curve (AUC) for the EA UV peak was calculated (Millenium[32], version 3.05.01) for each vial and quantified by regression analysis.

2.8 Standard Curve of AEME on HPLC

AEME was evaluated on HPLC with the following conditions: Zorbax SB-Phenyl reversed phase column (4.6 X 150mm, 5 μm); mobile phase consisting of acetonitrile:phosphate buffer (10 mM, pH 7.5) run at an isocratic ratio of 70:30; flow rate = 0.5 mL/min; λ= 220 nm. AEME concentrations ranging from 0.62 mg/mL to 0.019 mg/mL were injected (5 μL) onto column, and the area under the UV peak eluting at 10.7 minutes was computed by Millenium software. The mean AUC (n=3) was plotted versus AEME concentration to generate a six point best-fit regression line by Sigma Plot (r^2= 0.998). The equation describing the line was used to calculate relative AEME concentrations in incubations described next.

2.9 AEME plus GSH with Human Liver Cytosol

AEME (0.1 mM in 100% methanol), GSH (5 mM) and human liver cytosol (1 mg) were combined with phosphate buffer (pH 7.4) to a final volume of 1 mL. Control solutions omitted AEME, GSH or cytosol. Total [methanol] was 1.6% for each vial. All samples were pre-incubated at 37°C for 4 minutes. AEME was added in the final step and then the solutions were incubated at 37°C for one hour. Following which, solutions were quenched by the addition of ice cold acetonitile/1% formic acid and centrifuged at 10,000 rpm for 5 minutes to separate the cytosol from solution. Small aliquots of the supernatant in each reaction vial were injected separately onto the HPLC (conditions described in section 2.7) and analyzed for the presence of AEME that elutes at 11 minutes. Mean $AEME_{AUC}$ for each vial were tested for significance using a one-tailed Student's *t*-test.

A second set of incubations were conducted to evaluate the effect, if any, of varying pH levels on AEME-SG formation in the presence of soluble GST's. AEME (0.5 mM, 0.25 mM or 0.125 mM in DMSO), reduced GSH (1 mM) and human liver cytosol (1 mg) were combined with phosphate buffer (0.1 M; pH 6.5, 7.4 or 8.5) and incubated at 37°C for 60 minutes. Control solutions contained either boiled cytosol or omitted AEME or GSH. Total [DMSO] was 2.5% for each vial.

Following the incubation, vials were quenched with the addition (50 µL) of ice cold acetonitrile/0.1% formic acid, spiked with internal standard (cocaine HCl, 0.5 µg), and centrifuged for 8 minutes at 10,000 rpm. A small aliquot (10 µL) was injected onto an LC-MS system containing a SB-phenyl (Zorbax) analytical column and a solvent system of acetonitrile:ammonium acetate (10 mM, pH 6.8) in a ratio of 70:30 flowing at 0.5 mL/min.

Monitoring in the positive ion mode, the presence of AEME-SG (MH^+ 489), AEME (MH^+ 182), AE (MH^+ 168), GSH (MH^+ 308) and cocaine (MH^+ 304) were detected for each vial.

2.10 GST Activity after Exposure to AEME, Arecoline or EA

AEME (10 mM), arecoline (10 mM) or EA (5 mM) were separately combined with 50 μL (1 mg) of pooled human liver cytosol and incubated at 37°C for 20 hours. The GST activity of a 2 μL HLC sample was measured initially before drug exposure and after a 20 hour incubation at 37°C by a modification of the method described by Habig and co-workers (118). Briefly, DCNB (15 mM, 80 μL) and THAM buffer (100 mM, pH 7.42, 10 mL) were combined and pre-warmed at 37°C for five minutes. Reaction mixture (990 μL) was combined with 10 μL GSH solution (5 mM in distilled H_2O) and 2 μL HLC in a UV cuvette, covered with parafilm, then mixed by inversion for 20 seconds. A UV reading at 345 nm (published UV maximum of the DCNB-SG conjugate) was recorded every 15 seconds for one minute and a rate was calculated by the UV software (Beckman DU 640 spectrophotometer). Absorbance readings acquired at 20 hours were subtracted from both the initial readings (t= 0) and non-enzymatic chemical rate (blank). Mean absorbance (n=4) measurements were converted to relative activity (velocity), and compared to control enzyme solutions void of any drug using a one-tailed Student's t-test and F-distribution analysis (ANOVA). Blank solutions contained no cytosol, while control solutions contained cytosol with equivalent amounts of solvent (3.0 μL of 50% methanol) used to add the electrophilic compounds.

2.11 Enzymatic Conversion of CDNB to CDNB-SG

Enzymatic activities of cytosolic GST's towards CDNB, forming *S*-(2-chloro-4-nitrophenyl)-glutathione (CDNB-SG) adduct in the presence of reduced GSH, was assayed spectrophotometrically according to Habig *et al.* (118). Briefly, a reaction mixture containing THAM® buffer (0.1 M, pH 7.4) and CDNB (5 μM to 2560 μM in 100% methanol) were warmed to 37°C. Reaction mixture (972 μL), 50% methanol (18 μL), GSH (1 mM in THAM®) and single donor human liver cytosol (4 μL; 0.08 mg protein/mL) were added to a UV cuvette, mixed briefly by inversion, and then placed into the spectrophotometer to measure the absorbance at 340 nm continuously for 20 seconds. Following the short incubation, a relative rate (dA/min) was computed by the UV spectrophotometer software, and an apparent velocity (nmole product/mg/min) was calculated according to the following equation:

$$\text{mean rate} / [(\text{volume of sample}) \times (\text{protein concentration}) \times (0.0096 \text{ A/nmole})]$$

A blank UV recording performed prior to each analysis included all reaction components except GSH. Trials for 20 seconds were repeated for at least six separate experiments for each CDNB concentration point. Total methanol concentration was maintained at less than 5.0%, and was the same concentration for all incubation vials. The non-enzymatic conjugation rate was also evaluated in a similar fashion, excluding cytosol. Average non-enzymatic rates were subtracted from the apparent mean enzymatic rates to obtain a truer rate estimate, which was used to calculate velocity (above equation) and further evaluated in a non Michaelis-Menten model and Eadie-Hofstee plot (Sigma Plot 8.0). The

[CDNB] utilized in these plots was adjusted for a slight dilution, and corrected values varied by less than 10% from initial calculations (4.84 μM to 2358 μM).

2.12 Inhibition of Cytosolic GST Activity by AEME

The enzymatic inhibition of CDNB-SG adduct formation in single donor human liver cytosol by the presence of AEME (0, 50, 125, and 320 μM) was evaluated. Incubation conditions were adjusted from the above method (section 2.11). In brief, incubations included reaction mixture (972 μL) containing CDNB (5 μM to 80 μM), AEME (0 μM to 320 μM in 50 % methanol), GSH (1 mM) and cytosol (0.08 mg/mL). Components were combined as described above to obtain an apparent rate over 20 seconds ($n \geq 6$). The non-enzymatic rate (excluding cytosol) was subtracted from the enzymatic rate to obtain an apparent velocity calculation. Mean velocity calculations for AEME and CDNB concentrations were analyzed on a Lineweaver-Burk plot and Dixon plot, fitting the data to a non-linear regression model (Enzyme Kinetics Module, version 1.1.1).

2.13.1 Solid Phase Extraction of Cocaine and Metabolites from Urine

The solid phase extraction (SPE) method for analyzing cocaine and metabolites in urine was modified from a literature procedure (36). One mL of blank urine was spiked with known, varied concentrations of AEME, AEEE, AEME-NAC or cocaine. Urine from multiple drug overdose victims (obtained from the OCME of WV) was extracted under similar experimental conditions. Varian Bond Elut Certify (130 mg/3 mL) cartridges containing a mixed mode sorbent with non-polar and cation exchange mechanisms were used. Each SPE utilized an individual cartridge. Extraction cartridges were subjected to reduced pressure (to facilitate

solvent flow) on a PrepTorr (Fisher Scientific) vacuum manifold connected to a water aspirator.

Extraction was initiated by preconditioning the cartridge with 2 mL of acetonitrile (or methanol) at a flow rate under vacuum (8 kPa) of 0.75 mL/minute, followed by 3 mL of potassium phosphate buffer (0.1M, pH= 6.0). Next, a well mixed, pre-prepared solution (5 mL) consisting of 1 mL thawed urine diluted in 4 mL phosphate buffer, was loaded onto the extraction cartridge. The cartridge was rinsed with 2 mL acetic acid solution (0.1M) followed by 3 mL of acetonitrile (or methanol), and the sorbent was dried under vacuum for one minute. The basic analytes were eluted with 6 mL of elution solvent consisting of a freshly prepared mixture of methylene chloride:2-propanol:22% ammonium hydroxide (78:20:2). Elution solvent washed through the column was initially collected in 1.5 mL centrifuge tubes, then transferred to a small round bottom flask (10 mL), evaporated *in vacuo* at room temperature using a rotavapor apparatus, and further dried in a vacuum dessicator. The small residue was carefully reconstituted in appropriate solvent and subjected to analysis via GC-MS, LC-MS, LC-MS/MS or direct inject ESI-MS.

The limit of detection of AEME-NAC on LC-MS or LC-MS/MS was obtained by injecting a diluted series of known concentrations of confirmed AEME-NAC until detection was not observed, and then repeated for verification.

2.13.2 Standard Curve of AEEE on GC-MS and LC-MS

A five point linear standard curve (r^2= 0.996) was generated on GC-MS by injecting authentic AEEE (in ethanol) in a concentration range of 0.4 to 6.3 μg/mL (t_R = 4.7 minutes). On the LC-MS (Waters, Micromass) system a six point linear standard curve (r^2= 0.999) was

created for AEEE in a range of 0.6 ng to 19 ng injected onto column (t_R = 6.8 minutes). For GC-MS, the abundance of ions 195 and 166 were monitored and quantified by HP software, and a linear regression line was computed (Sigma Plot 2001). For LC-MS, the ion peak corresponding to MH^+ 196 was integrated by MassLynx 3.5 software (Waters) and the resulting peak areas were quantified linearly by regression analysis (Sigma Plot 2001).

2.13.3 Analysis of Urine from a Known Free-base Cocaine/Ethanol Abuser

The case history for a drug overdose victim was obtained from James C. Kraner, Ph.D., Toxicologist at the Office of the Chief Medical Examiner in Charleston, WV.

Case History: The decedent, a 41 year old white male weighing 178 lbs. and standing 6'0" tall, was found dead, collapsed outside his vehicle one morning. His wife stated that he had left home after an argument at approximately 2330 hours. A friend reported that the decedent had been out drinking the previous night. The decedent's wife stated that he had a history of alcohol and illicit drug use but that he had been "clean" for the past 6-7 weeks.

Preliminary toxicological evaluation of the victim performed at the OCME is as follows. The body was brought to the state medical examiner's office and a complete autopsy was performed. Blood alcohol concentrations were determined by direct injection GC-FID analysis using *t*-butanol as an internal standard. Urine was screened for drugs of abuse and tricyclic antidepressants by enzyme mediated immunoassay (EMIT) using a Roche Cobas Mira with kits purchased from Dade Behring (Cupertino, CA). Urine was also screened for basic drugs using the Toxi-Lab A extraction system (Varian Inc.; Walnut Creek, CA) with Proadifen (SKF-525A) added as an internal standard. After a 20 minute period in which the sample was inverted then centrifuged, the organic layer was evaporated to dryness and reconstituted with

75 μL of ethyl acetate. One microliter was injected onto an Agilent 6980/5973 GC-MS and analyzed in full scan mode. Peak identification was accomplished by comparison to a house mass spectral library, the AAFS drug library and the National Institute of Standards and Technology (NIST) 2002 library. Confirmation and quantitation was by GC-MS. Oxycodone was present in the subclavian blood at 4.40 mg/L and methadone at 0.25 mg/L. Cocaine was confirmed at < 0.05 mg/L, benzoylecgonine at 0.18 mg/L and ethanol at 0.10%. Other compounds identified in the urine but not quantified include AEME, AEEE, cotinine, and two methadone metabolites, EDDP (2-ethylidene-1,5-dimethyl-3,3-diphenylpyrrolidine) and EMDP (2-ethyl-5-methyl-3,3-diphenylpyrroline). Cause of death was combined oxycodone, methadone, cocaine and alcohol intoxication. The manner of death was accidental.

In our laboratories, 1 mL of urine from this victim was subjected to SPE as described above, and peaks (or known fragments) corresponding to AEEE were compared to authentic, synthesized standard, quantified on GC-MS and LC-MS, and identified by LC-MS/MS.

2.14.1 Lung A549 Cells Exposed to AEME, AEEE, and AE

A549 lung fibroblast cells were seeded in 24-well plates (3.75×10^5 cells/well) and incubated at 37°C with 5% CO_2 for 48 hours until roughly 80% confluence was observed microscopically. Cells were washed with 1 mL of Hank's balanced salt solution, then 1 mL of HyQ Ham's/F-12 media was added to each well. Confirmed AEME fumarate (1 mM, 0.5 mM and 0.25 mM in DMSO), AE HCl (1 mM in DMSO), and AEEE fumarate (1 mM in DMSO) were added to cells in triplicate. Control wells (also created in triplicate) included 0.10% ethyl alcohol, 18 μL DMSO (2%), or nil. Cells were incubated at 37°C with 5% CO_2 for 24 hours. Following incubation, media was removed and the cells were trypsinized by the addition of

500 μL trypsin/0.25% EDTA. Upon another short incubation, 10 μL of cell solution were combined with 99 μL trypan blue (0.4%) in a 96 well culture tissue plate. Five μL of the resulting mixture were pipetted onto the hemacytometer and the percent cell viability was calculated, as observed under microscope for 5 separate grids, using the following equation:

$$\% \text{ cell viability} = \# \text{ viable cells per grid} / \# \text{ total cells per grid} \times 100\%$$

Viable cells were counted as such if they displayed no staining, whereas dead cells exhibited uptake of the trypan blue dye, which readily permeates damaged or destroyed cellular membranes. The calculated mean percent viability for each compound was compared to control cells only spiked with DMSO. Significant variability in cell viability was tested by the student's *t*-test, using a one-tailed test.

2.14.2 A549 Cell Cytotoxicity Observed by Flow Cytometry

Lung A549 fibroblast cells were prepared as described above (section 2.12.1). Following incubation for 48 hours, confluent cells were separately spiked (in duplicate) with the following compounds: 20% ethyl alcohol, DMSO, DMSO + distilled water, NAC (5 mM in distilled water), styrene oxide (1 mM in DMSO), AEME fumarate (1 mM, 0.5 mM or 0.25 mM in DMSO), AE HCl (1 mM in DMSO), AEEE fumarate (1 mM in DMSO), cocaine HCl (1 mM in DMSO), AEME (1 mM, 0.5 mM or 0.25 mM) plus NAC (5 mM), AE (1 mM) plus NAC, AEEE (1 mM) plus NAC, styrene oxide (1 mM) plus NAC. The final concentration of DMSO in each cell was 2 % (v/v) or less. Cells were then incubated for 24 hours at 37°C with 5% CO_2, following which, images where captured of each well for comparison. Media was

removed and set aside, and then the cells were trypsinized by the addition of trypsin with 0.5% EDTA. Saved media was centrifuged and the resulting pellet was combined with trypsinized cells to achieve a final cellular mixture. Solutions were spiked with 2 μL propidium iodide, transferred to a 10 mL test tube, and analyzed on a flow cytometer located in the WVU Core Facility. A region of increased fluorescence was indicative of cellular death and the percentage of dead cells was computed. Comparisons between compounds and control (DMSO alone) were evaluated using a one-tailed student's *t*-test.

Chapter 3: Results

3. Results

3.1 Synthesis of Arecoline Congeners

The ESI-MS, MS/MS and MS^3 spectra of the chemically synthesized arecoline-NAC adduct are presented below (Fig. 3.1). The full scan spectrum of arecoline-NAC (Fig. 3.1.A) shows a low intensity ion peak (MH^+ 156) corresponding to arecoline, suggesting that the final product was not pure. However, the ^1H NMR spectrum of arecoline-NAC (not shown) indicates pure product, as the vinylic proton (ca. 7.0 ppm) corresponding to arecoline alone was not observed. Therefore, it is likely that the electrospray analysis of arecoline-NAC facilitated some retrogression of the adduct to starting materials.

Propyl ester salts (hydrochloride and sulfate) of arecaidine were also synthesized and exhibited a slightly greater retention time on TLC analysis, as compared to arecoline, the methyl ester, and standard, arecaidine (R_f= 0.8, 0.78 and 0.0, respectively). The full ESI-MS scan of the chemically synthesized arecoline-SG conjugate showed the parent ion (MH^+ 464), Na^+ adduct (MH^+ 486) and a fragment (MH^+ 335), which represents the loss of a glutamic acid moiety (Fig. 3.2.1), a commonly seen fragment when analyzing glutathione adducts on ESI-MS. Interestingly, ESI-MS analysis (spectra not shown) of a small aliquot of the synthesized arecaidine propyl ester-SG adduct (10 μg/mL in methanol) showed two predominant ion peaks (MH^+ 492 and 464), representing the propyl ester and methyl ester adducts, respectively. Apparently, the ESI process, in the presence of an excess of methanol, catalyzed the propyl to methyl transesterification of the analyte.

3.2 Synthesis of AEME, AEEE and Derivatives

Starting with cocaine HCl, AE HCl, then AEME fumarate was synthesized and the NMR spectra are reported for AE and AEME (Fig 3.3, 3.4.1 and 3.4.2). AEME-NAC was synthesized from AEME, and the proton assignments, as well as stereochemical assignments about C-2 and C-3 were elucidated (Fig 3.2.2 and 3.5). The ESI-MS spectra of AEME-NAC and AEME-SG are reported below (Fig 3.6 and 3.7, respectively), providing additional structural evidence of each compound. The specific mass fragmentation patterns of AEME-NAC are included in Fig 3.2.1.

^{1}H and COSY spectra (Fig 3.5) of AEME-NAC present fairly equally intensive peaks for most of the protons (53:47). The stereochemistry of AEME-NAC was evaluated using the one-dimensional cycleNOE experiment. Parameters for this experiment were optimized on two individual reference solutions, dimethyl acrylic acid (10 mg in DMSO-d_6) and camphor (15 mg in DMSO-d_6). Saturation of the H-2 peak on AEME-NAC (3.4 ppm) resulted in NOE effects of H-1 (4.28 ppm), H-3 (3.6 ppm) and H-4 (2.6 ppm). Saturation of the other peak corresponding to H-2 (3.37 ppm) resulted in only one NOE effect of H-1 (4.17 ppm). These findings are consistent with the epimers drawn below (Fig 3.2.2).

AE-SG was also synthesized and the adduct ion of MH^+ 475 (MS/MS: 346, 308, 168) was detected by ESI-MS (spectrum not shown). The relative amount of AE-SG formed was less than the amount of glutathione adducts formed by using similar synthetic procedures with arecoline, AEME and ethacrynic acid. The ethyl transesterification product of AEME in the presence of ethanol, AEEE, was also synthesized. A ^{1}H NMR spectrum of AEEE fumarate is included below (Fig 3.8).

3.3 Synthesis of the EA-SG Conjugate

EA-SG phosphate, a potent inhibitor of cytosolic GST's, was chemically synthesized. An ESI-MS scan of the LC-collected product detected an adduct ion, MH^+ 610, and adduct ion fragments on MS/MS: MH^+ 481 and 335 (spectra not shown). NMR spectra of the adduct is shown below (Fig 3.9). Our NMR spectra shows evidence of two diastereoisomers, and our proton assignments are consistent with those reported in the literature (109).

3.4 GSH Depletion by Michael Acceptor Compounds

The relative rate of glutathione depletion over time in the presence of reactive compounds was assessed by Ellman's method (117). Glutathione concentration versus time was charted for each compound (arecoline, ethacrynic acid, acetaminophen and AEME) and included below (Fig 3.10, 3.11). The control reaction included acetaminophen (10 mM), which has no appreciable reactivity with GSH. Calculated GSH concentration values were the arithmetic mean of three separate experiments. Some additional graphs were created depicting GSH^{-1} concentration versus time and log [GSH] versus time. The log [GSH] versus time graphs (not shown) were not linear, suggesting that the reaction is not of the first order. Slopes ($mM^{-1}min^{-1}$), or second order rate constants (k_1), of the best-fit linear regression lines for each compound (Fig 3.12.1, 3.12.2) and calculated half-life values (min) are as follows: arecoline (2.2×10^{-1}, 14.7), ethacrynic acid (4.1×10^{-1}, 5.3), AEME (6.8×10^{-3}, 459), and acetaminophen (3.1×10^{-3}, 1001).

3.5 Chemical Formation of the DCNB-SG Adduct

The chemical formation of the DCNB-SG conjugate was monitored in the presence of EA (10 mM), arecoline (10 mM) or AEME (10 mM). Collected data points were plotted over time and included below for each compound beside control (Fig. 3.13, 3.14, and 3.15). EA ($p < 0.005$), arecoline ($p < 0.025$) and AEME ($p < 0.100$) exhibited a significantly reduced absorbance reading at 20 minutes compared to control. The AEME trial contained greater variance; therefore, it was found only significant at the 10% level, in spite of the pronounced reduction in conjugate formation over 20 minutes, as compared to arecoline.

3.6 Degradation of Selected Glutathione Conjugates in Solution

Synthetically prepared arecoline-SG and AEME-SG conjugates were dissolved in buffer at physiological pH and the approximate rate of glutathione release over time was measured using Ellman's reagent. The measured extent of glutathione appearance over time is charted below for both conjugates (Fig 3.16). The negative control, GSH alone (1 mg/mL) in buffer, exhibited no significant changes in concentration over time (data not shown). Assuming a first-order rate of degradation, the relative rate constants (k_{-1}) for arecoline-SG and AEME-SG decay were calculated from the slope of the regression line fitting log [GSH] versus time (2.1×10^{-5} and 3.9×10^{-4}, respectively). Although the calculated rate of degradation for AEME-SG was approximately 19-fold greater than arecoline-SG, the AEME-SG rate indicates only minimal reversion to the original reactants over 24 hours. The measured amount of GSH in AEME-SG solution after 4 hours was merely 0.005 mM, representing less than 1% degradation.

Direct injection ESI-MS was applied to detect adduct ions in the tested buffered solutions initially and 24 hours later. Chemical structures for arecoline-SG (MH^+ 463) and AEME-SG (MH^+ 489) were confirmed by MS/MS and MS^3 for each ion at 0 and 24 hours later, providing additional evidence of the stability for both conjugates at the tested pH and temperature.

3.7 EA + GSH in Human Liver Cytosol

HPLC with UV detection of EA (k'= 5.5 min) quantified the amount of EA in each reaction vial following a 4 minute incubation at 37°C. In one incubation set, reaction vials containing EA (0.5 mM), GSH (2 mM) and cytosol (1 mg) contained less EA than vials with EA and GSH only (0.28 μg and 0.97 μg, respectively). A summary of incubation conditions and results is contained within Tables 3.1.1 and 3.1.2, and a portion of representative chromatograms for the analysis of two different reaction vials from the same incubation is also included below (Fig. 3.17).

3.8 AEME + GSH in Human Liver Cytosol

The first set of incubations utilized HPLC with UV detection to identify and quantify AEME in each reaction vial following a 60 minute incubation at 37°C. Preparations containing AEME, GSH and HLC contained significantly less AEME (Fig. 3.18) than preparations lacking HLC ($p < 0.005$).

In the second array of incubations, LC-MS was employed for detection of AEME-SG formation at varying pH levels. At all tested AEME concentrations (0.5 mM, 0.25 mM and 0.125 mM) we found no appreciable difference between vials containing viable HLC versus

those with boiled cytosol. Similarly, adjusting the incubation buffer pH from 6.5, 7.4 or 8.5 did not significantly alter product formation between the two preparations.

3.9 GST Activity after Exposure to AEME, Arecoline or EA

HLC (40 μg) was incubated at 37°C with AEME (10 mM), arecoline (10 mM) or EA (5 mM) for 20 hours. Following which, the GST activity (pmole product/mg/min) was measured as the rate of formation of the conjugate, DCNB-SG, as measured by the increase in absorbance at 345 nm (Fig. 3.19). AEME and EA substantially reduced GST activity ($p < 0.005$) after 20 hours. Arecoline, however, displayed considerable variability in the reduction of GST activity and was not found to be statistically significant from cytosol control.

3.10 Enzymatic Conversion of CDNB to CDNB-SG

Single donor HLC (0.08 mg/mL) was briefly incubated over 20 seconds at 37°C in the presence of GSH (1 mM) and various concentrations of CDNB (5 μM to 2560 μM). CDNB concentration points versus mean apparent velocity (nmole product/mg protein/min), calculated from the apparent rate derived from the non-enzymatic rate subtracted from the enzymatic rate, are depicted in a non-Michaelis-Menten plot (Fig 3.20). An Eadie-Hofstee plot (Fig. 3.21) was also generated from the data, depicting velocity versus velocity/ [CDNB], and also suggests a biphasic or atypical kinetic profile for this reaction (119).

3.11 Inhibition of Cytosolic GST Activity by AEME

In an analogous fashion to the aforementioned experiments (section 3.10), single donor HLC (0.08 mg/mL), GSH (1 mM), CDNB (5 μM to 80 μM) and AEME (0 μM to 320 μM)

were incubated at 37°C for 20 seconds. The apparent velocity was calculated after 20 seconds (n=6) and an evaluation of the type of inhibition was performed using simulated enzyme kinetics software (Enzyme Kinetics Module, version 1.1.1). The software fit the experimental data best to a competitive and mixed inhibition model (r^2= 0.985 and 0.986, respectively). A Lineweaver-Burk plot (Fig. 3.22.1), depicting 1/velcocity versus 1/ [CDNB] for four fixed AEME concentrations (0, 50, 125, and 320 μM), and Dixon plot (Fig. 3.22.2), depicting 1/velocity versus AEME concentration, are displayed for a mixed (full)-linear inhibition model. The following kinetic parameters, V_{max} (nmole/mg/min), K_m (μM), and K_i (μM) values, were derived from the analysis: 311, 96, and 334, respectively. The relative inhibition constant, K_i, was calculated for the mixed (334 μM) and competitive (262 μM) models, indicating that AEME is a weak inhibitor of cytosolic GST activity.

3.12 Solid Phase Extraction of AEME-NAC

Blank urine was spiked with varying concentrations of authentic AEME-NAC and extracted by solid phase extraction. Using direct injection ESI-MS, the limit of detection of AEME-NAC was approximately 15 ng/mL. A positive identification of the adduct ion in the blank urine sample included three data points, including full scan (MH^+ 345), MS/MS (MH^+ 216 and 182), and MS^3 of 216 (MH^+ 182). The limit of detection on LC-MS was approximately 1.9 ng, whereas the detection limit on LC-MS/MS was nearly 50 ng. Using SPE followed by direct injection ESI-MS, LC-MS or LC-MS/MS analyses, we were unable to detect this adduct in the urine of two different known crack cocaine users, obtained from the OCME of West Virginia.

3.13 Analysis of the Urine from a Known Free-base Cocaine/Ethanol Abuser

Three different analytical approaches were employed to analyze the urine of a decedent who co-abused freebase cocaine and ethanol. AEEE was identified in a urine sample that also contained cocaine, cocaethylene and AEME. By GC-MS, the peak eluting at 4.67 minutes corresponded to AEEE (Fig 3.23). By comparison with a standard curve, the approximate concentration of AEEE in the urine sample was about 1.0 μg/mL. The other compounds, although not quantified, exhibited the following retention times (min): AEME (4.28), cocaine (8.79), cocaethylene (9.04). A comparison of peak heights from 0 to 12.5 minutes showed relative concentrations of AEME, cocaine and cocaethylene. The relative peak height ratio of AEME:AEEE was 1.5:1. In addition, the relative peak height ratio of cocaine:cocaethylene was 1.7:1, whereas the ratios of cocaine or cocaethylene to there related breakdown product, AEME or AEEE, was 2.8:1 and 2.4:1, respectively. The possibility that AEEE is an artifact produced in the GC injector port by thermal decomposition of cocaethylene was not ruled out.

To address the possible thermal breakdown of cocaethylene on GC-MS, an analytical process was applied for the detection of AEEE that would have less potential for producing AEEE as an artifact. Urine from the same overdose victim was analyzed by SPE followed by LC-MS (Fig 3.24). Reconstituted urine SPE extract (40 μL) was injected and the corresponding compounds (with retention times in minutes) were detected: AEME (6.63), AEEE (6.83), cocaine (7.33) and cocaethylene (8.13). Relative peak height ratios were as follows: cocaine:cocaethylene (1.6:1); AEME:AEEE (3.5:1); cocaine:AEME (1381:1); and cocaethylene:AEEE (3812:1).

Authentic AEEE (10 μg/mL in acetonitrile) was injected directly into an ion trap ESI-MS and the mass fragmentation was recorded. Confirmed AEEE in a similar concentration

was injected (20 μL) onto the LC-MS (Shimadzu/ Thermoquest system) and MS/MS analysis on the parent mass, MH^+= 196, with collision energy of 20%, was performed up to 15 minutes. In the urine sample, a low intensity ion peak at a similar retention time to standard, ca. 8.44 minutes, was detected for the following MS/MS ions: 168, 150, 122, and 91, confirming the presence of AEEE in the sample. An additional ion peak at 10.42 minutes was assigned as cocaethylene based on an analysis of its mass spectrum. It is interesting to note the presence of a cocaethylene fragment at the same *m/z* value as the AEEE MH^+ ion (*m/z* 196), indicating that the ESI ionization process produces the same product as does thermal degradation. Thus, separation of AEEE from cocaethylene by LC or other chromatographic processes is necessary to give an accurate identification of AEEE.

Two different control urine samples were analyzed under the same experimental conditions as the case sample. LC-MS (Waters/Micromass system) on a 1 mL blank urine sample showed no trace of cocaine, cocaethylene, or pyrolysis products. Another urine sample obtained from the OCME was analyzed, and the compounds identified included cocaine and AEME. This sample contained no detectable levels of either cocaethylene or AEEE.

3.14 Lung A549 Cells Exposed to AEME, AEEE, and AE

The percent cell viability of A549 lung fibroblasts exposed to cocaine pyrolysis products for 24 hours was measured by a trypan blue exclusion dye assay. Mean percent viability (n=3) for each compound and controls are depicted below (Fig. 3.25). Viability of cells exposed to AEME (1 mM) or AEEE (1mM) were significantly less than 2% DMSO control ($p < 0.01$). AEME (0.5 and 0.25 mM) and AE (1 mM) exposed cells also exhibited significantly less cell viability ($p < 0.005$). Their greater level of significance resulted from

less variance among the 3 tested wells, even though AEME (0.5 and 0.25 mM) contained greater percent viabilities (Fig. 3.25) than AEME (1 mM) or AEEE (1mM).

3.15 A549 Cell Cytotoxicity Observed by Flow Cytometry

Percentages of dead cells, resulting from a 24 hour incubation with various compounds were calculated by flow cytometry and averaged (Table 3.2). DMSO control (2%) exhibited a high percentage of cellular death (45%), resulting in weak comparisons with other cells spiked with cocaine and pyrolysis products. 1 mM of AEME fumarate (46%) did exhibit a greater percentage of cell death than 1 mM of cocaine HCl (37%), but only significant at the 10% level. AEEE fumarate (1 mM) showed the greatest percentage of cell death (57%) of the tested cocaine pyrolysis products. Styrene oxide (1 mM) displayed similar toxicity as 20% ethanol (87% and 87.2%, respectively) to A549 cells, and clearly more toxic than cocaine or any of the pyrolysis products. The addition of NAC (5 mM) to styrene oxide, AEME, AEEE and AE was also tested in duplicate in this cell line (Table 3.3). Although the addition of NAC appears to lower cell toxicity with styrene oxide, AEME (1.0, 0.5, and 0.25 mM), AEEE (1 mM) but not with AE (1 mM), this effect was not statistically significant.

(A)

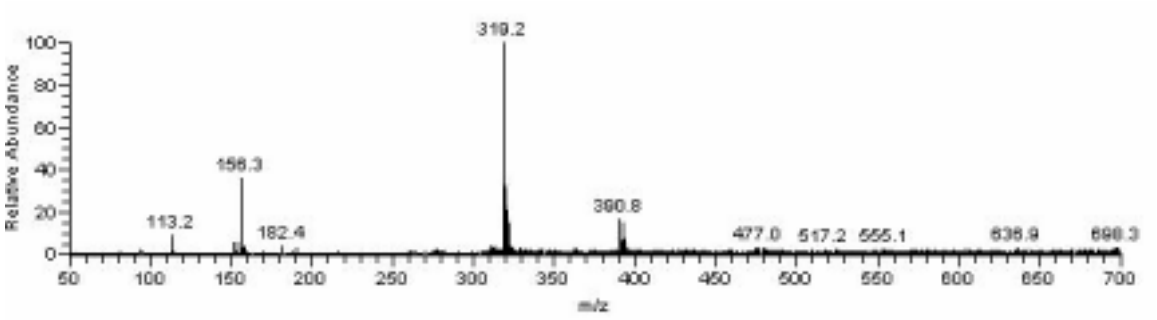

(B)

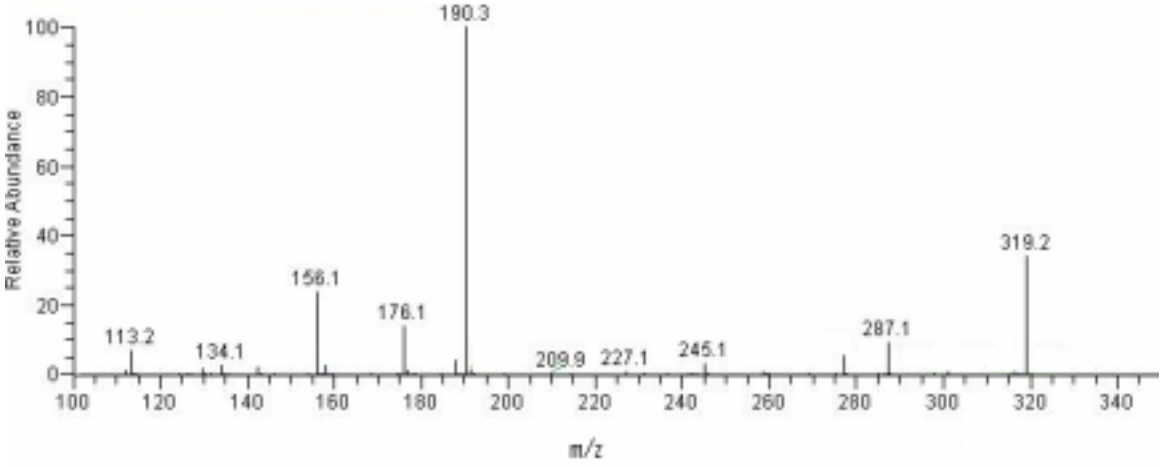

(C)

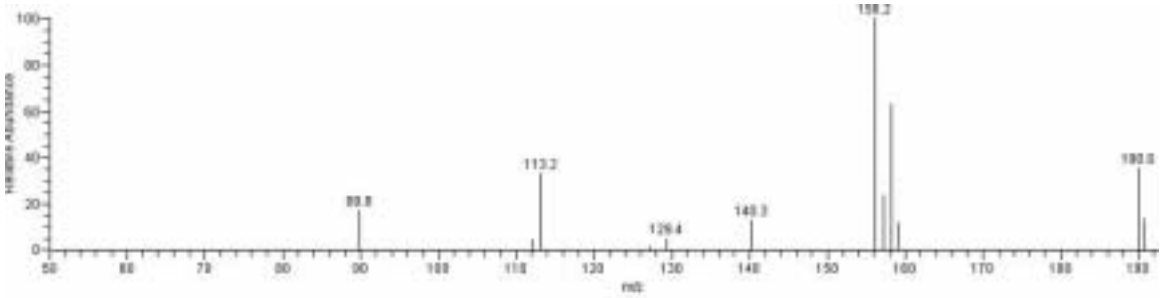

Figure 3.1: ESI-MS spectra of arecoline-NAC adduct. **(A)** Full scan. **(B)** MS/MS fragmentation of the protonated adduct ion at *m/z* 319. **(C)** MS^3 of the fragment ion, *m/z* 190, producing the major fragment *m/z* 156, protonated arecoline.

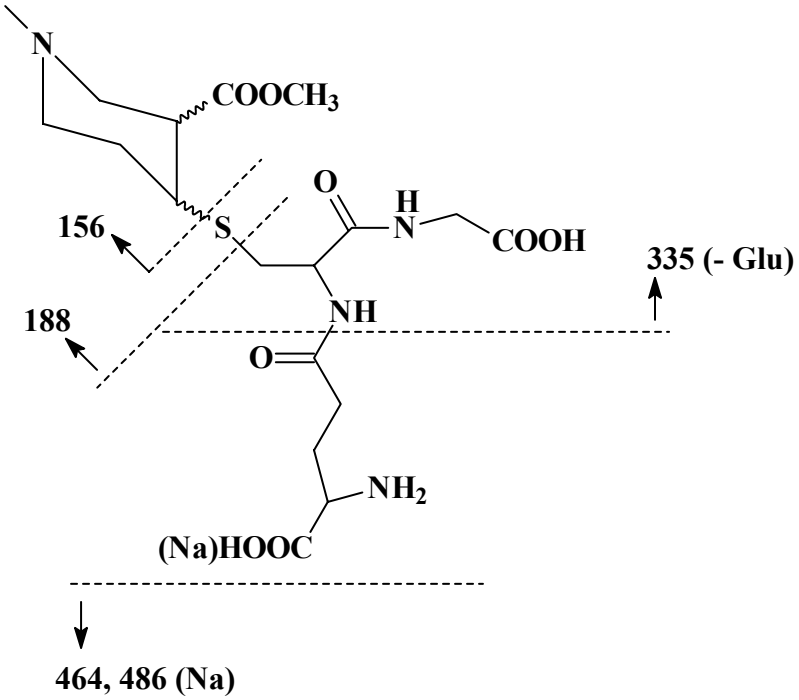

Arecoline-SG

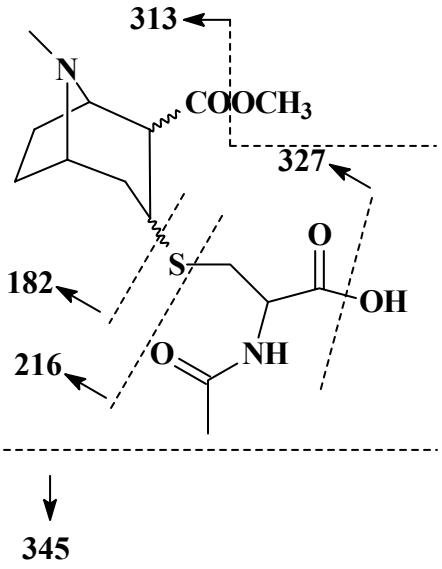

AEME-NAC

Figure 3.2.1: Mass fragmentation patterns of the synthesized arecoline-SG and AEME-NAC adducts on ESI-MS in the positive ion mode.

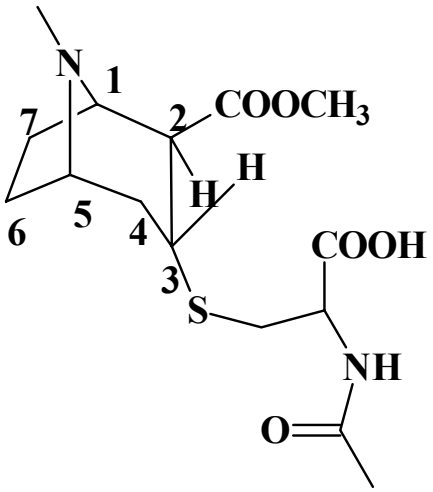

A

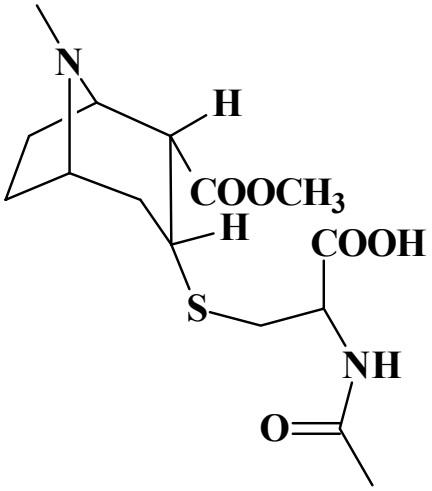

B

Figure 3.2.2: Chemically synthesized AEME-NAC epimers. **A** is the 2β,3α isomer, while **B** is the 2α,3α isomer.

(A)

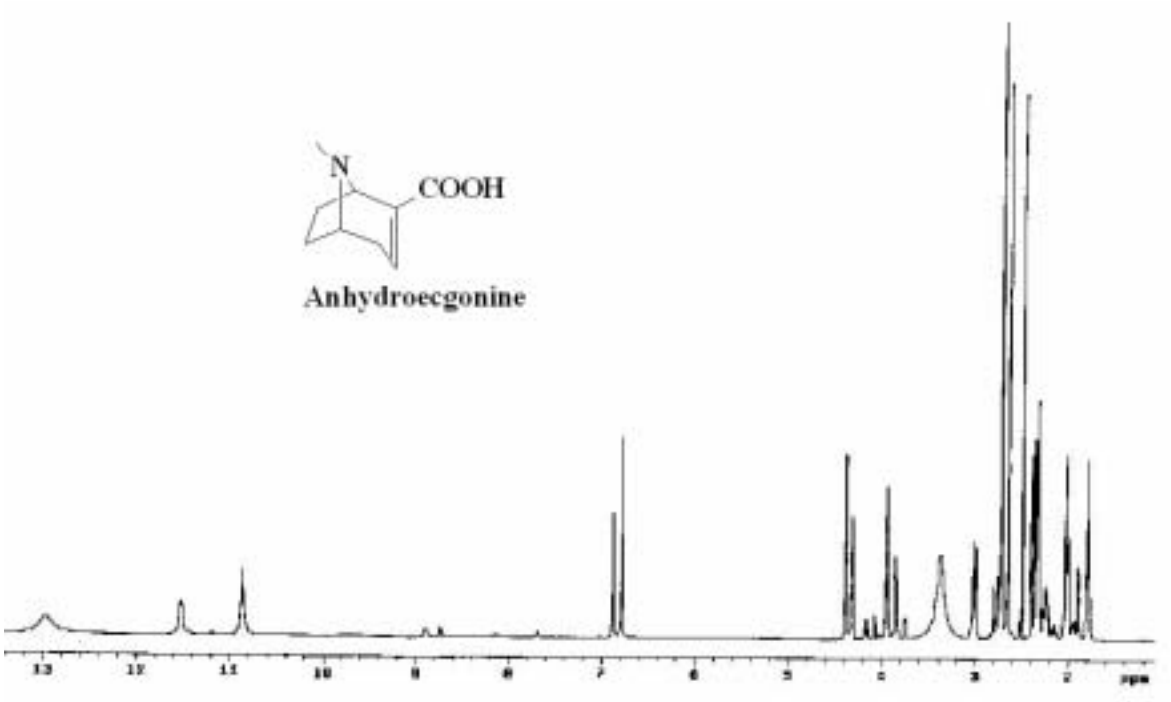

(B)

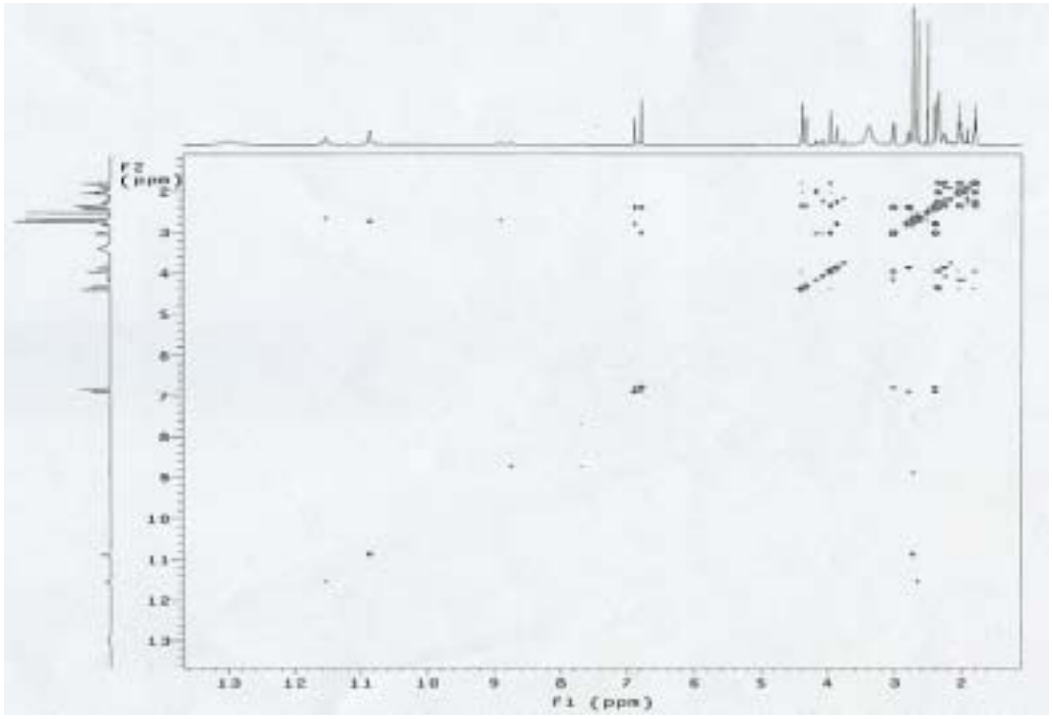

Figure 3.3: NMR spectra of AE HCl in DMSO-d_6. **(A)** ^{1}H **(B)** COSY.

(A)

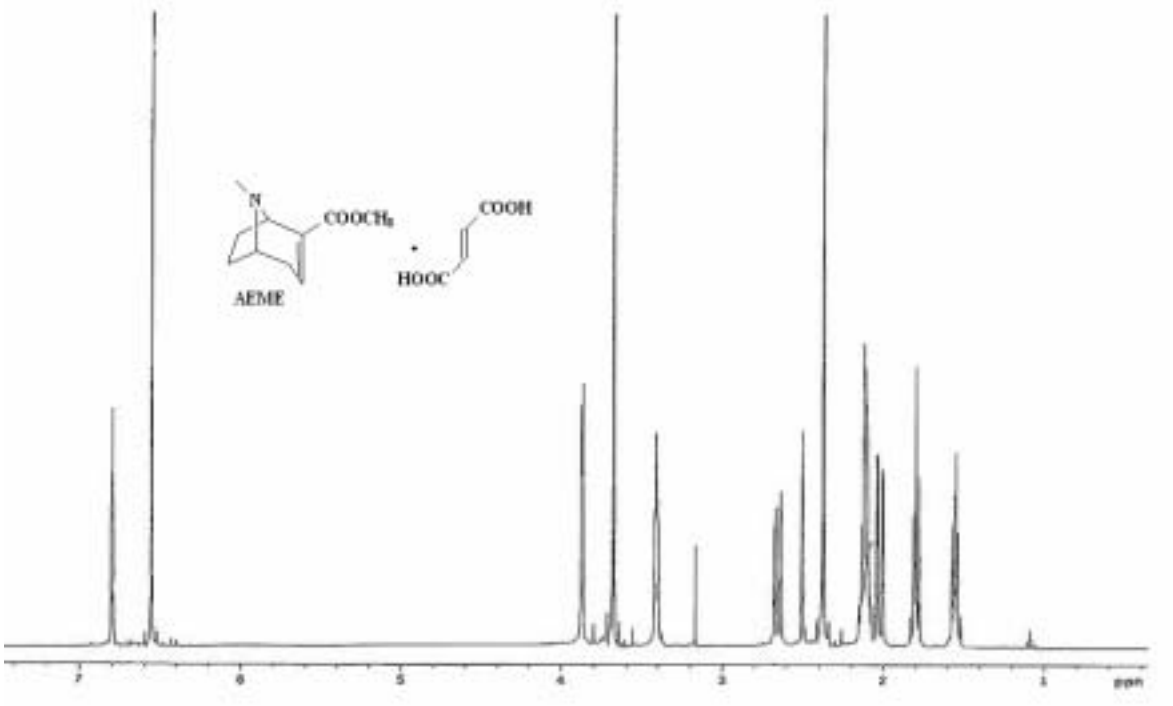

(B)

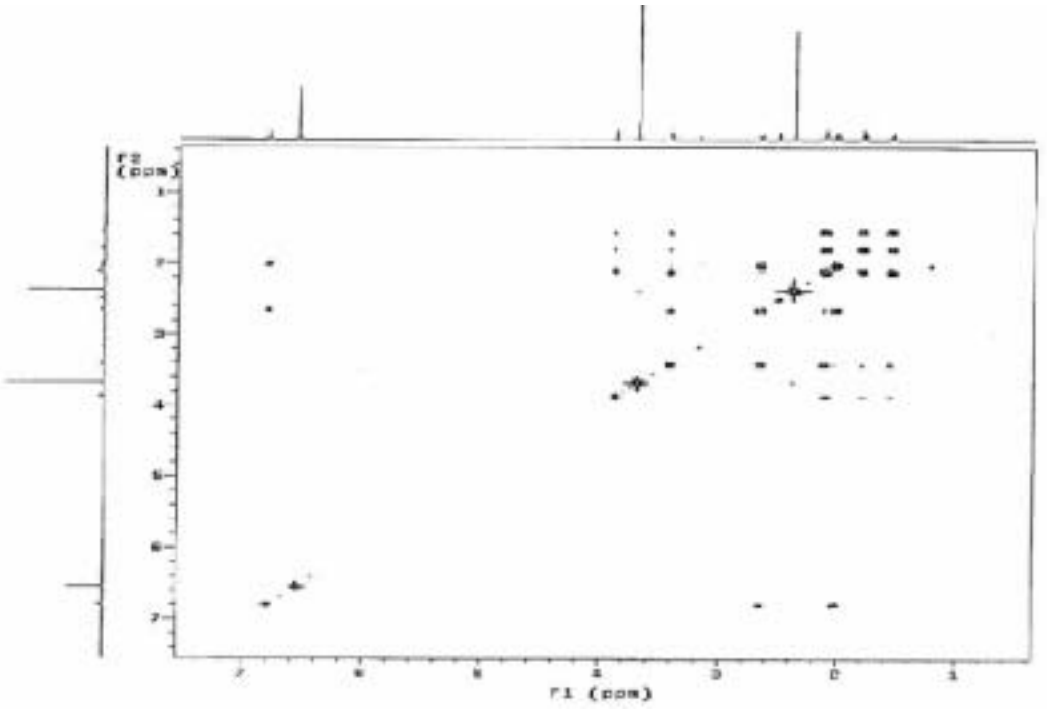

Figure 3.4.1: NMR analysis of AEME fumarate in DMSO-d_6. **(A)** ^{1}H **(B)** COSY.

(C)

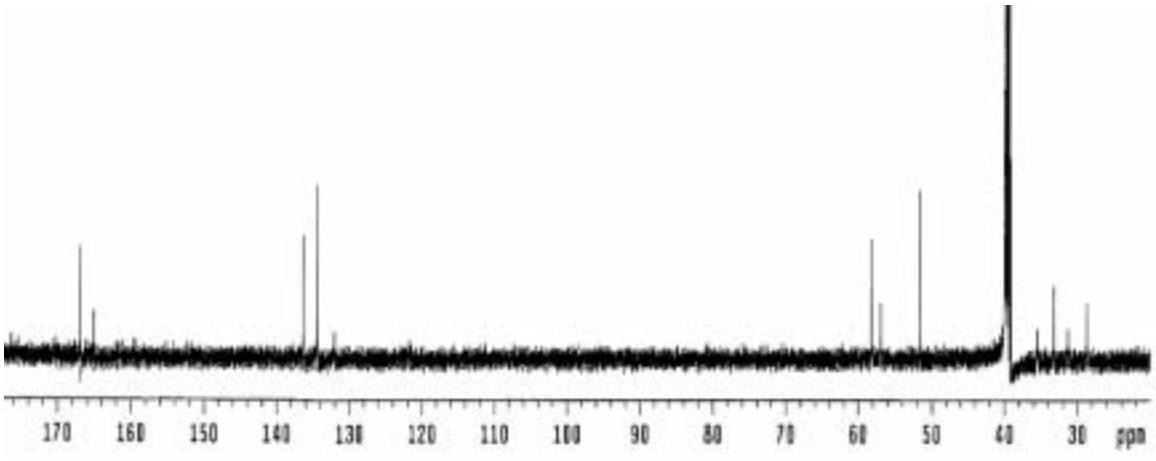

(D)

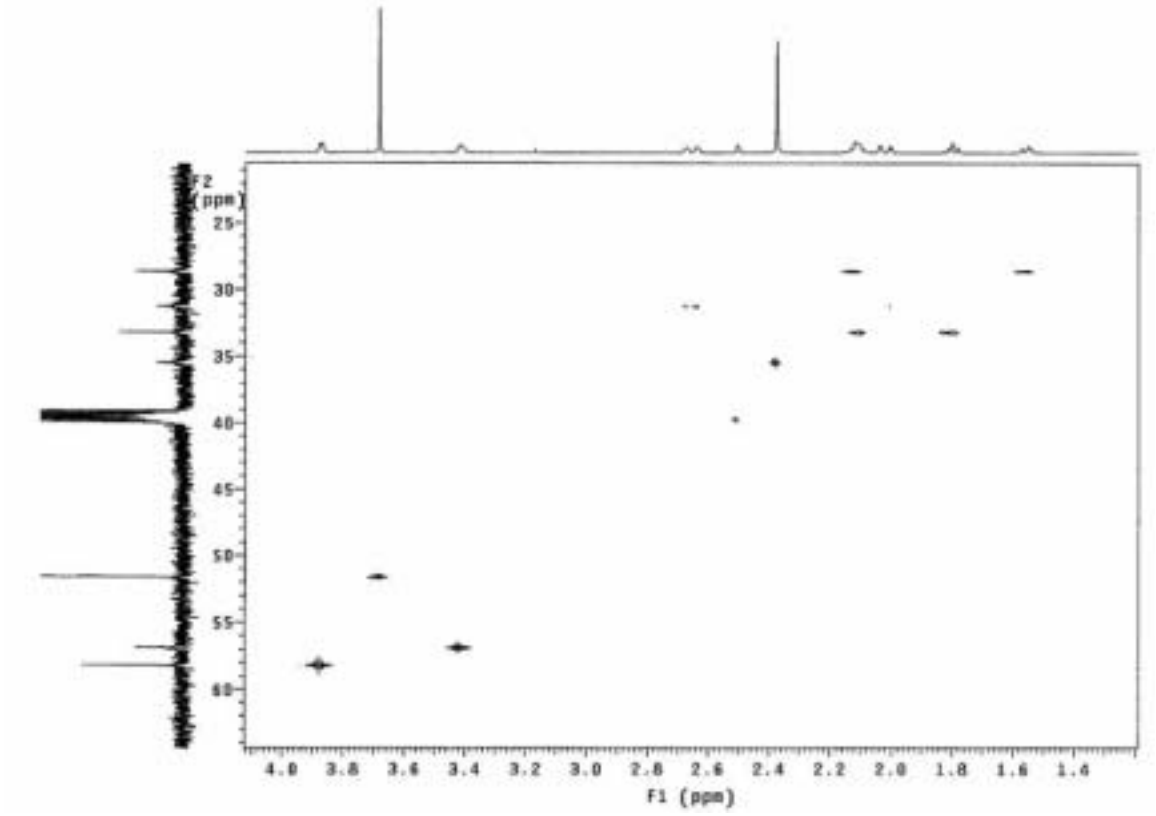

Figure 3.4.2: NMR analysis of AEME fumarate in DMSO-d_6. **(C)** ^{13}C **(D)** HETCOR.

(A)

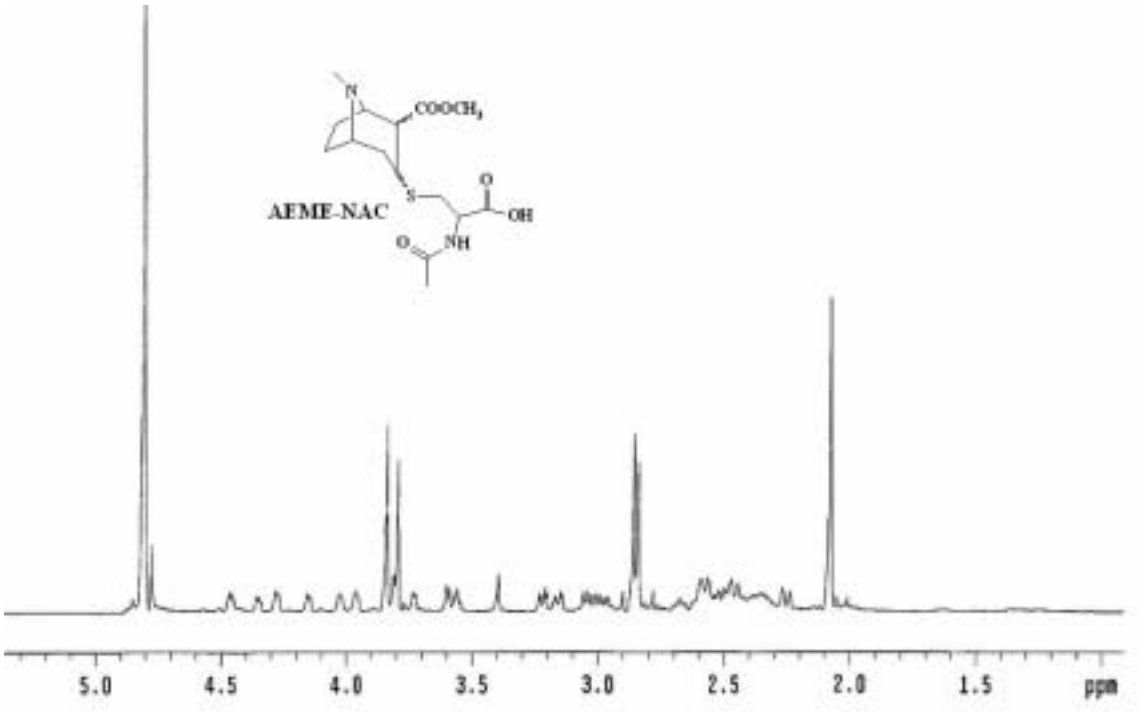

(B)

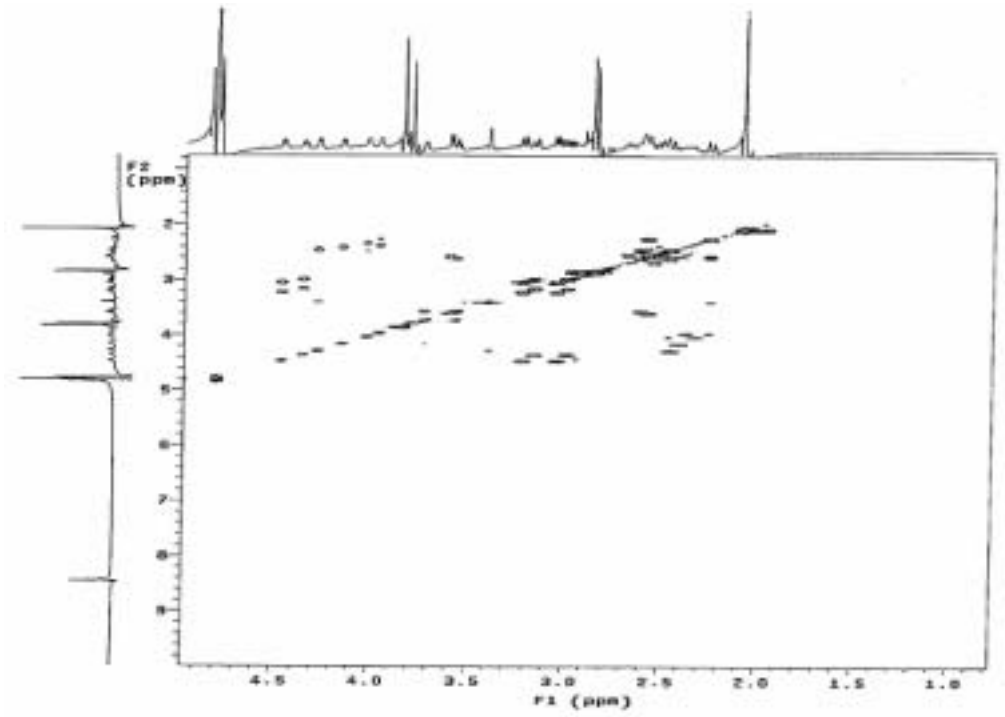

Figure 3.5: NMR spectra of AEME-NAC in D_2O. **(A)** ^1H **(B)** COSY.

(A)

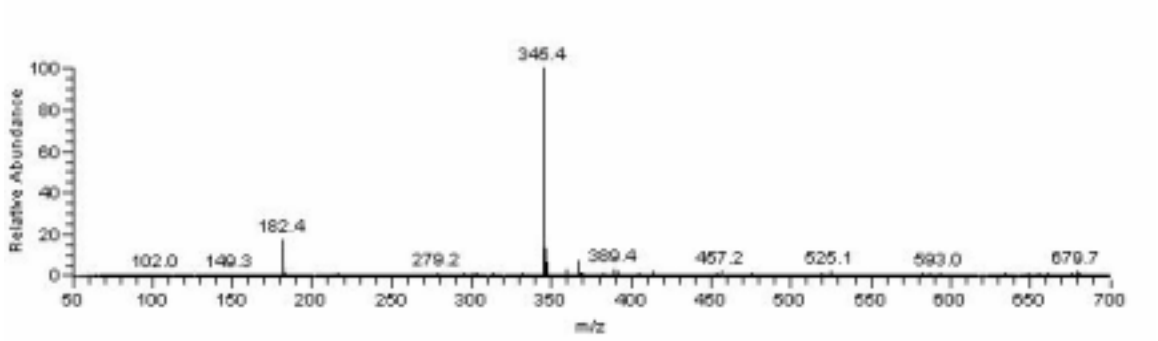

(B)

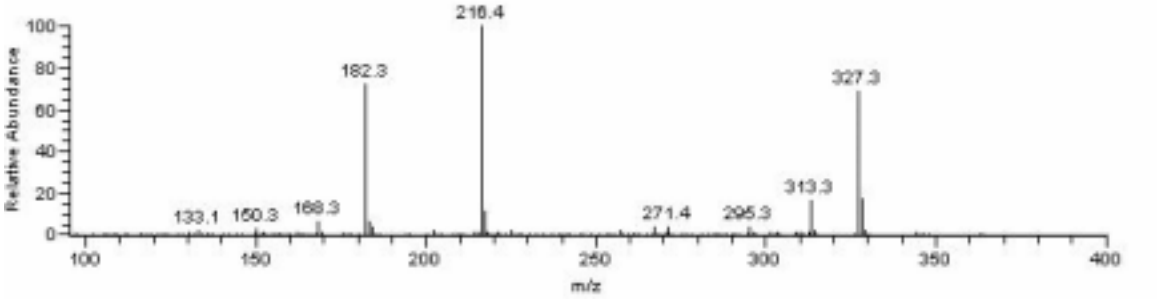

(C)

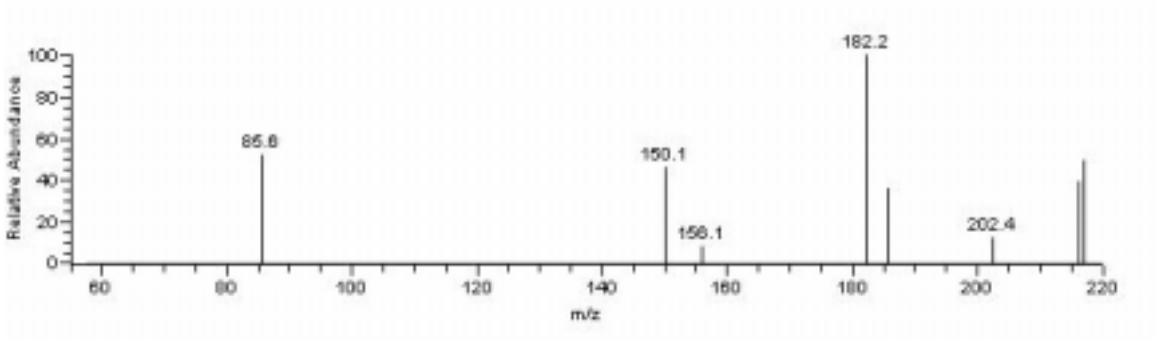

Figure 3.6: ESI-MS spectra of synthesized AEME-NAC. **(A)** Full scan. **(B)** MS/MS of adduct ion, producing the primary fragments: MH^+ 327, 216 and 182. **(C)** MS^3 of fragment ion MH^+ 216, producing MH^+ 182, protonated AEME.

(A)

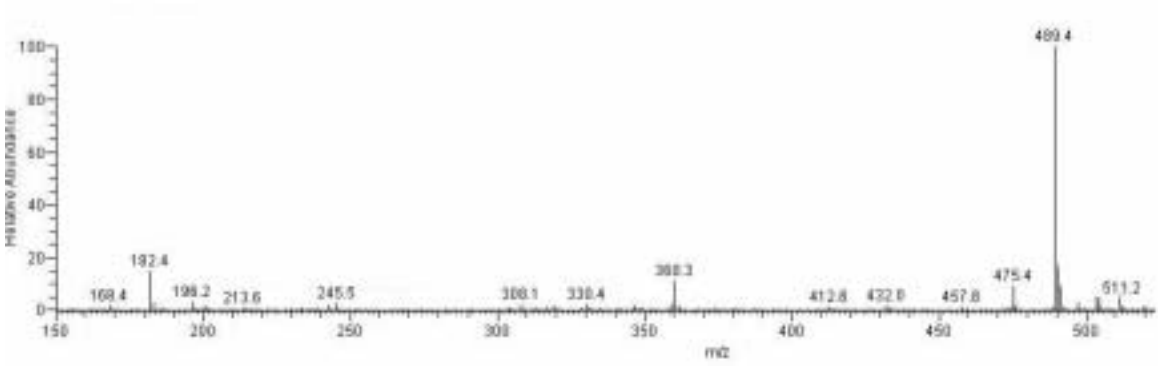

(B)

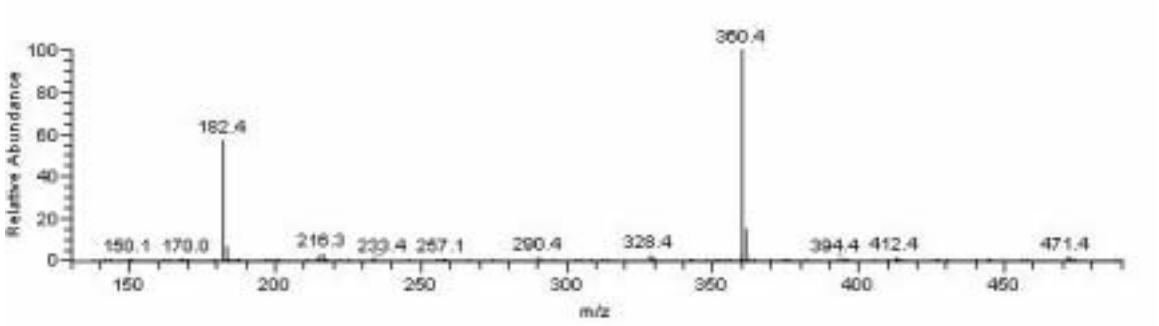

(C)

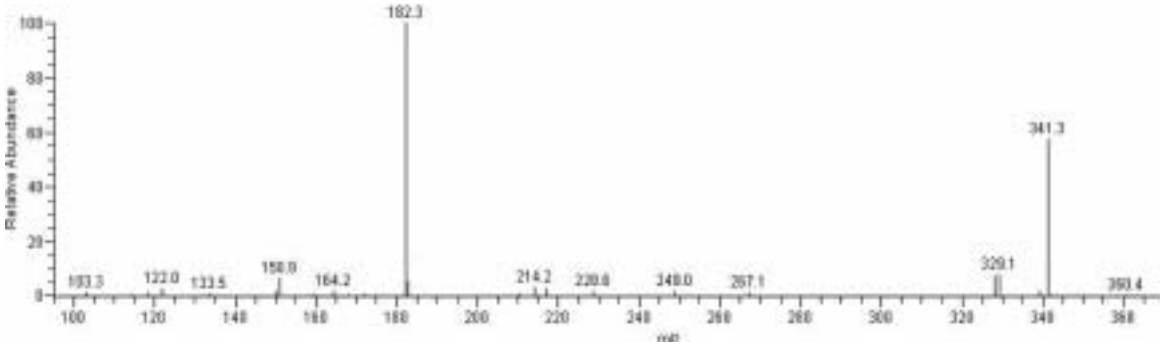

Figure 3.7: ESI-MS spectra of synthesized AEME-SG. **(A)** Full scan. **(B)** MS/MS of adduct ion MH^+ 489, producing the ion fragments, MH^+ 360 and 182. **(C)** MS^3 of fragment ion MH^+ 360, producing primarily MH^+ 182, protonated AEME.

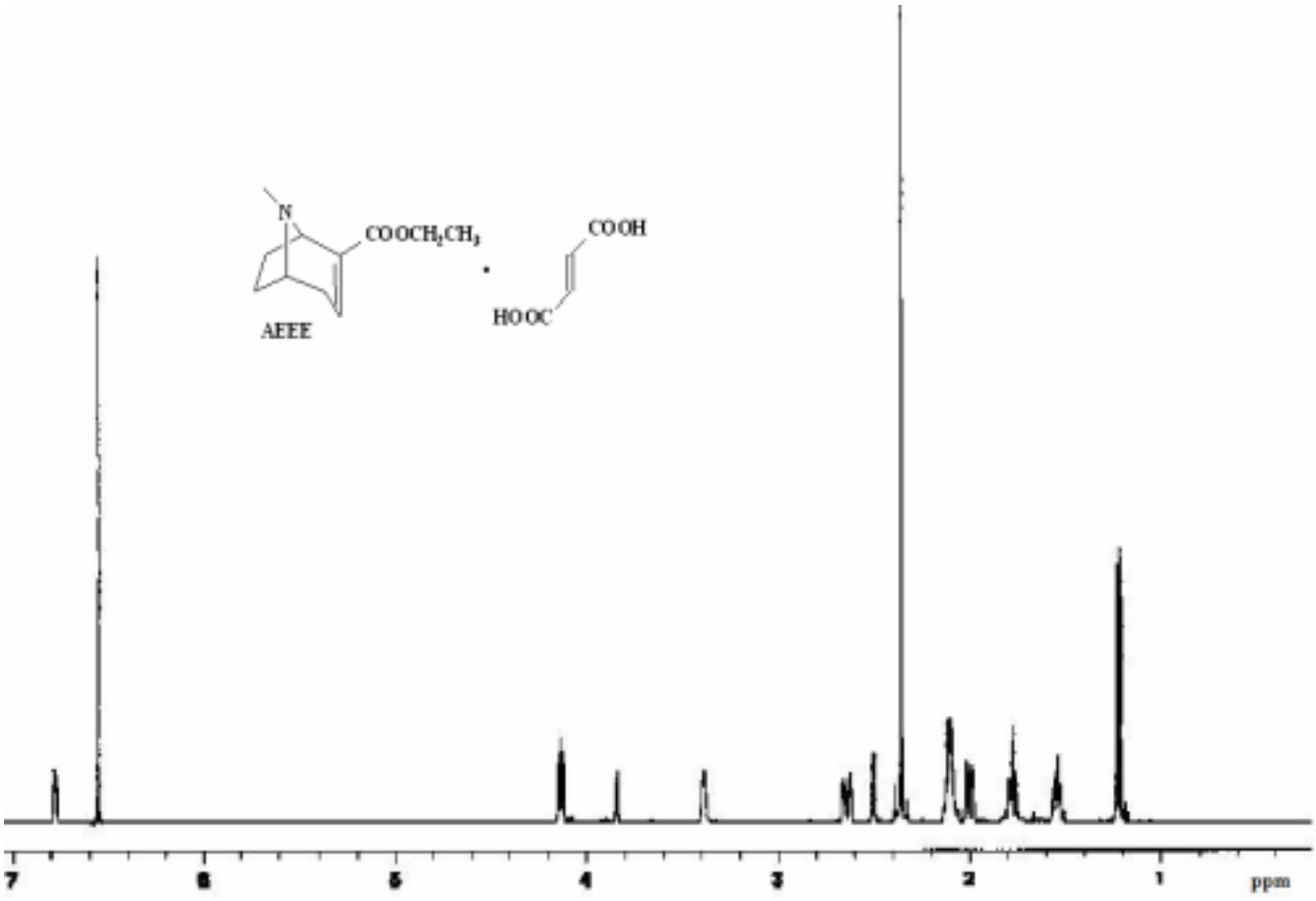

Figure 3.8: ^{1}H NMR spectrum of chemically synthesized AEEE fumarate in DMSO-d_6.

(A)

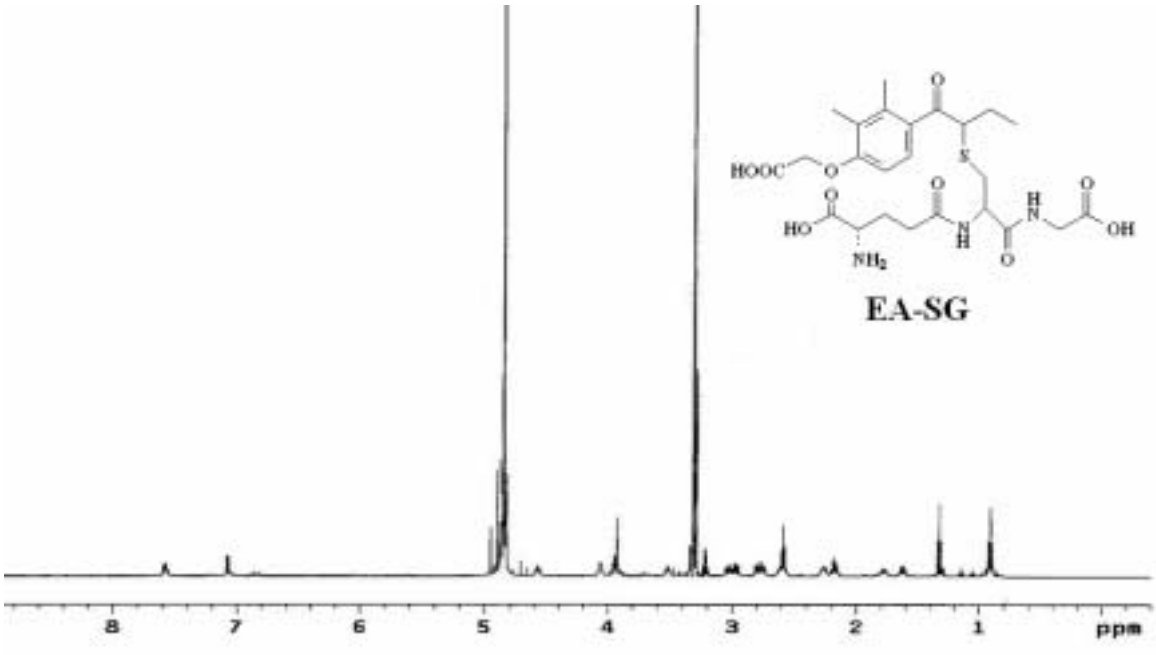

(B)

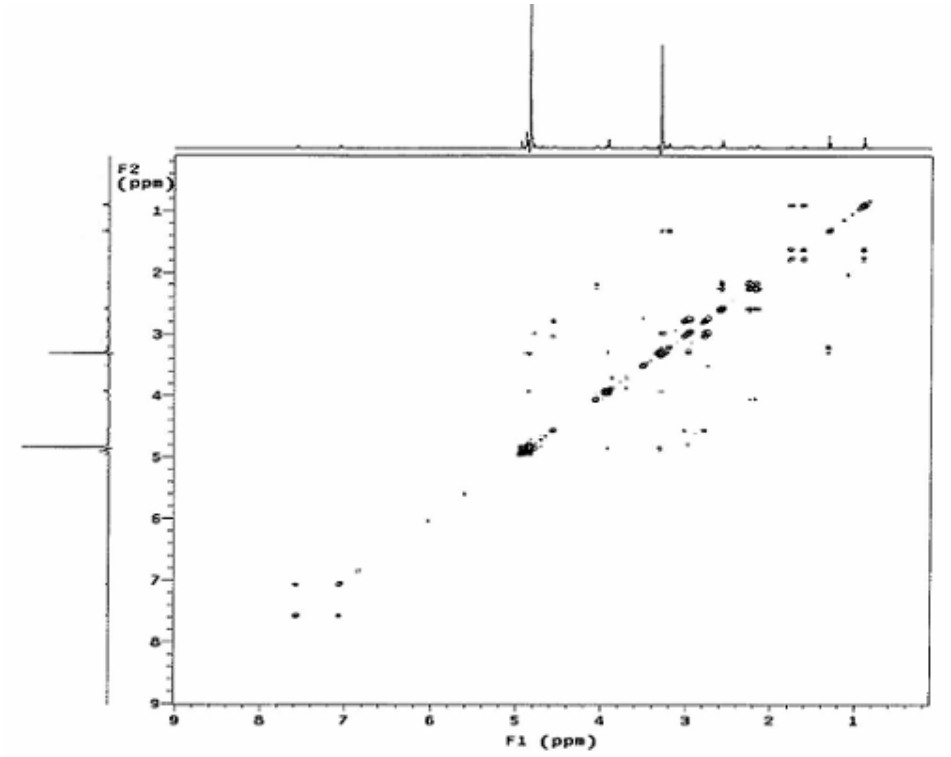

Figure 3.9: NMR spectra of synthesized EA-SG in CD_3OD. **(A)** ^1H **(B)** COSY.

(A)

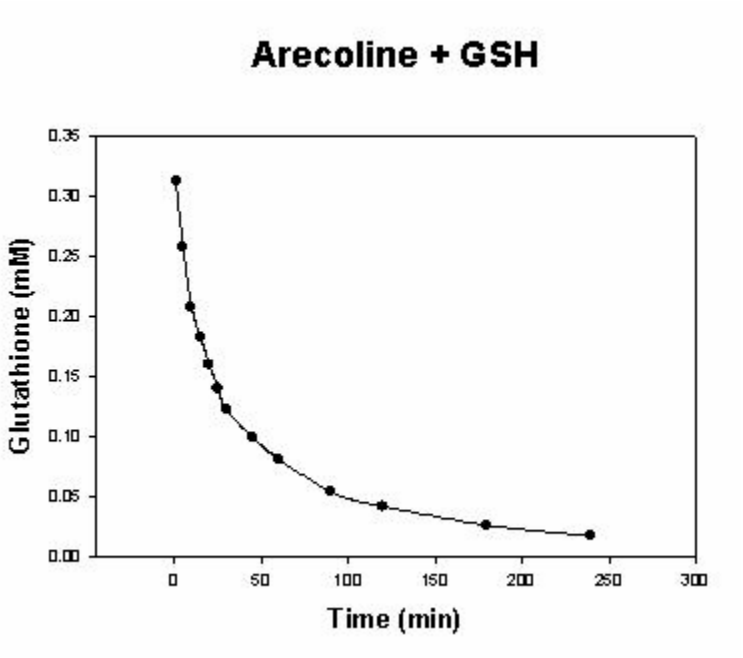

(B)

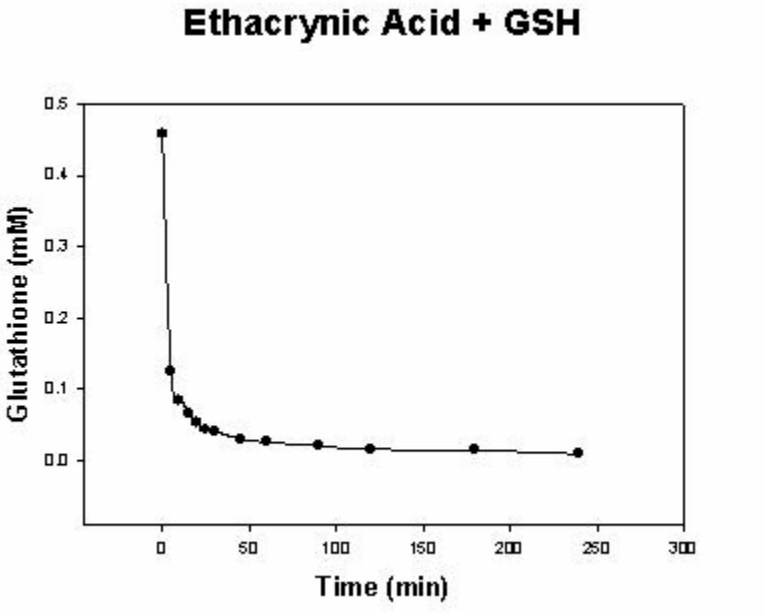

Figure 3.10: Glutathione depletion over time. **(A)** Arecoline, 10 mM **(B)** EA, 10 mM.

(A)

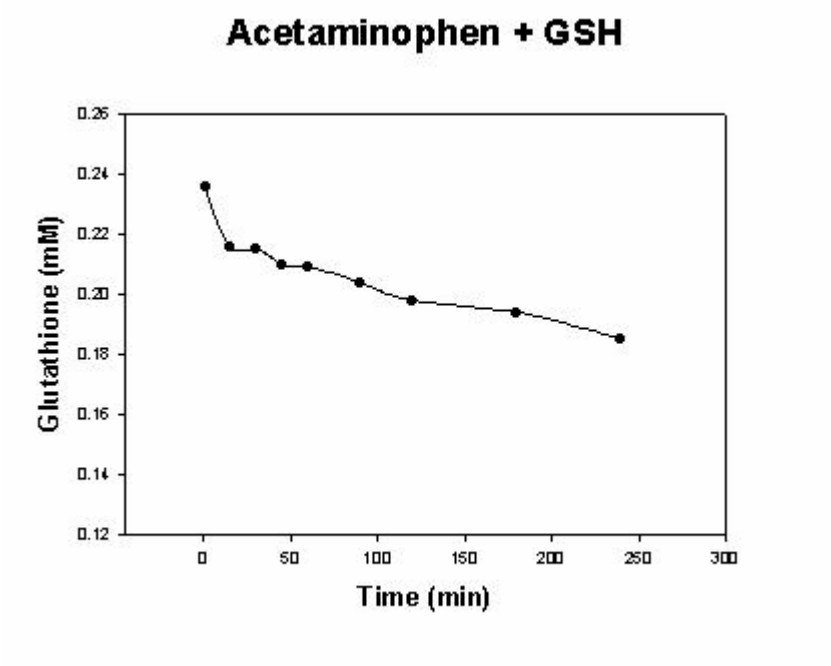

(B)

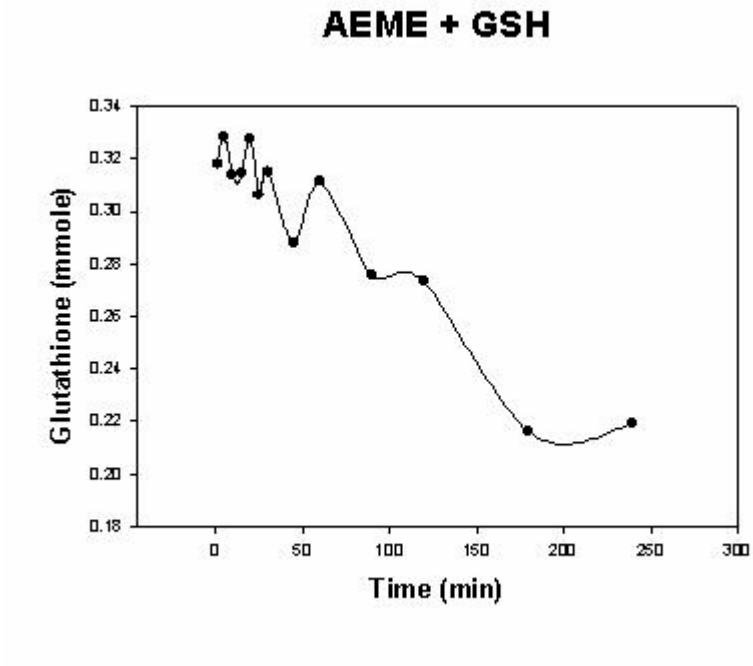

Figure 3.11: Glutathione depletion over time. **(A)** APAP, 10 mM **(B)** AEME, 10 mM.

(A)

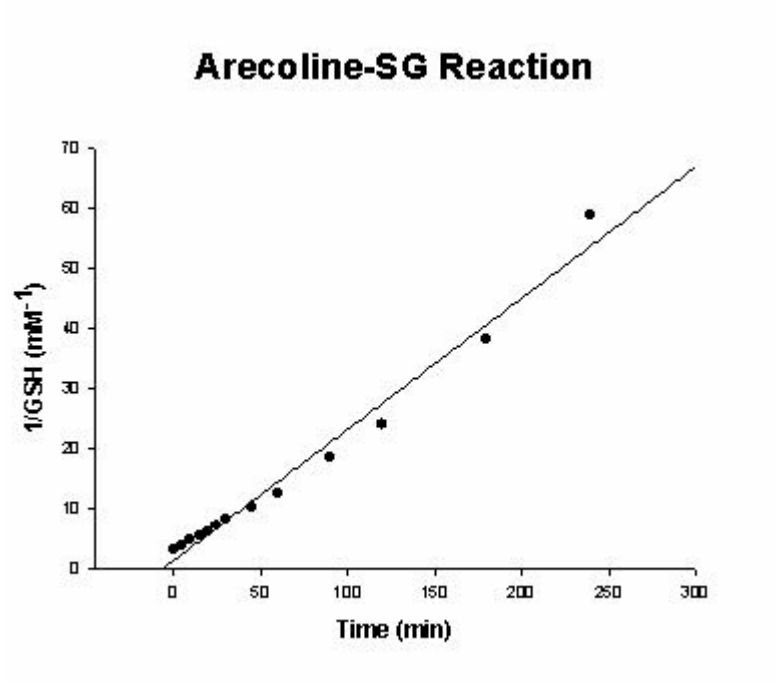

(B)

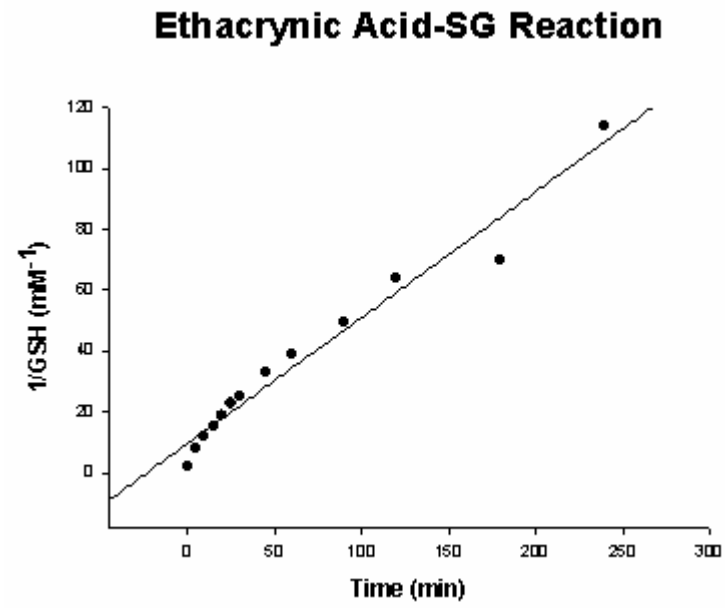

Figure 3.12.1: Inverse 2nd order reaction graphs. **(A)** Arecoline **(B)** EA.

(C)

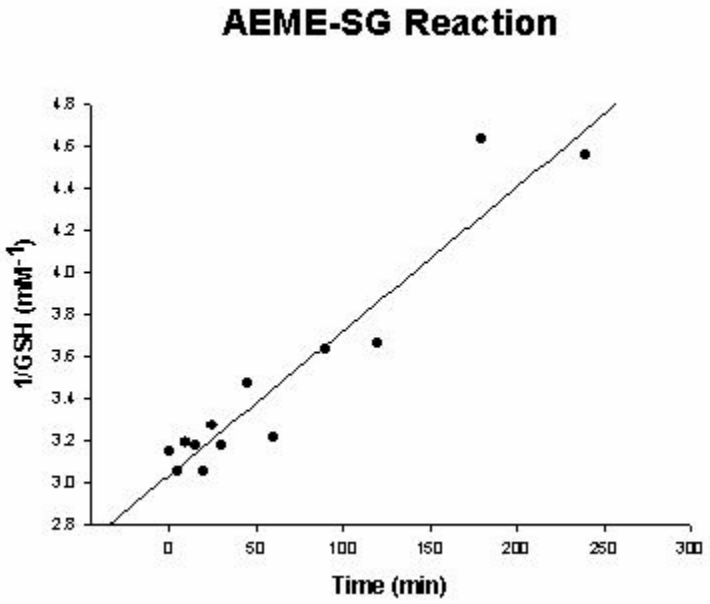

(D)

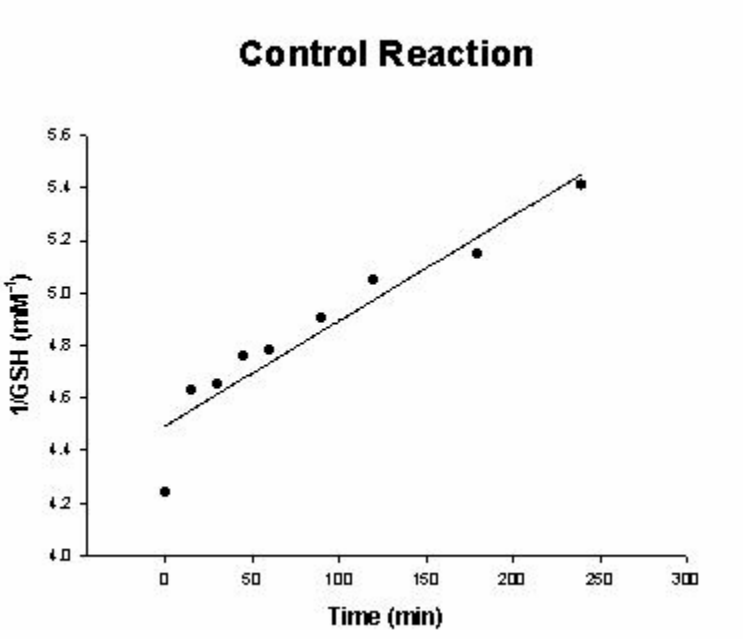

Fig 3.12.2: Inverse 2nd order reaction graphs. **(C)** AEME **(D)** APAP (Control).

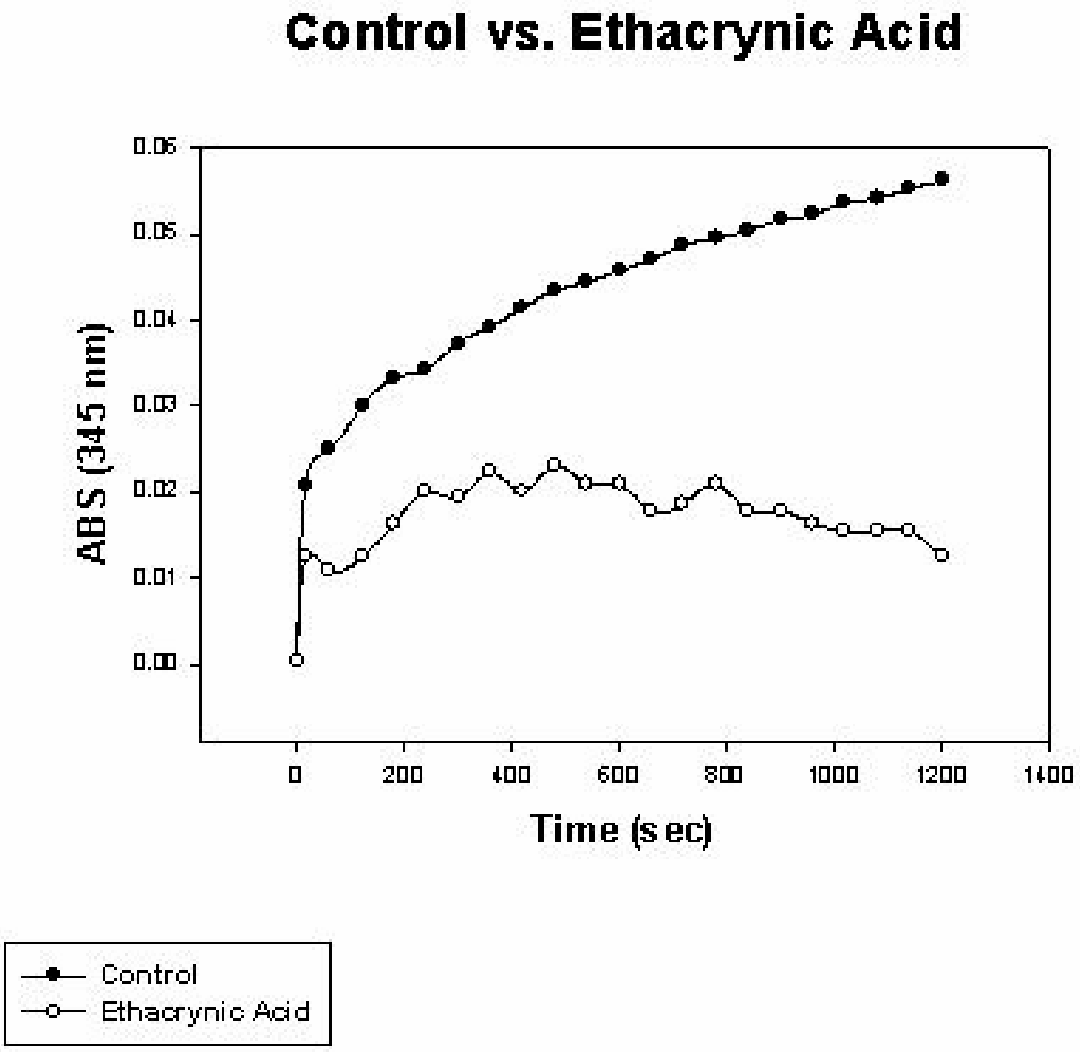

Figure 3.13: Chemical formation of DCNB-SG in the presence of ethacrynic acid (10 mM).

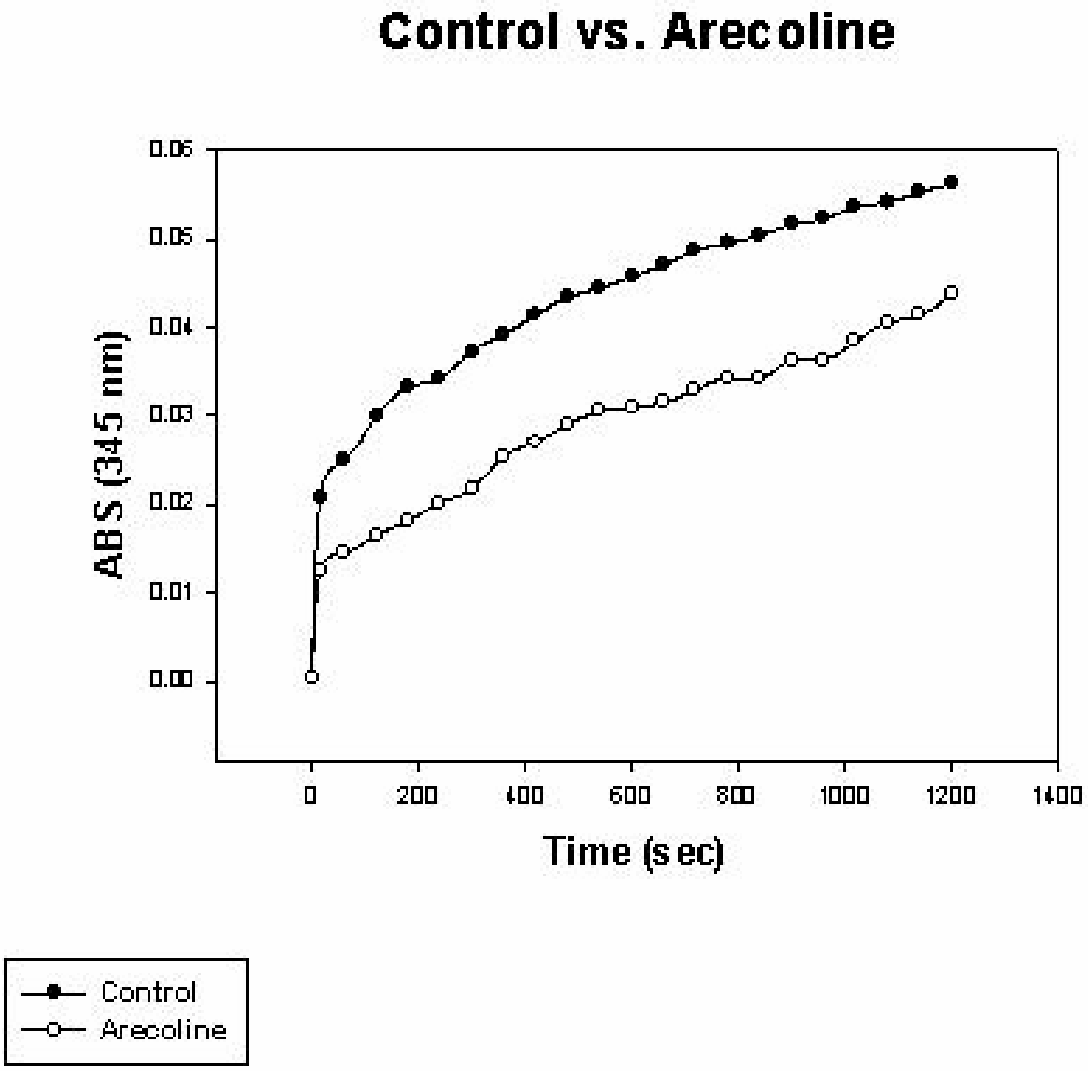

Figure 3.14: Chemical formation of DCNB-SG in the presence of arecoline (10 mM).

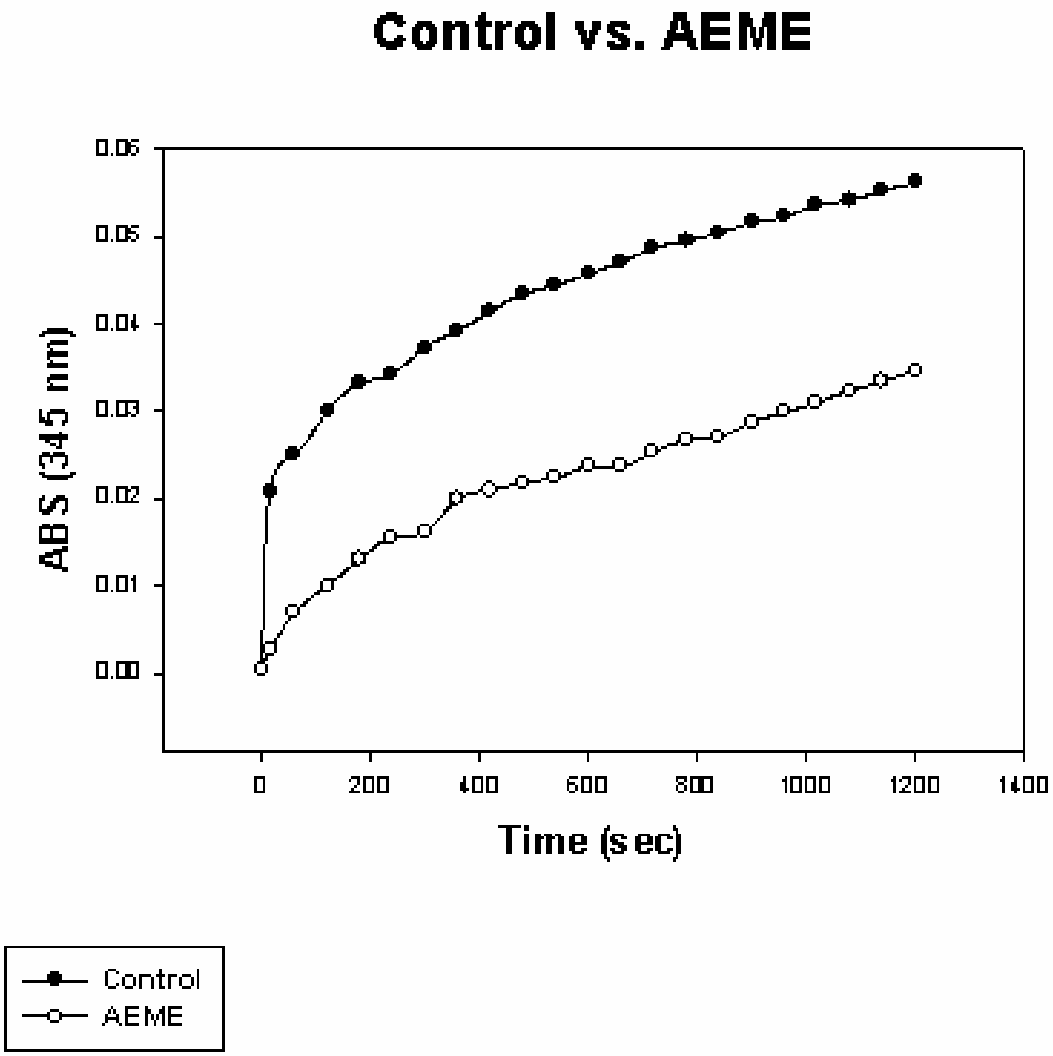

Figure 3.15: Chemical formation of DCNB-SG in the presence of AEME (10 mM).

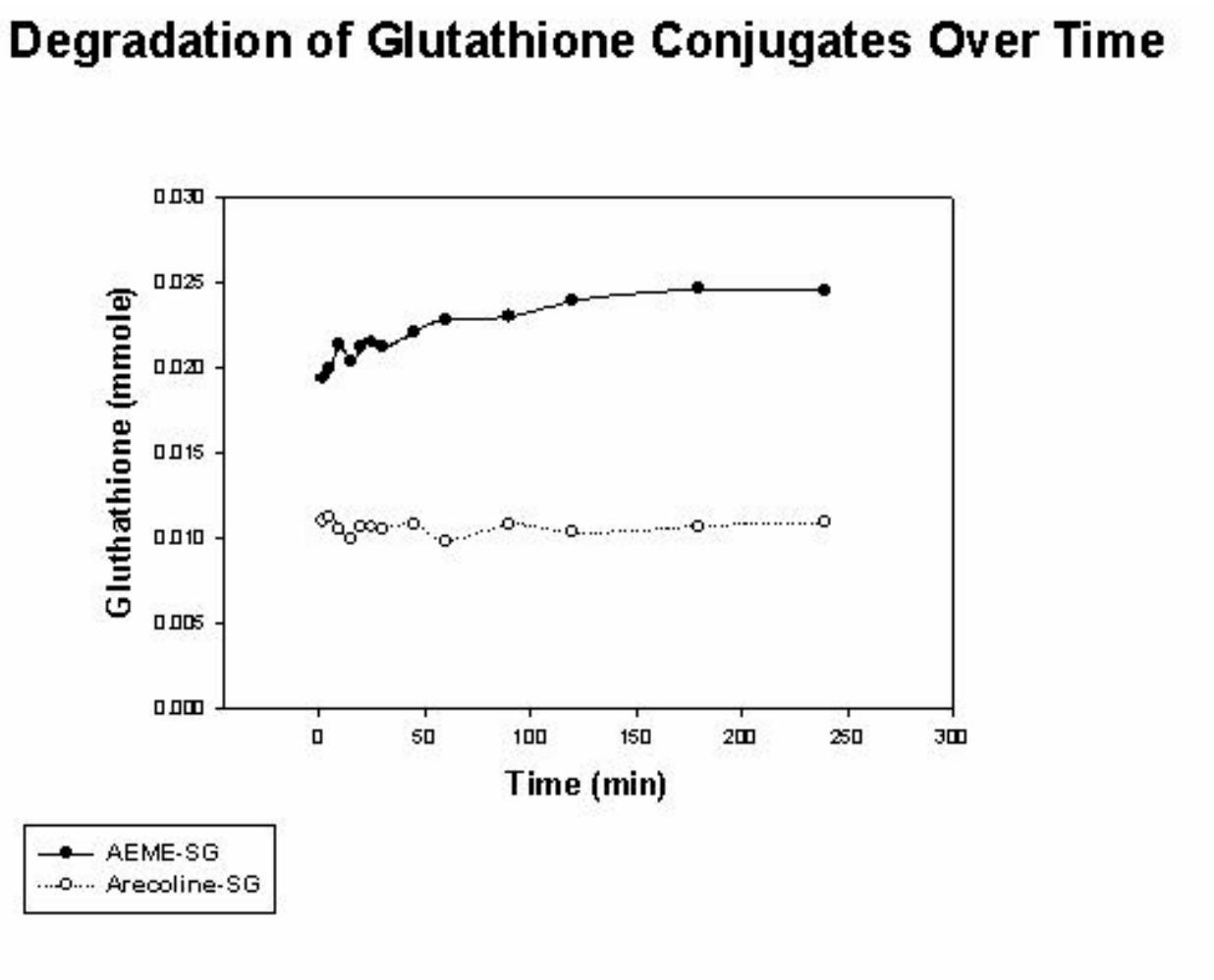

Fig. 3.16: The slow degradation of chemically synthesized AEME-SG (1 mg/mL) and arecoline-SG (1 mg/mL) conjugates over time at 25°C.

Reaction Vial	[EA]	[GSH]	HLC	Total Volume
#1	1.0 mM	2 mM	1 mg	1.0 mL
#2	1.0 mM	2 mM	-----	1.0 ml
#3	0.5 mM	2 mM	1 mg	1.0 mL
#4	0.5 mM	2 mM	-----	1.0 mL

Table 3.1.1: Summary of EA + GSH incubations with or without HLC.

Reaction Vial	EA Peak Area	[EA]
#1	5.5×10^6	0.86 μg
#2	1.5×10^7	2.32 μg
#3	1.8×10^6	0.28 μg
#4	6.3×10^6	0.97 μg

Table 3.1.2: Quantification of EA from standard curve after 4 min. incubation.

(A)

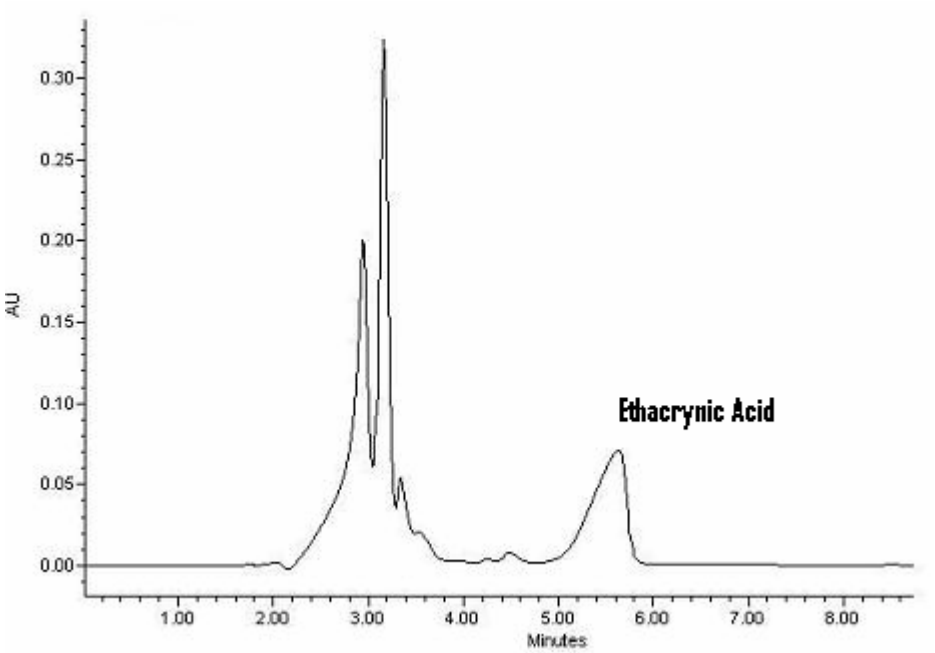

(B)

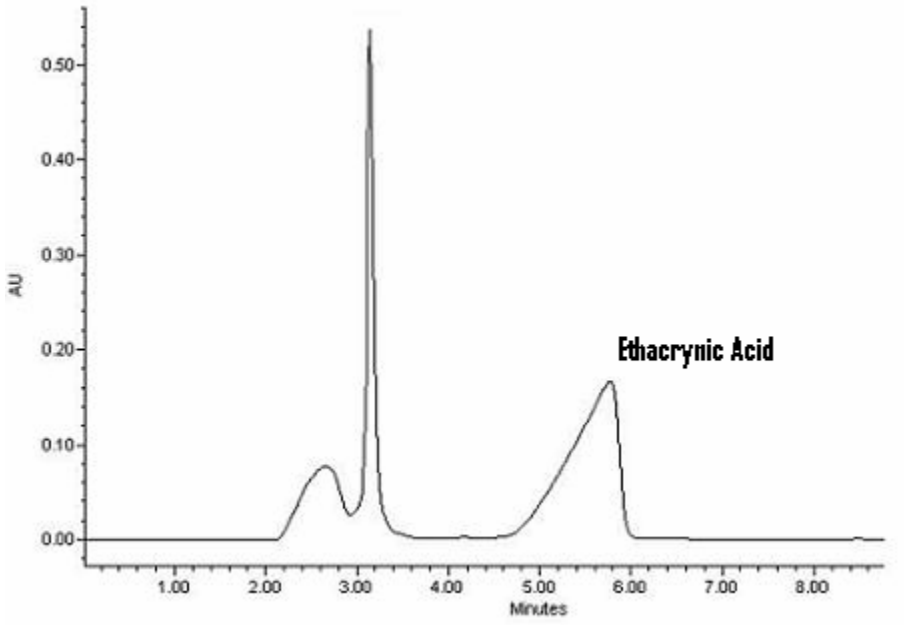

Fig. 3.17: Sample HPLC chromatograms following 4 min. incubation from the conditions described on the previous page. **(A)** vial #3 **(B)** vial #4.

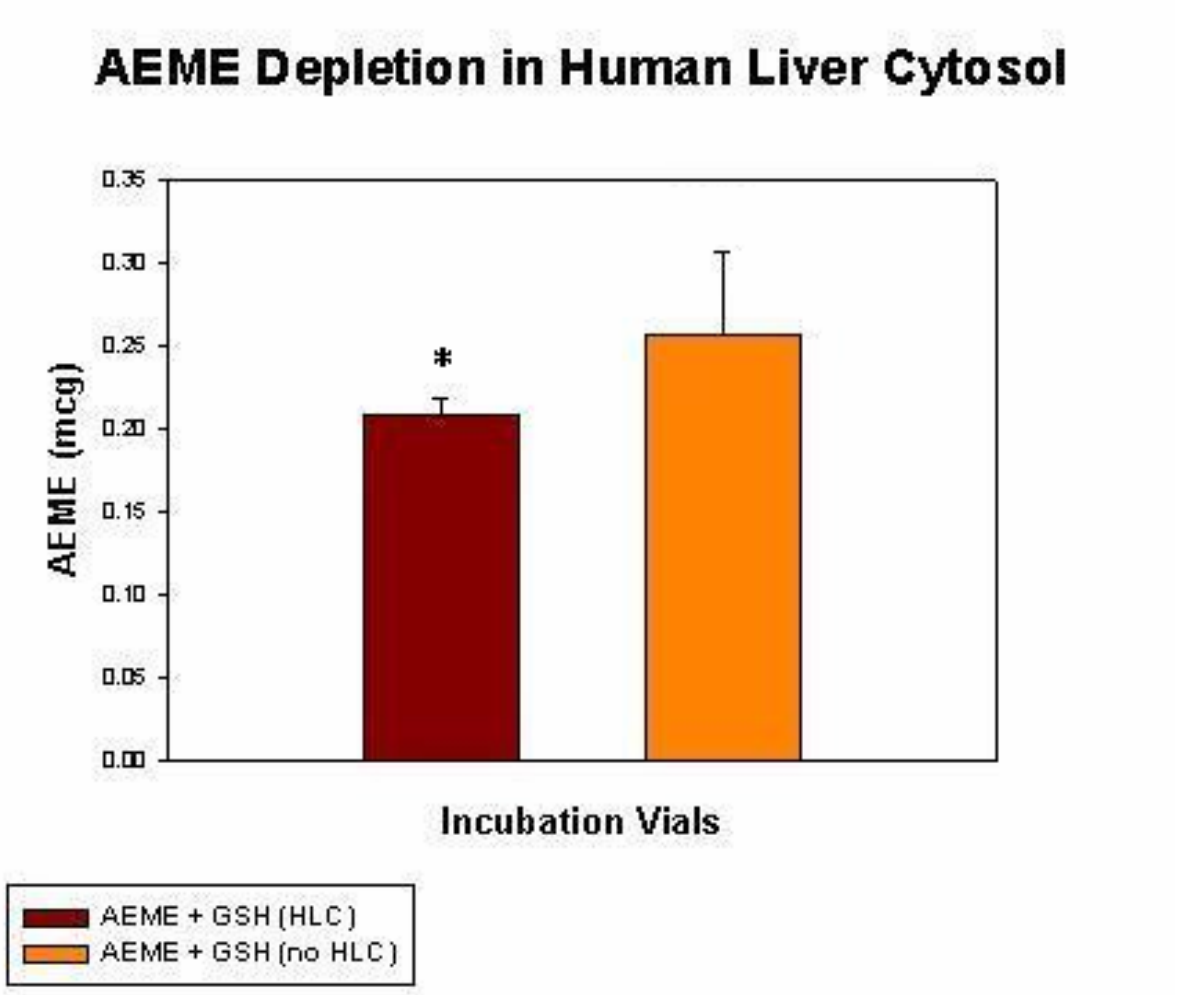

Figure 3.18: AEME depletion in preparations with or without human liver cytosol after 60 min. incubation. (* indicates $p < 0.005$).

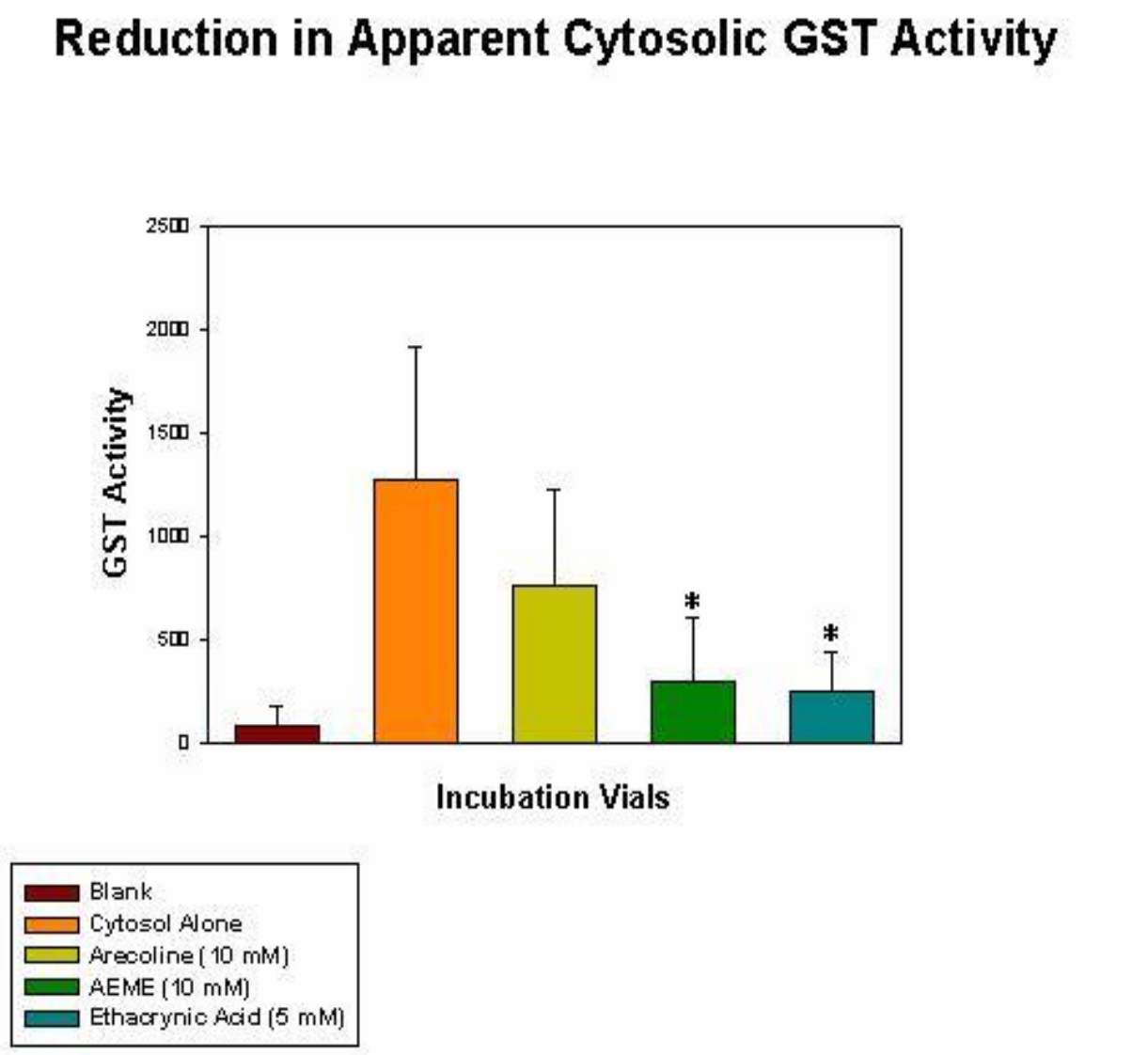

Figure 3.19: Reduction of presumed cytosolic GST activity by AEME (10 mM) and EA (5 mM) after 20 hr. incubation. (* $p < 0.005$).

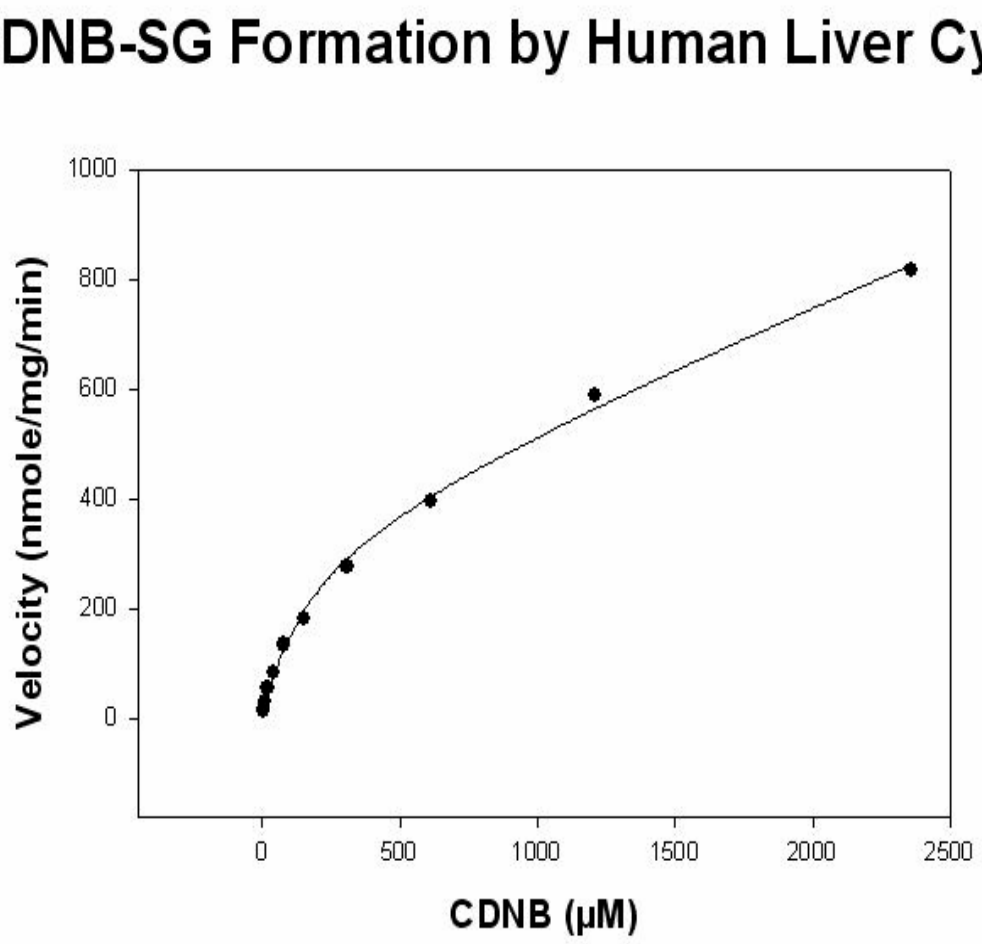

Fig 3.20: CDNB-SG conjugate formation by HLC (0.08 mg/mL) fitted to an atypical or non-Michaelis-Menten kinetic model.

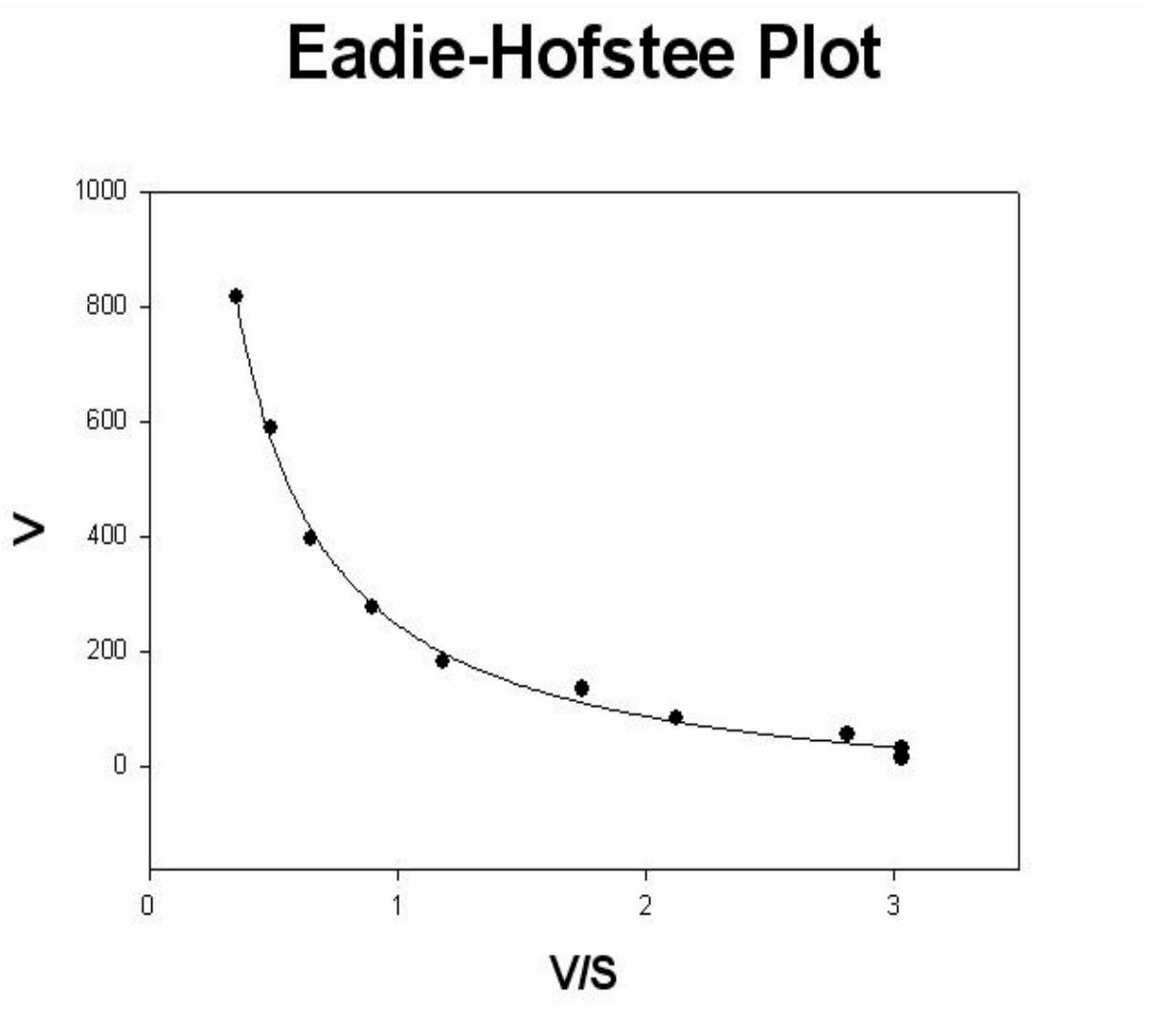

Fig 3.21: Eadie-Hofstee plot of CDNB-SG conjugation by HLC, providing further evidence of an atypical kinetic profile (119).

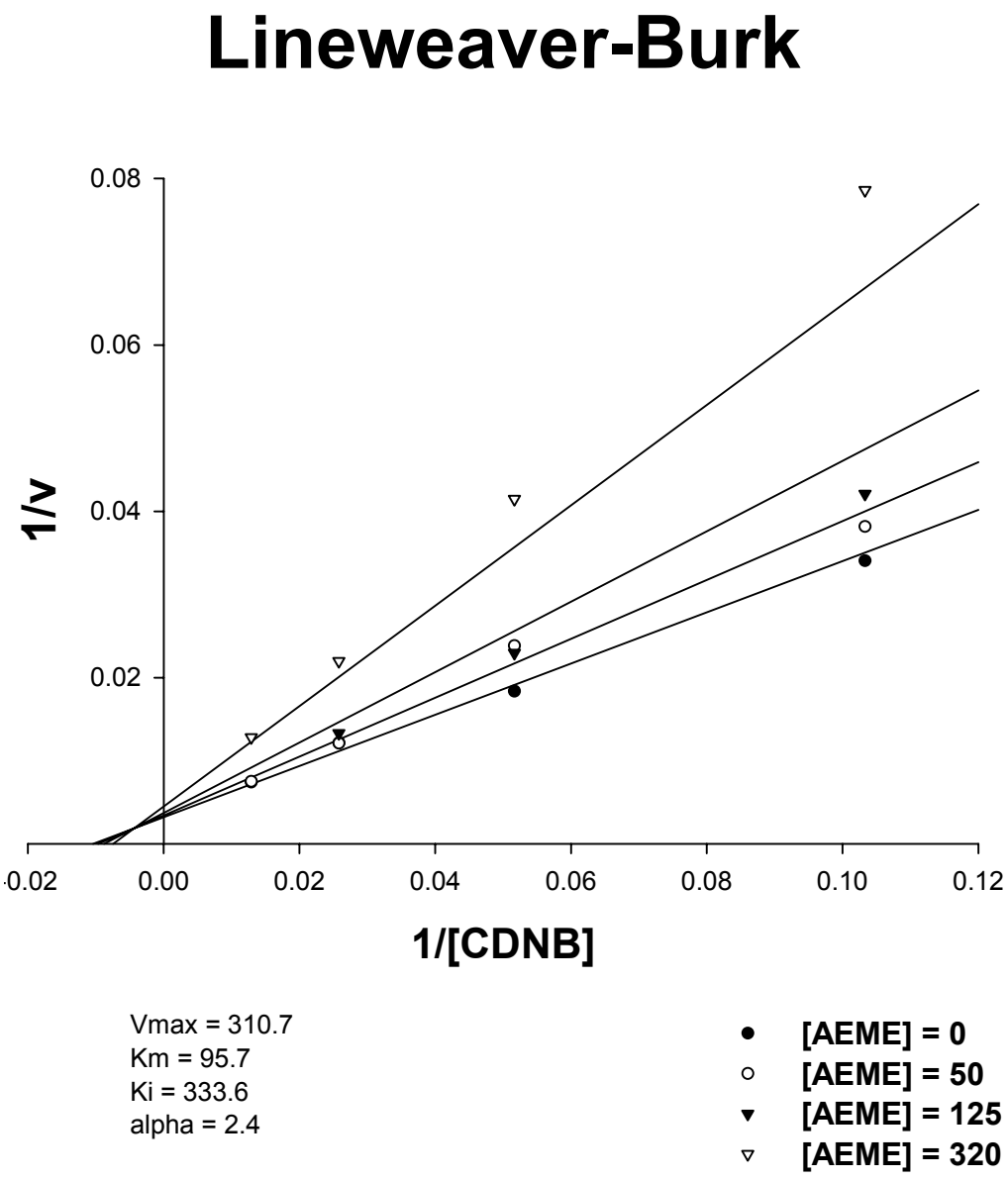

Fig 3.22.1: Lineweaver-Burk plot showing mixed-linear inhibition of cytosolic CDNB-SG formation using various concentrations of AEME.

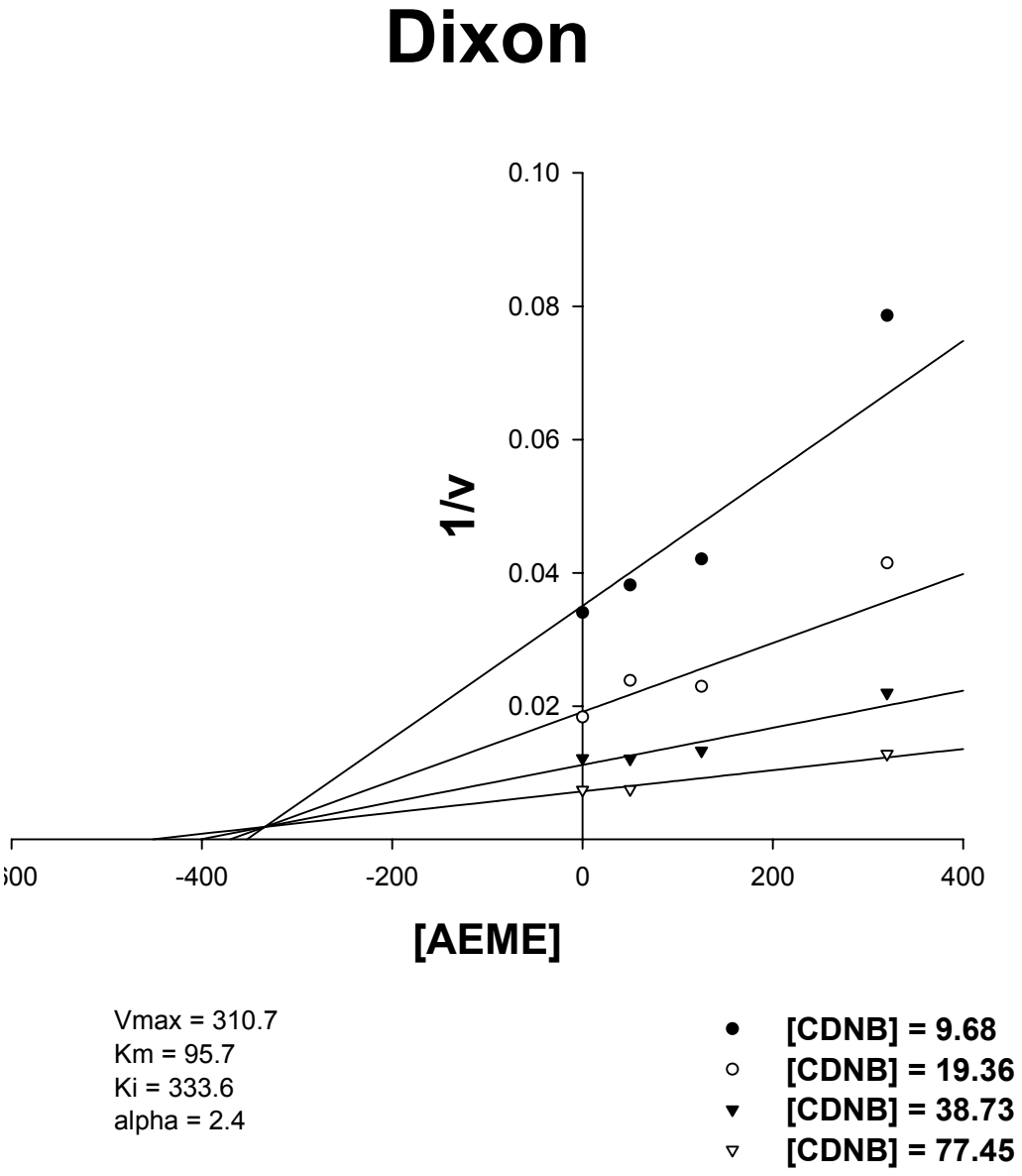

Fig 3.22.2: Dixon plot representing mixed-linear inhibition of cytosolic GST activity by AEME. The relative inhibition constant, K_i, was calculated as 334 μM.

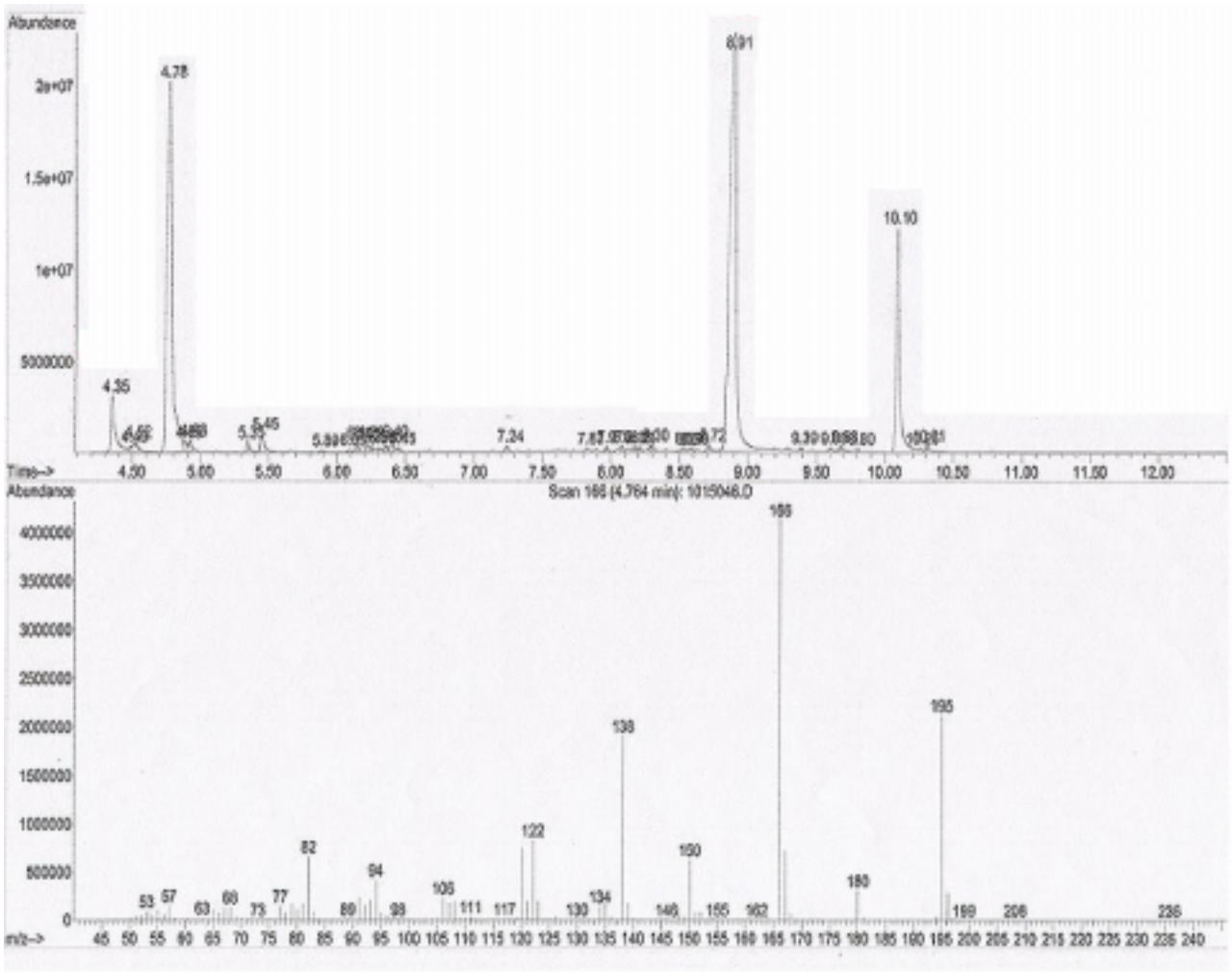

Fig. 3.23: GC-MS spectrum of the decedent's urine following SPE, showing total ion current (top spectrum). The fragmentation spectrum (bottom spectrum) of the peak at 4.7 minutes structurally confirms the presence of AEEE in the urine.

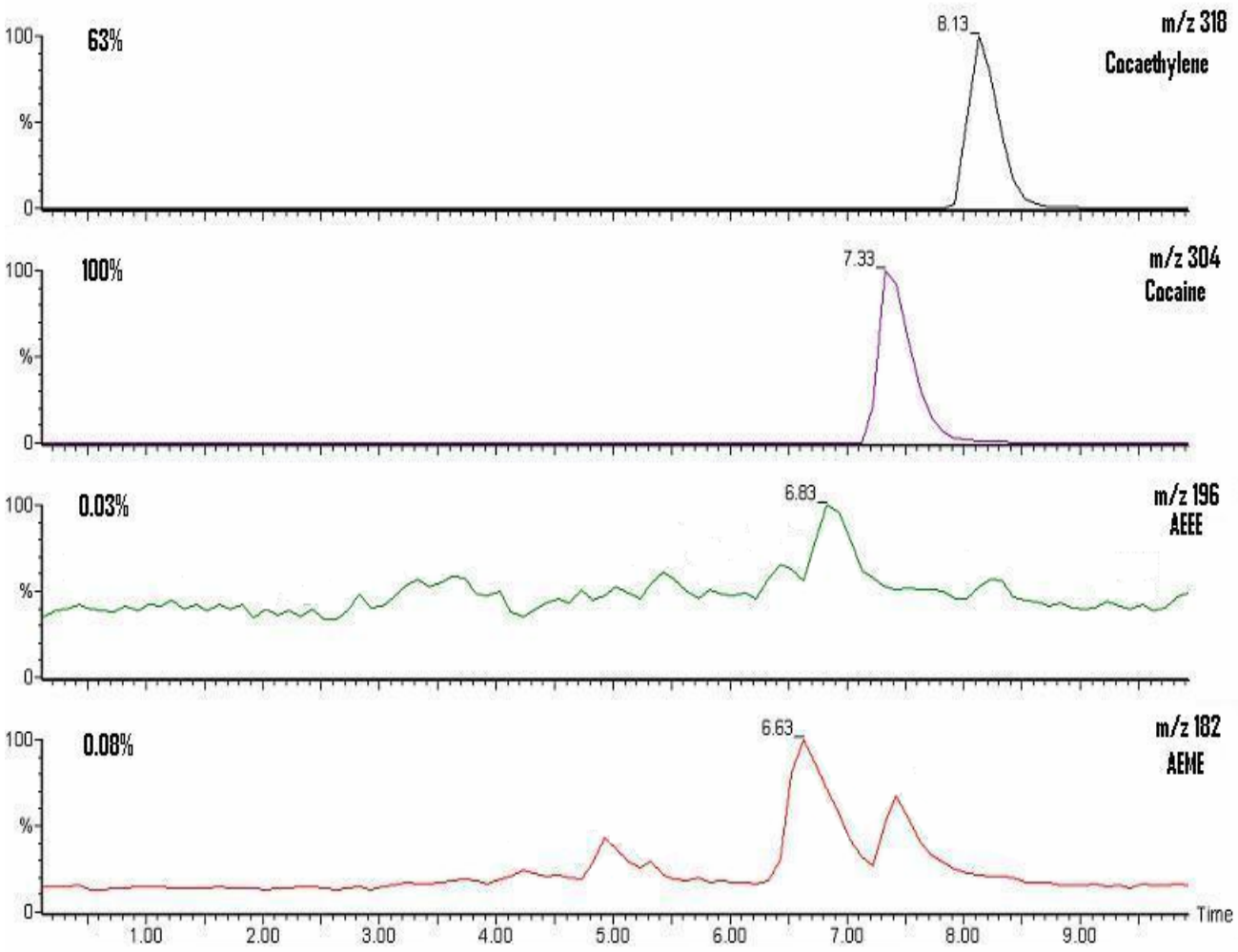

Fig. 3.24: LC-MS spectra (selected ion monitoring) of the decedent's urine sample following SPE. The appropriate protonated ion mass is indicated to the right of each SIM chromatogram, and the relative intensity (top left) for each compound were normalized from the most intense peak. Retention times (min) for each compound, similar to authentic material, are listed above each peak.

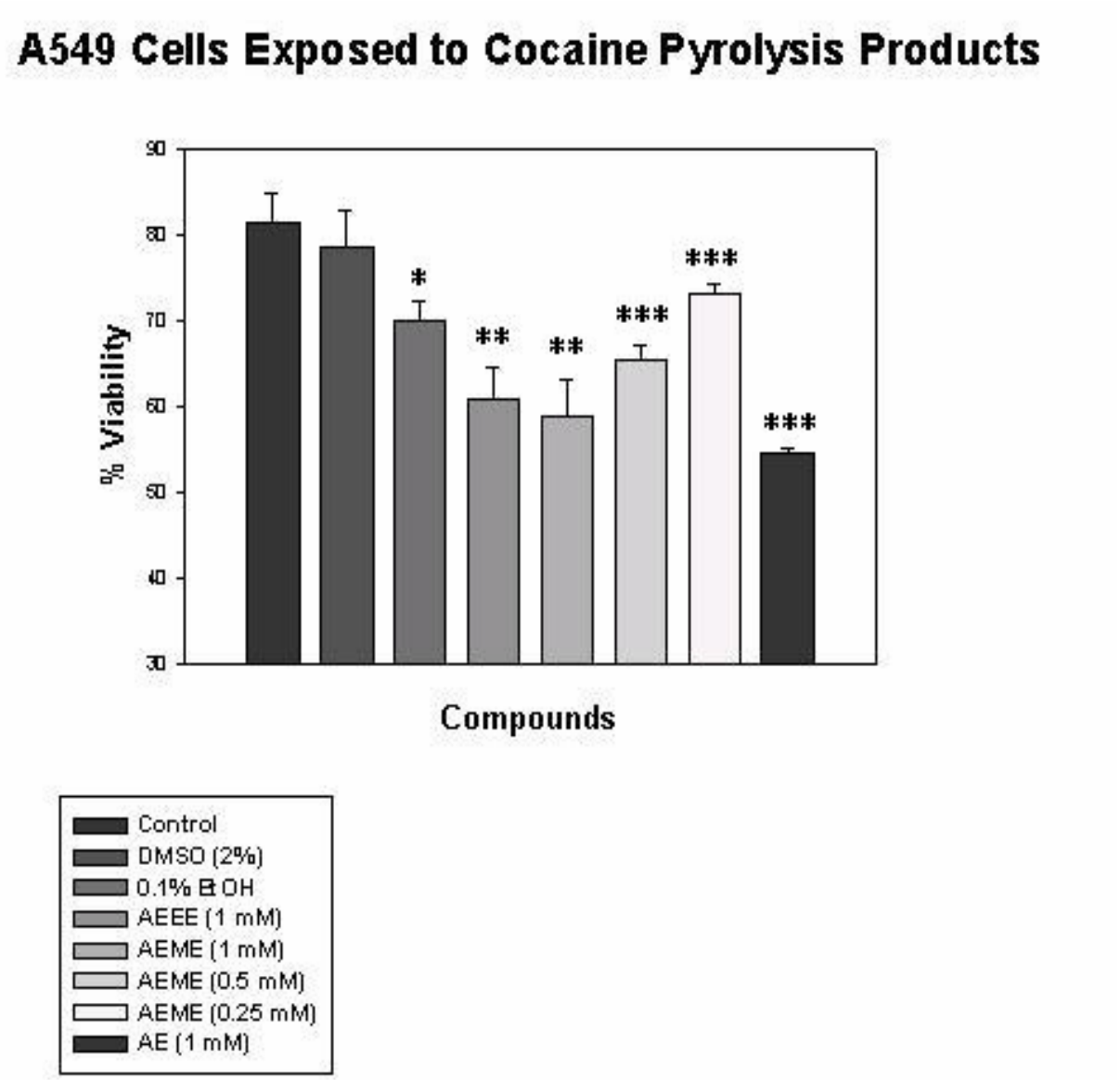

Fig. 3.25: Calculated percent cell viability of A549 lung fibroblasts based on trypan blue exclusion. (* $p < 0.025$; ** $p < 0.01$; *** $p < 0.005$).

Compound	% Cell Death
DMSO (2 %)	45
Nil	21
NAC (5 mM)	10
EtOH (20%)	87
Styrene oxide (1 mM)	87
AEME (1 mM)	46
AEME (0.5 mM)	34
AEME (0.25 mM)	31
AE (1 mM)	42
AEEE (1 mM)	57
Cocaine (1 mM)	37

Table 3.2: Tabulation of cellular death to A549 lung fibroblasts, as measured by flow cytometry, following exposure to various compounds, including styrene oxide and cocaine pyrolysis products.

Compound(s)	% Cell Death
Styrene oxide (1 mM)	87
Styrene oxide (1 mM) + NAC (5 mM)	79
AEME (1 mM)	46
AEME (1 mM) + NAC (5 mM)	36
AEME (0.5 mM)	34
AEME (0.5 mM) + NAC (5 mM)	19
AEME (0.25 mM)	31
AEME (0.25 mM) + NAC (5 mM)	23
AE (1 mM)	42
AE (1 mM) + NAC (5 mM)	44
AEEE (1 mM)	57
AEEE (1 mM) + NAC (5 mM)	38

Table 3.3: Apparent effect of NAC addition on the toxicity of A549 cells induced by styrene oxide, cocaine and pyrolysis products.

Chapter 4: Discussion

4.1 Discussion

Our studies presented here contain biological significance. The following questions developed early during our investigations: Does the *in vivo* metabolism of AEME to AEME-SG occur in known free-base cocaine users? If so, does this phenomenon have toxicological implications, or represent the formation of an additional metabolite for identification of crack cocaine use in a forensic laboratory? Some of our initial studies have primarily addressed these questions. Firstly, the relevance of AEME-SG conjugate formation *in vivo* from primarily *in vitro* data is discussed.

We have demonstrated the chemical synthesis of AEME conjugates, mainly AEME-NAC and AEME-SG, and verified the chemical structures by NMR and multistage ESI-MS. Interestingly, the chemical synthesis of AEME-NAC resulted in two epimers (Fig. 3.2.2). Epimer **A** results from NAC addition on the endo side of AEME, due to increased steric hindrance produced by the *N*-methyl on the exo side of the ring. The structure of epimer **B** is speculated from previous work on phenylthio derivatives of AEME (120). It is likely the result of base-catalyzed epimerization of epimer **A** at C-2 in an attempt to reduce steric repulsion between the *N*-methyl and carbonyl groups (120).

In order to further study the Michael addition of GSH to electrophiles we utilized Ellman's method (117) to quantify GSH concentrations over time in the presence of AEME, ethacrynic acid or arecoline. Diagnostic graphs depicting log [GSH] versus time (not shown) were not linear; therefore, we assumed a 2nd order reaction for all compounds (A + B $\rightleftharpoons$ C), first-order in each reactant. Thus, we calculated relative 2nd order rate constants (k_1) for AEME (6.8×10^{-3}), arecoline (2.2×10^{-1}) and ethacrynic acid (4.1×10^{-1}). Furthermore,

AEME reduced GSH concentrations by approximately 30%, whereas arecoline and ethacrynic acid reduced GSH by nearly 95% and 98%, respectively.

Largely, the observed AEME rate suggests that chemically, AEME reacts slowly with GSH. We speculate that the observed slower reactivity of AEME with GSH, compared to the chemically similar arecoline, is due to the presence of an additional two carbon methylene bridge on AEME, producing increased steric hindrance that potentially slows nucleophile addition. EA chemically contains a methylenebutyryl side chain with an α,β-unsaturated ketone moiety that is freer to react with nucleophiles than AEME or arecoline, which contain a more complicated ring structure. Moreover, it is likely that the ketone moiety on EA is capable of producing greater stabilization of the carbanion, on C-9 or C-10, following nucleophile addition, increasing conjugate formation.

Habig *et al.* (118) reported the extinction coefficient ($mM^{-1}cm^{-1}$) and maximum absorbance wavelength (nm) of 3,4-dichloronitrobenzene (DCNB) and 1-chloro-2,4-dinitrobenzene (CDNB): 8.5, 345; 9.6, 340, respectively. Both aromatic compounds are substrates for cytosolic GST's, readily react with free sulfhydryls, and commonly utilized in GSH experiments. AEME significantly slows the chemical conversion of DCNB to DCNB-SG (Fig 3.15). In contrast to the *chemical* reaction studied by Ellman's method (Fig 3.11.B), AEME reduced the chemical formation of DCNB-SG intermediary to EA and arecoline. One source of error in these experiments involves the potential conversion of DCNB to a hydroxylated metabolite, which likely contains a strong absorbance at 345 nm. Chiefly, these experiments are also suggestive of AEME reacting with GSH.

Despite moderate reactivity with GSH, the potential for AEME as a substrate for cytosolic glutathione *S*-transferases was postulated, and is certainly biologically significant. If

found as a substrate for GST's, then the likelihood of detecting AEME conjugates in biological fluids of free-base cocaine users increases. In the presence of pooled HLC and reduced GSH, AEME concentration was significantly reduced in comparison to control vials lacking HLC. However, the high likelihood of liver esterases being present in the HLC may catalyze the hydrolysis of AEME to AE, a polar, amphoteric compound that elutes quicker than AEME on our HPLC system. A second array of experiments using LC-MS found no statistical difference in AEME-SG formation between native cytosol versus boiled cytosol preparations. Furthermore, varying pH levels appears to not appreciably alter product formation. Therefore, in our hands we report no clear evidence suggesting that AEME is a substrate for soluble GST's contained within human liver cytosol. One explanation for the lack of enzyme catalysis in our experiments includes the *possibility* that AEME inhibits or blocks GST's. We have shown that AEME and EA, a known GST inhibitor, significantly reduce GST activity towards DCNB-SG conjugation after a 20 hour incubation (Fig 3.15).

Since these preliminary GST inhibitory experiments were only suggestive, we then engaged in a more detailed kinetic analysis to study the potential of AEME as an inhibitor of cytosolic GST's. If discovered as a GST inhibitor, chronic AEME exposure may potentially predispose chronic free-base cocaine users to toxicity from electrophilic xenobiotics that are normally detoxified by GST's. Several studies have shown a predisposition to cancer development in cocaine smokers (121,122), and chemical carcinogens are often electrophilic agents that are also substrates for GST's (77).

Using CDNB (1-chloro-2,3-dinitrobenzene) as a probe GST substrate, we observed an atypical or non-Michaelis-Menten kinetic profile (Fig. 3.20) in the presence of an excess of GSH (119). Although an ordered sequential pathway with high GSH concentrations and a

ping-pong pathway at low concentrations of GSH have been postulated regarding the GST kinetic mechanism (123), most studies support the idea that the kinetic mechanism is random sequential (124-126). The studies do agree that the kinetic profile is biphasic, which agrees with our current findings. Our Eadie-Hofstee plot (Fig. 3.21) is also indicative of a biphasic kinetic mechanism (119). The presence of multiple isoforms of GST's in human liver cytosol may also complicate kinetic analysis.

After studying the inhibition of cytosolic GST activity by AEME, the type of inhibition was diagnosed as a mixed (full)-linear model ($\alpha > 1$, $\beta = 0$), based on correlation coefficients. Mixed inhibition, containing a likely combination of competitive (increase in K_m) and pure non-competitive inhibition (decrease in V_{max} with no overall change in K_m) (127,128), was previously observed with ethacrynic acid towards GST's (80,129). Ethacrynic acid ($K_i < 10$ μM) strongly competes competitively with CDNB while showing non-competitive inhibition towards GSH (80). Based on our current data, a similar scenario is postulated to occur with AEME ($K_i = 334$ μM), CDNB and GSH. To conclude, AEME is a weak inhibitor of cytosolic GST's, suggesting limited biological significance since only a small proportion of free-base cocaine is thermolytically converted to AEME (≤ 5%), leading to low physiological serum levels, and AEME retains an overall insubstantial K_i constant compared to other known GST inhibitors.

The relative rate of degradation of chemically prepared arecoline-SG and AEME-SG is reported here. Both conjugates exhibited insignificant reversion to original reactants in buffered solution (pH 7.4) at room temperature. Although AEME exhibited retro release of GSH over time, this amount approximated to only 0.25% loss over 4 hours. In general, the measured stability at physiological pH suggests that these metabolites, or their mercapturic

acid derivatives, are favorable, stable candidates for detection in human subjects. Arecoline-NAC and arecaidine-NAC have been found in arecoline-dosed rats (64). Currently, there are no documented peer-reviewed articles, to our knowledge, reporting the identification of AEME-SG, AEME-NAC or related conjugates in human crack cocaine users.

Glutathione conjugates formed *in vivo* are enzymatically converted to mercapturic acid derivatives prior to excretion in the urine (75). Therefore, if AEME is conjugated to AEME-SG *in vivo*, then AEME-SG would be partially metabolized to AEME-NAC. Our method including SPE clean-up followed by LC-MS, was developed to detect the AEME mercapturate in the urine of known free-base cocaine users. In two urine samples (both positive for AEME and cocaine by LC-MS) from multiple drug overdose victims we failed to identify AEME-NAC by direct-injection ESI-MS, LC-MS or LC-MS/MS.

Several pitfalls exist that potentially deter the detection of AEME-NAC in human urine. Firstly, the limit of detection of AEME-NAC on the more sensistive, quadrupole LC-MS system (Water, Micromass) was approximately 2.0 ng. Perhaps, AEME-NAC was present in the urine, but existing in the picogram range, which is clearly below our detection limit. Also, the inherent problems of ion suppression during ESI-MS analysis can impede nanoscale or lower detection of analytes (130).

The extent of free-base cocaine abuse is also a concern for analysis. We were unable to determine from the case history data if the decedent's under investigation were chronic or acute free-base cocaine users. The literature suggests that up to 5% of cocaine is converted to AEME (42), leaving only a small amount of AEME available *in vivo* to conjugate with GSH. Therefore, the identification of AEME-SG in the bile or AEME-NAC in the urine of human subjects may indicate chronic cocaine use, a potentially useful piece of evidence in judicial

proceedings. Several conservative calculations, starting with a solo free-base cocaine dose of 100 mg, results in the formation of roughly 33 ng/mL of AEME-NAC in the urine, assuming normal hepatic and renal function with a total urine volume of 1.5 L (131). More frequent crack cocaine use, obviously, would result in greater accumulation of AEME conjugates, leading to easier detection of these metabolites.

AEME is also chemically and enzymatically hydrolyzed to AE (46,56), a less reactive compound with GSH based on our preliminary findings (data not shown). A possible explanation of the reduced reactivity of AE, containing a carboxylic acid moiety, includes the possible decreased stability of the resulting carbanion of AE-SG, leading to increased retrogression. In fact, arecaidine, the hydrolysis product of arecoline and chemically similar to AE, reacted much slower with GSH and NAC than arecoline, partly due to the relative instability of the arecaidine-thiol products (64). Moreover, AEME is significantly converted *in vivo* to AE, deterring contributable conjugation to AEME-SG (and later degradation, followed by acetylation to AEME-NAC) in free-base cocaine users.

The OCME of West Virginia detected cotinine, a nicotine metabolite with an approximately 8-fold greater plasma half-life than nicotine (132), in one decedent's urine we analyzed for the presence of AEME-NAC, suggesting that this individual was a smoker. Benzo(a)pyrene is a polycyclic aromatic hydrocarbon (PAH) contained in inhaled mainstream tobacco smoke and capable of inducing Phase I and Phase II mRNAs and their corresponding proteins, including isoforms of GST's (133). Furthermore, nicotine induced mitochondrial GST A4-4 activity in the rat brain (134). Another study found a weak, positive correlation between the number of cigarettes smoked per subject and GST activity of human lung tissue (135). Although Graziano and co-workers (136) failed to report an increase in GST activity in

laboratory rats nasally exposed to cigarette smoke, they did conclude that smoking reduced hepatic glutathione content by almost 15%. Moreover, they suggest that smokers are potentially less capable of detoxifying xenobiotics by GSH conjugation mechanisms (136).

Evaluated together, this conglomerate of literature reports suggests that nicotine or metabolites of tobacco smoking influence GST activity and/or the normal capacity to detoxify electrophilic compounds. Therefore, the decedent who smoked may have rapidly created AEME-SG *in vivo* and excreted the mercapturate before expiring, after which the urine was collected. On the other hand, it is also possible that the decedent had decreased hepatic GSH stores from chronic nicotine exposure, resulting in very minor or no appreciable levels of the GSH and NAC conjugates in his urine.

Finally, consider an additional mention regarding the potential detection of AEME-NAC in biological fluids. Forensic laboratories commonly employ GC-MS for analysis of biological fluids (137). Furthermore, the aforementioned conjugates contain a peptide-like moiety that is susceptible to degradation upon thermal analysis, such as GC-MS, and more appropriately analyzed on a less thermal system, such as LC-MS. Nonetheless, the potential exists for these conjugates as unique, forensic markers. With significant concerns of artifactually producing AEME during GC-MS analysis of cocaine (36) and more recently AEEE from cocaethylene (138) and AE from benzoylecgonine, ecgonine or *m*-hydroxybenzoylecgonine (37), the time is ripe for the identification of novel markers of smoked cocaine use.

As mentioned earlier, stable glutathione conjugates formed *in vivo* are potentially cytotoxic (75). Less stable adducts can release the parent, electrophilic compound at target

sites and exhibit toxicity (83). One pertinent example, discussed in more detail here, is the loop diuretic, ethacrynic acid, that readily forms conjugates with glutathione (85).

An interesting but deleterious adverse drug reaction to ethacrynic acid therapy is the development of ototoxicity, often co-existing with renal impairment (139). As little as 100 mg EA orally or 50 mg IV sodium ethacrynate have produced severe, transient hearing losses (139). Approximately 20-30% of administered EA is converted to the cysteine conjugate of EA (EA-cys), a metabolite of EA-SG (139). Some experimental evidence exists that suggests that EA-cys is the causative agent in EA induced ototoxicity (139-142).

For instance, EA (5.0 mg/kg) and EA-cys (2.0 mg/kg) were administered intravenously to healthy, adult cats (139). Ototoxicity was measured by the extent of cochlear N_1 depression. EA-cys exhibited an approximately 4-fold greater potency in producing N_1 depression than EA alone (139). Additionally, EA exhibited a longer latent period until the development of N_1 depression, suggesting EA is converted to EA-cys before ototoxic effects occur (139).

Another study revealed that EA-cys (2.4 mg/kg) administered IV to adult cats was more potent in inducing ototoxicity than EA (5.0 mg/kg) or furosemide (12.0 mg/kg), a loop diuretic chemically similar to EA (140). The duration of ototoxicity induced by EA or EA-cys was prolonged in comparison to furosemide (140). Similar to an earlier study, EA-cys displayed increased potency in inducing cochlear N_1 depression than EA (140).

These studies indicate that EA-cys may be a directly toxic agent to cochlear cells. In fact, EA-cys (MK-597) was withdrawn from clinical trials due to a high incidence of hearing loss (143). Contrary, another theory has been proposed that may explain the enhanced ototoxicity seen with EA-cys (144). EA binds plasma proteins nearly two fold greater than equal concentrations of EA-cys at 37°C (142). Under physiological conditions, EA-cys can

spontaneously reverse to regenerate EA (142). Therefore, free EA-cys, which is less extensively bound to plasma proteins, can conceivably liberate more EA at cochlear sites and exert toxicity (145).

The *in vitro* conversion of AEME to AEME-SG is documented in this report. Although likely, whether AEME is conjugated to AEME-SG *in vivo* and subsequently degraded to AEME-cys or AEME-NAC remains to be detected in free-base cocaine users. AEME-cys, if present, may play a role in cocaine related hearing losses in infants and newborns. Several studies have documented significant hearing losses in cocaine exposed unborn children (146-148). Whether AEME, AEME-SG or AEME-cys are toxic to human cochlear cells remains to be studied.

Besides hearing loss, cocaine also exhibits pulmonary toxicities that are well documented (9,149,150). The exact mechanism(s) of injury, however, are still largely unexplained. Current literature reports conflict on the pulmonary effects of AEME. One study reputes that AEME relaxes airway smooth muscle (58), while another reports suggests that it may play a role in bronchoconstriction observed in crack smokers (59).

We attempted to provide initial evidence regarding the likely cytotoxic effects of AEME and other pyrolysis products. Using a trypan blue exclusion assay, we report that AE, AEME and to a lesser extent, AEEE are toxic to A549 lung fibroblast cells following a 24 hour incubation. Using flow cytometry (151,152), we attempted to measure A549 cytotoxicity, but obtained significant cellular death with DMSO (2%) control, leading to weak comparisons with cells spiked with cocaine or pyrolysis products. DMSO, a documented membrane transport facilitator of low molecular weight, uncharged molecules (153), likely increased cellular uptake of propidium iodide (PI), leading to enhanced fluorescence not necessarily indicative of

cellular death. Actual reports of DMSO increasing PI permeability in cell lines are largely anecdotal and not well documented, although it is suggested to keep DMSO concentration ≤ 0.1% (personal communication with Dr. Cynthia Cunningham, West Virginia University).

We did observe, using flow cytometry, enhanced toxicity of pyrolysis products to A549 cells as compared to cocaine alone, a known toxin (Table 3.2). Furthermore, the addition of NAC appeared to reduce the cytotoxicity of AEME and AEEE but not with AE, suggesting that a likely mechanism of toxicity involves the Michael addition of electrophilic pyrolysis products to reactive groups on proteins. Another explanation, although not studied by us, implies that these alkaline thermolytic products, containing an oxidizable tertiary amine group, may form reactive *N*-oxides. Further experimentation is needed to clarify the exact mechanism of injury.

An interesting chapter evolved from our studies. Studies suggest that 60-85% of cocaine abusers also abuse alcohol, and concomitant consumption of cocaine and alcohol is common (26). The Drug Abuse Warning Network (DAWN) has consistently reported that the co-administration of cocaine and ethyl alcohol is the number one drug-drug interaction leading to emergency room admissions (154). The co-administration of cocaine and ethanol forms the ethylated product, cocaethylene. In an analogous fashion, AEME forms AEEE in the presence of ethanol when studied in rat liver microsomes (56). The idea of AEEE as a metabolite of cocaine and ethanol co-abuse has only been *proposed* earlier (57).

We report the identification of AEEE in a human subject who co-abused crack cocaine and ethanol. GC-MS was initially used to detect AEEE in 1 mL urine sample. However, the amount of AEEE in the urine quantified by standard curve on GC-MS was inflated due to pyrolysis of cocaethylene to AEEE in the heated GC injector port. Several reports have

documented the analogous generation of an artifact AEME peak from pyrolysis of cocaine during GC-MS analysis (36,155). Furthermore, artifact AEME production is linearly dependent on cocaine concentration and attenuated by the use of a clean insert liner (36). Identification of AEME by GC-MS analysis is equivocal because of the potential for artifactual production in heated injector ports of gas chromatographs. Analogously, application of GC-MS methods to the identification of AEEE in the presence of cocaethylene is also equivocal.

A more reliable alternative to the recently reported internal or external standardization method (36) is the use of a less thermolytically driven analytical step, such as LC-MS. Our LC-MS assay detected AEEE in urine following SPE at a concentration of approximately 50 ng/mL. This extrapolated value estimates the relative amount of AEEE in the urine and further confirms its presence. The concentrations of cocaine and cocaethylene in the sample were substantially greater than their respective thermolytic products, but were about equally concentrated. The data suggests that the transesterification of cocaine to cocaethylene proceeds at a faster rate than the analogous reaction of AEME to AEEE. Furthermore, it may be likely, although not proven by our investigations, that cocaine is a better substrate than AEEE for hCE-1, the putative transesterification enzyme (19,51,156,157).

Our multistage mass spectrometry LC-MS analysis represents a third analytical approach for identifying AEEE in the urine sample. Our analysis found that the electrospray ionization process also fragments cocaethylene to yield an ion of the same molecular weight as protonated AEEE, but LC was capable of separating the ions. These findings point to the need for LC separation of cocaethylene from AEEE to correctly identify AEEE in future samples. Although GC-MS fragmentation pathways are more reliable and more commonly employed in

forensic laboratories, our concern for artifactual production of AEEE warrants confirmation by LC-MS ion trap analysis.

Chapter 5: Future Directions

5.1 Future Directions

Some of the future work outlined below was speculated earlier in the previous chapter. Since our outlined studies failed to identify the AEME mercapturate in the urine, a more sensitive method is needed to evaluate numerous biological matrices (urine, bile, blood) of known free-base cocaine smokers for AEME-SG, AEME-NAC or other related conjugates. In addition, the availability of urine (or other fluid) with case evaluations from many crack cocaine users would allow an interesting side experiment that investigates the potential relationship between extent of cocaine use and detection of conjugates. Arecoline, a practice compound chemically similar to AEME and a drug of abuse in the Orient, also forms GSH adducts (and derivatives) in rats, which may be detected in the urine and bile of human betel nut users.

The literature conflicts on the particular effects of arecoline on GST activity; therefore, a potential future study could evaluate whether arecoline is a substrate for cytosolic GST's. Similarly, since our studies presented here only identify AEME as a mixed inhibitor of cytosolic GST's, future studies would determine if AEME is an inhibitor of specific GST isoforms, such as alpha or pi. Following which, *in silico* modeling could be applied to examine the orientation of AEME within the H (hydrophobic or electrophilic) binding site of the GST isoform(s). Also interesting includes a series of studies evaluating if the AEME-SG conjugate also inhibits GST's, and if so, can the conjugate bind to both substrate sites within the active site of GST's.

We provided initial cytotoxic data regarding several cocaine pyrolysis products (AEME, AEEE and AE). Continued research with flow cytometry and other applicable techniques using lung fibroblasts and other pertinent cell lines (i.e. myocytes and renocytes)

would assist in unraveling potential mechanisms of injury previously unexplained with free-base cocaine abuse. Finally, the pharmacology of AE is currently unknown and remains an important biological question, since it is a formidable metabolite of AEME hydrolysis.

Chapter 6: Summary and Conclusions

6.1 Summary and Conclusions

Smoking continues today as a major route of abuse for psychoactive drugs, leading to the formation of potentially toxic thermolytic products. The pyrolysis of cocaine to AEME has been well-documented since the early 1990's. Chemically, we maintain that AEME contains an electrophilic α,β-unsaturated carbonyl functional group, and we were successful in documenting the chemical reactivity of AEME with glutathione, a nucleophilic compound ubiquitously occurring in humans. Glutathione and mercapturic acid derivatives of AEME were synthesized. Also, AEME depleted glutathione concentrations over 4 hours *in vitro* and slowed the chemical conversion of DCNB to DCNB-SG over 20 minutes. However, our data suggests that AEME reacts modestly with glutathione, as compared to arecoline and ethacrynic acid, indicating that AEME conjugates are minor metabolites of free-base cocaine use and potentially undetectable.

We are unable, at this time, to conclude that AEME is a substrate for cytosolic GST's, the soluble enzymes that catalyze glutathione addition to electrophilic compounds. AEME did block apparent cytosolic GST activity. Our studies displayed a significant reduction of GST activity in the presence of AEME after a 20 hour co-incubation with human liver cytosol. More detailed kinetic studies proved that AEME inhibits cytosolic GST activity by a mixed-linear model, but retains a weak inhibition constant. We also observed in cellular toxicity studies using trypan blue exclusion and flow cytometry, that AEME and other pyrolysis products exhibited a greater toxicity to A549 lung fibroblasts than equally concentrated cocaine. AEME, AE, AEEE and related conjugates are potentially novel players in the sequelae of pulmonary toxicity exhibited in crack cocaine users.

Finally, we detected AEEE in the urine of a drug overdose victim with a history of drug abuse by GC-MS, LC-MS, and LC-MS/MS. To our knowledge, this is the first documented report of the identification of this metabolite in humans. AEEE is a potential additional forensic marker, besides cocaethylene and ecgonine ethyl ester, for the detection of crack cocaine abused concomitantly with ethanol. The inherent dangers of erroneously identifying AEEE in a biological sample, also containing cocaethylene, by GC-MS analytical methods exists today in forensic laboratories. Therefore, our alternative LC-MS and LC-MS/MS methods, capable of chromatographically separating artifactually created compound from authentic metabolite present in urine, provide the basis for a useful analytical method in forensic cases involving suspected free-base cocaine/ethanol use.

References

(1) Pearman K. Cocaine: a review. J Laryngol Otol 1979;93:1191-9.

(2) Cornish JW, O'Brien CP. Crack cocaine abuse: an epidemic with many public health consequences. Annu Rev Public Health 1996;17:259-73.

(3) Martin BR, Boni J. Pyrolysis and inhalation studies with phencyclidine and cocaine. NIDA Res Monogr 1990;99:141-58.

(4) National Institute on Drug Abuse. Cocaine abuse and addiction. Bethesda, MD: National Institute on Drug Abuse; 1999. Report No.: NIH Pub No. 99-4342.

(5) Jeffcoat AR, Perez-Reyes M, Hill JM, Sadler BM, Cook CE. Cocaine disposition in humans after intravenous injection, nasal insufflation (snorting), or smoking. Drug Metab Dispos 1989;17(2):153-9.

(6) Cook CE, Jeffcoat AR. Pyrolytic degradation of heroin, phencyclidine, and cocaine: identification of products and some observations on their metabolism. NIDA Res Monogr 1990;(99):97-120.

(7) Catterall W, Mackie K. Local Anesthetics. In: Hardman JG, Limbird LE, editors. Goodman and Gillman's The Pharmacological Basis of Therapeutics. 9th ed. New York: McGraw-Hill; 1996. p. 331-47.

(8) Cone EJ, Yousefnejad D, Hillsgrove MJ, Holicky B, Darwin WD. Passive inhalation of cocaine. J Anal Toxicol 1995;19:399-411.

(9) Haim DY, Lippmann ML, Goldberg SK, Walkenstein MD. The pulmonary complications of crack cocaine: a comprehensive review. Chest 1995;107(1):233-40.

(10) Perez-Reyes M, Guiseppi SD, Ondrusek G, Jeffcoat AR, Cook CE. Free-base cocaine smoking. Clin Pharmacol Ther 1982;32:459-65.

(11) Peterson KL, Logan BK, Christian GD. Detection of cocaine and its polar transformation products and metabolites in human urine. Forensic Science International 1995;73:183-96.

(12) Bencharit S, Morton CL, Xue Y, Potter PM, Redinbo MR. Structural basis of heroin and cocaine metabolism by a promiscuous human drug-processing enzyme. Nature Structural Biology 2003;10(5):349-56.

(13) Isenschmid IS, Levine BS, Caplan YH. A comprehensive study of the stability of cocaine and its metabolites. J Anal Toxicol 1989;13:250-6.

(14) Rafla FK, Epstein RL. J Anal Toxicol 1979;3:59-63.

(15) Smith RM. Ethyl esters of arylhydroxy- and arylhydroxymethoxycocaines in the urines of simultaneous cocaine and ethanol users. J Anal Toxicol 1984;8(1):38-42.

(16) Jatlow P, Elsworth JD, Bradberry CW, Winger G, Taylor JR, Russell R, Roth RH. Cocaethylene: a neuropharmacologically active metabolite associated with concurrent cocaine-ethanol ingestion. Life Sci 1991;48:1787-94.

(17) Jatlow P, Hearn WL, Elsworth JD, Roth RH, Bradberry CW, Taylor JR. Cocaethylene inhibits uptake of dopamine and can reach high plasma concentrations following combined cocaine and ethanol use. NIDA Res Monogr 1991;105:572-3.

(18) Hearn WL, Rose S, Wagner J, Ciarleglio A, Mash DC. Cocaethylene is more potent than cocaine in mediating lethality. Pharmacol Biochem Behav 1991;39:531-3.

(19) Laizure SC, Mandrell T, Gades NM, Parker RB. Cocaethylene metabolism and interaction with cocaine and ethanol: role of carboxylesterases. Drug Metab Dispos 2003;31(1):16-20.

(20) Pennings EJM, Leccese AP, de Wolf FA. Effects of concurrent use of alcohol and cocaine. Addiction 2002;97:773-83.

(21) Pellinen P, Honkakoski P, Stenback F, Niemitz M, Alhava E, Pelkonen O, Lang MA, Pasanen M. Cocaine N-demethylation and the metabolism-related hepatoxicity can be prevented by cytochrome P450 3A inhibitors. Eur J Pharmacol 1994;270:35-43.

(22) Ladona MG, Gonzalez ML, Rane A, Peter RM, de la Torre R. Cocaine metabolism in human fetal and adult liver microsomes related to cytochrome P450 3A expression. Life Sci 2000;68:431-43.

(23) Kloss MW, Rosen GM, Rauckman EJ. Biotransformation of norcocaine to norcocaine nitroxide by rat brain microsomes. Psychopharmacology 1984;84:221-4.

(24) Jenkins AJ, Goldberger BA. Identification of unique cocaine metabolites and smoking by-products in postmortem blood and urine specimens. J Forensic Sci 1997;42(5):824-7.

(25) Cone EJ, Tsadik A, Oyler J, Darwin WD. Cocaine metabolism and urinary excretion after different routes of administration. Ther Drug Monit 1998;20(5):556-60.

(26) McCance-Katz EF, Kosten TR, Jatlow P. Concurrent use of cocaine and alcohol is more potent and potentially more toxic than use of either alone--a multiple-dose study. Biol Psychiatry 1998;44(4):250-9.

(27) Braslavsky A. First Cocaine Vaccine Being Tested in Humans. WebMD Medical News; 2000 Mar 31.

(28) Kosten TR, Rosen M, Bond J, Settles M, Roberts JSC, Shields J, Jack L, Fox B. Human therapeutic cocaine vaccine: safety and immunogenicity. Vaccine 2002;20:1196-204.

(29) Mets B, Winger G, Cabrera C, Seo S, Jamdar S, Yang G, Zhao K, Briscoe RJ, Anders MW, Woods JH, Landry DW. A catalytic antibody against cocaine prevents cocaine's reinforcing and toxic effects in rats. Proc Natl Acad Sci 1998;95:10176-81.

(30) Sekine H, Nakahara Y. Abuse of smoking methamphetamine mixed with tobacco: II. The formation mechanism of pyrolysis products. J Forensic Sci 1990;35(3):580-90.

(31) Sekine H, Nakahara Y. Abuse of smoking methamphetamine mixed with tobacco: I. Inhalation efficiency and pyrolysis products of methamphetamine. J Forensic Sci 1987;32(5):1271-80.

(32) Cook CE, Jeffcoat AR. Cocaine thermal degradation. Chem Eng News 1986;64:4.

(33) Sanga M. Methamphetamine toxicity: thermal degradation, CYP450-mediated metabolic activation and cytotoxic epoxide formation. Dissertation: West Virginia University; 2004.

(34) Cook CE, Jeffcoat AR, Perez-Reyes M. Pharmacokinetic Studies of Cocaine and Phencyclidine in Man. In: Barnett G, Chiang CN, editors. Pharmacokinetics and pharmacodynamics of psychoactive drugs.Rockville, MD: Biomedical Publication; 1985. p. 48-74.

(35) Lowry WT, Lomonte JN, Hatchett D, Garriott JC. Identification of two novel cocaine metabolites in bile by gas chromatography and gas chromatography/mass spectrometry in a case of acute intravenous cocaine overdose. J Anal Toxicol 1979;3:91-5.

(36) Toennes SW, Fandino AS, Hesse FJ, Kauert G. Artifact production in the assay of anhydroecgonine methyl ester in serum using gas chromatography-mass spectrometry. J Chromatogr B Analyt Technol Biomed Life Sci 2003;792:345-51.

(37) Cardona PS, Chaturvedi AK, Soper JW, Canfield DV. Simultaneous determination of cocaine, cocaethylene, and their possible pentafluoropropylated metabolites and pyrolysis products by gas chromatography/mass spectrometry. Springfield, VA: National Technical Information Service; 2003. Report No.: DOT/FAA/AM-03/24.

(38) Jacob P, Lewis ER, Elias-Baker BA, Jones RT. A pyrolysis product, anhydroecgonine methyl ester (methylecgonidine), is in the urine of cocaine smokers. J Anal Toxicol 1990;14:353-7.

(39) Zhang JY, Foltz RL. Cocaine metabolism in man: identification of four previously unreported cocaine metabolites in human urine. J Anal Toxicol 1990;14:201-5.

(40) Kintz P, Sengler C, Cirimele V, Mangin P. Evidence of crack use by anhydroecgonine methylester identification. Hum Exp Toxicol 1997;16:123-7.

(41) Toennes SW, Fandino AS, Kauert G. Gas chromatographic-mass spectrometric detection of anhydroecgonine methyl ester (methylecgonidine) in human serum as

evidence of recent smoking of crack. J Chromatogr B Biomed Sci Appl 1999;735(1):127-32.

(42) Wood RW, Shojaie J, Fang CP, Graefe JF. Methylecgonidine coats the crack particle. Pharmacol Biochem Behav 1996;53(1):57-66.

(43) Scheidweiler KB, Plessinger MA, Shojaie J, Wood RW, Kwong TC. Pharmacokinetics and pharmacodynamics of methylecgonidine, a crack cocaine pyrolyzate. J Pharmacol Exp Ther 2003;307(3):1179-87.

(44) Nakahara Y, Ishigami A. Inhalation efficiency of free-base cocaine by pyrolysis of 'crack' and cocaine hydrochloride. J Anal Toxicol 1991;15:105-9.

(45) Shimomura ET, Hodge GD, Paul BD. Examination of postmortem fluids and tissues for the presence of methylecgonidine, ecgonidine, cocaine, and benzoylecgonine using solid-phase extraction and gas chromatography-mass spectromety. Clin Chem 2001;47:1040-7.

(46) Fandino AS, Toennes SW, Kauert GF. Studies on in vitro degradation of anhydroecgonine methyl ester (methylecgonidine) in human plasma. J Anal Toxicol 2002;26:567-70.

(47) Fandino AS, Karas M, Toennes SW, Kauert G. Identification of anhydroecgonine methyl ester *N*-oxide, a new metabolite of anhydroecgonine methyl ester, using electrospray mass spectrometry. J Mass Spectrom 2002;37:525-32.

(48) Bourland JA, Martin DK, Mayersohn M. *In vitro* transesterification of cocaethylene (ethylcocaine) in the presence of ethanol. Drug Metab Dispos 1998;26(3):203-6.

(49) Boyer CS, Petersen DR. Enzymatic basis for the transesterification of cocaine in the presence of ethanol: evidence for participation of microsomal carboxylesterases. J Pharmacol Exp Ther 1992;260:939-46.

(50) Dean RA, Christian CD, Sample RHB, Bosron WF. Human liver cocaine esterases: ethanol mediated formation of ethylcocaine. FASEB J 1991;5:2735-9.

(51) Bourland JA, Martin DK, Mayersohn M. Carboxylesterase-mediated transesterification of meperidine (demerol) and methylphenidate (ritalin) in the presence of [$^{2}H_{6}$]ethanol: preliminary in vitro findings using a rat liver preparation. J Pharm Sci 1997;86(12):1494-6.

(52) Markowitz JS, Devane CL, Boulton DW, Nahas Z, Risch SC, Diamond F, Patrick KS. Ethylphenidate formation in human subjects after the administration of a single dose of methylphenidate and ethanol. Drug Metab Dispos 2000;28(6):620-4.

(53) Patrick KS, Williard RL, VanWert AL, Dowd JJ, Oatis JE, Middaugh LD. Synthesis and pharmacology of ethylphenidate enantiomers: the human transesterfication metabolite of methylphenidate and ethanol. J Med Chem 2005;48:2876-81.

(54) Larsen FG, Jakobsen P, Knudsen J, Weismann K, Kragballe K, Nielsen-Kudsk F. Conversion of acitretin to etretinate in psoriatic patients is influenced by ethanol. J Invest Dermatol 1993;100(5):623-7.

(55) Schmitt-Hoffmann AH, Dittrich S, Saulnier E, Schenk P, Chou RC. Mechanistic studies on the ethyl-esterification of acitretin by human liver preparations in vitro. Life Sci 1995;57(26):PL407-PL412.

(56) Fandino AS, Toennes SW, Kauert GF. Studies on hydrolytic and oxidative metabolic pathways of anhydroecgonine methyl ester (methylecgonidine) using microsomal preparations from rat organs. Chem Res Toxicol 2002;15:1543-8.

(57) Isenschmid DS. Cocaine. In: Levine B, editor. Principles of Forensic Toxicology. 2nd ed. Washington D.C.: AACC Press; 2003. p. 207-28.

(58) El-Fawal HA, Wood RW. Airway smooth muscle relaxant effects of the cocaine pyrolysis product, methylecgonidine. J Pharmacol Exp Ther 1995;272(3):991-6.

(59) Chen LC, Graefe JF, Shojaie J, Willetts J, Wood RW. Pulmonary effects of the cocaine pyrolysis product, methylecgonidine, in guinea pigs. Life Sci 1995;56(1):PL7-PL12.

(60) Erzouki HK, Allen AC, Newman AH, Goldberg SR, Schindler CW. Effects of cocaine, cocaine metabolites and cocaine pyrolysis products on the hindbrain cardiac and respiratory centers of the rabbit. Life Sci 1995;57(20):1861-8.

(61) Huang L, Woolf JH, Ishiguro Y, Morgan JP. Effect of cocaine and methylecgonidine on intracellular Ca^{2+} and myocardial contraction in cardiac myocytes. Am J Physiol 1997;273:H893-H901.

(62) Newman AH, Allen AC, Witkin JM, Izenwasser S, Mash D, Katz JL. The thermal decomposition product of "crack," AEME, and analogs do not appear to contribute acutely to the pharmacological or toxicological actions of cocaine. Med Chem Res 1994;4:93-110.

(63) Klaassen CD, Fitzgerald TJ. Metabolism and biliary excretion of ethacrynic acid. J Pharmacol Exp Ther 1974;191(3):548-56.

(64) Boyland E, Nery R. Mercapturic acid formation during the metabolism of arecoline and arecaidine in the rat. Biochem J 1969;113:123-30.

(65) Delbressine LPC, van Balen HCJG, Seutter-Berlage F. Isolation and identification of mercapturic acid metabolites of phenyl substituted acrylate esters from urine of female rats. Arch Toxicol 1982;49:321-30.

(66) Ishida T, Kumagai Y, Ikeda Y, Ito K, Yano M, Toki S, Mihashi K, Fujioka T, Iwase Y, Hachiyama S. (8*S*)-(Glutathion-*S*-yl)Dihydromorphinone, a novel metabolite of morphine from guinea pig bile. Drug Metab Dispos 1989;17(1):77-81.

(67) Shenhav H, Rappoport Z, Saul P. Nucleophilic attacks on carbon-carbon double bonds. XII. Addition of amines to electrophilic olefins and reactivity order of the activating groups. J Chem Soc B: Phys Org 1970;3:469-76.

(68) Tarbell DS, Tarbell AT. Essays on the History of Organic Chemistry in the United States, 1875-1955. Nashville, TN: Folio Publishers; 1986.

(69) Fuson RC. Advanced Organic Chemistry. New York: John Wiley & Sons, Inc.; 1950.

(70) Matthews WS, Bares JE, Bartmess JE, Bordwell FG, Cornforth FJ, Drucker GE, Margolin Z, McCallum RJ, McCollum GJ, Vanier NR. Equilibrium acidities of carbon acids. VI. Establishment of an absolute scale of acidities in dimethyl sulfoxide solution. J Am Chem Soc 1975;97(24):7006-14.

(71) Carey FA, Sundberg RJ. Carbanions and other nucelophilic carbon species. Advanced Organic Chemistry Part A: Structure and Mechanisms. 4th ed. New York: Kluwer Academic/ Plenum Publishers; 2000. p. 405-48.

(72) Bergmann ED, Ginsburg D, Pappo R. The Michael Reaction. In: Adams R, Blatt AH, Boekelheide V, Cope AC, Curtin DY, McGrew FC, Niemann C, editors. Organic Reaction.New York: John Wiley & Sons, Inc.; 1959. p. 179-555.

(73) March J. Advanced Organic Chemistry: Reactions, Mechanisms, and Structure. 4th ed. New York: John Wiley & Sons; 1992.

(74) Oare DA, Heathcock CH. Topics in Stereochemistry. Eliel EL, Wilen SH, editors. [19], 227-407. 1989. New York, John Wiley & Sons.
Ref Type: Serial (Book,Monograph)

(75) Commandeur JNM, Stijntjes GJ, Vermeulen NPE. Enzymes and transport systems involved in the formation and disposition of glutathione S-conjugates. Pharmacol Rev 1995;47(2):271-330.

(76) Kosower EM. Chemical Properties of Glutathione. In: Arias IM, Jakoby WB, editors. Glutathione: Metabolism and Function.New York: Raven Press; 1976. p. 1-15.

(77) Chasseud LF. The role of glutathione and glutathione *S*-transferases in the metabolism of chemical carcinogens and other electrophilic agents. Adv Cancer Res 1979;29:175-275.

(78) Meister A, Anderson ME. Glutathione. Ann Rev Biochem 1983;52:711-60.

(79) Silverman RB. Drug Metabolism. The Organic Chemistry of Drug Design and Drug Action.San Diego: Academic Press, Inc.; 1992. p. 277-351.

(80) Ploemen JHTM, Ommen BV, Bladeren PJV. Inhibition of rat and human glutathione *S*-transferase isoenzymes by ethacrynic acid and its glutathione conjugate. Biochem Pharmacol 1990;40(7):1631-5.

(81) Ploemen JHTM, Van Ommen B, Bogaards JJ, van Bladeren PJ. Ethacrynic acid and its glutathione conjugate as inhibitors of glutathione S-transferases. Xenobiotica 1993;23(8):913-23.

(82) Monks TJ, Anders MW, Dekant W, Stevens JL, Lau SS, van Bladeren PJ. Contemporary issues in toxicology: glutathione conjugate mediated toxicities. Toxicol Appl Pharmacol 1990;106:1-19.

(83) Witz G. Biological interactions of alpha,beta-unsaturated aldehydes. Free Radic Biol Med 1989;7:333-49.

(84) Schauenstein E, Taufer M, Esterbauer H, Kylianek A, Seelich T. The reaction of protein-SH-groups with 4-hydroxy-pentenal. Monatsh Chem 1971;102:517-29.

(85) Ploemen JHTM, Van Schanke A, Van Ommen, van Bladeren PJ. Reversible conjugation of ethacrynic acid with glutathione and human glutathione S-transferase P1-1. Cancer Res 1994;54:915-9.

(86) Booth J, Boyland E, Sims P. Metabolism of polycyclic compounds: 15. The conversion of napthalene into a derivative of glutathione by rat liver slices. Biochem J 1960;74:117-22.

(87) Daniel V. Glutathione *S*-transferases: gene structure and regulation of expression. Crit Rev Biochem Mol Biol 1993;28(3):173-207.

(88) Strange RC, Spiteri MA, Ramachandran S, Fryer AA. Glutathione-*S*-transferase family of enzymes. Mutat Res 2001;482:21-6.

(89) Hayes JD, Strange RC. Glutathione-*S*-transferase polymorphisms and their biological consequences. Pharmacology 2000;61:154-66.

(90) Salinas AE, Wong MG. Glutathione S-transferases: a review. Curr Med Chem 1999;6:279-309.

(91) Van Ommen B, Bogaards JJ, Peters WHM, Blaauboer B, van Bladeren PJ. Quantification of human hepatic glutathione S-transferases. Biochem J 1990;269:609-13.

(92) Wilce MCJ, Parker MW. Structure and function of glutathione-*S*-transferases. Biochim Biophys Acta 1994;1205:1-18.

(93) Dirven HAAM, Megens L, Oudshoorn MJ, Dingemanse MA, Van Ommen B, van Bladeren PJ. Glutathione conjugation of the cytostatic drug ifosfamide and the role of human glutathione s-transferases. Chem Res Toxicol 1995;8:979-86.

(94) Tsuchida S, Sato K. Glutathione transferases and cancer. Crit Rev Biochem Mol Biol 1992;27:337-84.

(95) Hanigan MH, Pitot HC. gamma-Glutamyl transpeptidase: its role in hepatocarcinogenesis. Carcinogenesis 1985;6:165-72.

(96) Campbell BJ, Forrester LJ, Zahlen WL, Burks M. Beta-lactamase activity of purified and partially characterized human renal dipeptidase. J Biol Chem 1984;259:14586-90.

(97) Hughey R, Rankin B, Elce J, Curthois N. Specificity of a particulate rat renal peptidase and its localization along with other enzymes of mercapturic acid synthesis. Arch Biochem Biophys 1978;186:211-7.

(98) Ishikawa T. The ATP-dependent glutathione S-conjugate export pump. Trends Biochem Sci 1992;17:463-8.

(99) Nagamatsu K, Kido Y, Terao T, Ishida T, Toki S. Protective effect of sulfhydryl compounds on acute toxicity of morphinone. Life Sci 1982;30:1121-7.

(100) Ishida T, Yano M, Toki S. In vivo formation of codeinone-glutathione adduct: isolation and identification of a new metabolite in the bile of codeine-treated pig. J Anal Toxicol 1998;22:567-72.

(101) Kumagai Y, Todaka T, Toki S. A new metabolic pathway of morphine: *in vivo* and *in vitro* formation of morphinone and morphinone-glutathione adduct in guinea pig. J Pharmacol Exp Ther 1990;255(3):504-10.

(102) Rollins DE, Buckpitt AR. Liver cytosol catalyzed conjugation of reduced glutathione with a reactive metabolite of acetaminophen. Toxicol Appl Pharmacol 1979;47:331-9.

(103) Robbers JE, Speedie MK, Tyler VE. Alkaloids. In: Balado D, editor. Pharmacognosy and Pharmacobiotechnology.Baltimore: Williams & Wilkins; 1996. p. 144-85.

(104) Brown JH, Taylor P. Muscarinic receptor agonists and antagonists. In: Hardman JG, Limbird LE, editors. Goodman and Gilman's The Pharmacological Basis of Therapeutics. 9th ed. New York: McGraw-Hill; 1996. p. 141-60.

(105) Chang MC, Ho YS, Lee PH, Chan CP, Lee JJ, Hahn LJ, Wang YJ, Jeng JH. Areca nut extract and arecoline induced the cell cycle arrest but not apoptosis of cultured oral KB epithelial cells: association of glutathione, reactive oxygen species and mitochondrial membrane potential. Carcinogenesis 2001;22(9):1527-35.

(106) Singh A, Rao AR. Effects of arecoline on phase I and phase II drug metabolizing system enzymes, sulfhydryl content and lipid peroxidation in mouse liver. Biochem Mol Biol Int 1993;30(4):763-72.

(107) Chang YC, Hu CC, Tseng TH, Tai KW, Lii CK, Chou MY. Synergistic effects of nicotine on arecoline-induced cytotoxicity in human buccal mucosal fibroblasts. J Oral Pathol Med 2001;30(8):458-64.

(108) Jackson EK. Diuretics. In: Hardman JG, Limbird LE, editors. Goodman and Gilman's The Pharmacological Basis of Therapeutics. 9th ed. New York: McGraw-Hill; 1996. p. 685-713.

(109) Van Iersel MLPS, Van Lipzig MMH, Rietjens IMCM, Vervoort J, van Bladeren PJ. GSTP1-1 stereospecifically catalyzes glutathione conjugation of ethacrynic acid. FEBS Lett 1998;441:153-7.

(110) Awasthi S, Srivastava SK, Ahmad F, Ahmad H, Ansari GAS. Interactions of glutathione S-transferase-pi with ethacrynic acid and its glutathione conjugate. Biochim Biophys Acta 1993;1164:173-8.

(111) Holmquist CR, Parham KR, Holleman JA, Carroll FI. An improved procedure for the synthesis of anhydroecgonine methyl ester. OPPI 1997;29(3):308-11.

(112) Zhang C, Lomenzo SA, Ballay II CJ, Trudell ML. An improved synthesis of (+)-2-tropinone. J Org Chem 1997;62:7888-9.

(113) Zirkle CL, Geissman TA, Bloom M, Craig PN, Gerns FR, Inkik ZK, Pavloff AM. 3-substituted tropane derivatives. I. The synthesis and stereochemistry of the tropane-3-carboxylic acids adn their esters. A comparison of positional isomers in the tropane series. J Org Chem 1962;27:1269-79.

(114) Kline RH, Wright J, Fox KM, Eldefrawi ME. Synthesis of 3-arylecgonine analogues as inhibitors of cocaine binding and dopamine uptake. J Med Chem 1990;33:2024-7.

(115) Scheidweiler KB, Shojaie J, Plessinger MA, Wood RW, Kwong TC. Stability of methylecgonidine and ecgonidine in sheep plasma in vitro. Clin Chem 2000;46(11):1787-95.

(116) Carroll FI, Coleman ML, Lewin AH. Syntheses and conformational analyses of isomeric cocaines: a proton and carbon-13 nuclear magnetic resonance study. J Org Chem 1982;47:13-9.

(117) Ellman GL. Tissue sulfhydryl groups. Arch Biochem Biophys 1959;82:70-7.

(118) Habig WH, Pabst MJ, Jakoby WB. Glutathione S-transferases. J Biol Chem 1974;249(22):7130-9.

(119) Hutzler JM, Tracy TS. Atypical kinetic profiles in drug metabolizing reactions. Drug Metab Dispos 2002;30(4):355-62.

(120) Thiruvazhi M, Abraham P, Kuhar MJ, Carroll FI. Synthesis of the isomers of (1R)-3-(phenylthio)tropane-2-carboxylic acid methyl ester. A new class of ligands for the dopamine transporter. Chem Commun 1997;6:555-6.

(121) Barsky SH, Roth MD, Kleerup EC, Simmons M, Tashkin DP. Histopathologic and molecular alterations in bronchial epithelium in habitual smokers of marijuana, cocaine, and/or tobacco. J Natl Cancer Inst 1998;90(16):1198-205.

(122) Duarte JG, do Nascimento AF, Pantoja JG, Chaves CP. Chronic inhaled cocaine abuse may predispose to the development of pancreatic adenocarcinoma. Am J Surg 1999;178(5):426-7.

(123) Pabst MJ, Habig WH, Jakoby WB. Glutathione S-transferase A: a novel kinetic mechanism in which the major reaction pathway depends on substrate concentration. J Biol Chem 1974;249(22):7140-50.

(124) Askelof P, Guthenberg C, Jakobson I, Mannervik B. Purification and characterization of two glutathione *S*-aryltransferase activities from rat liver. Biochem J 1975;147:513-22.

(125) Jakobson I, Warholm M, Mannervik B. Multiple Inhibition of glutathione *S*-transferase A from rat liver by glutathione derivatives: kinetic analysis supporting a steady-state random sequential mechanism. Biochem J 1979;177:861-8.

(126) Jakobson I, Askelof P, Warholm M, Mannervik B. A steady-state-kinetic mechanism for glutathione *S*-transferase A from rat liver. Eur J Biochem 1977;77:253-62.

(127) Cornish-Bowden A. Inhibitors and Activators. Fundamentals of Enzyme Kinetics.London: Butterworths; 1979. p. 73-98.

(128) Segel IH. Rapid Equilibrium Partial and Mixed-Type Inhibition. Enzyme Kinetics.New York: John Wiley & Sons; 1975. p. 161-226.

(129) Phillips MF, Mantle TJ. The initial-rate kinetics of mouse glutathione S-transferase YfYf. Biochem J 1991;275:703-9.

(130) Annesley TM. Ion suppression in mass spectrometry. Clin Chem 2003;49(7):1041-4.

(131) Spence AP, Mason EB. Human Anatomy and Physiology. 3rd ed. Menlo Park, CA: The Benjamin/Cummings Publishing Company, Inc.; 1987.

(132) Perez-Stable E, Herrera B, Jacob P, Benowitz N. Nicotine metabolism and intake in black and white smokers. JAMA 1998;280:152-6.

(133) Spivack SD, Hurteau GJ, Fasco MJ, Kaminsky LS. Phase I and II carcinogen metabolism gene expression in human lung tissue and tumors. Clin Cancer Res 2003;9:6002-11.

(134) Bhagwat SV, Vijayasarathy C, Raza H, Mullick J, Avadhani NG. Preferential effects of nicotine and 4-(*N*-methyl-*N*-nitrosamino-1-(3-pyridyl)-1-butanone on mitochondrial glutathione *S*-transferase A4-4 induction and increased oxidative stress in the rat brain. Biochem Pharmacol 1998;56:831-9.

(135) Bluhm C. Effects of smoking on benzo(α)pyrene- and glutathione-metabolizing enzymes in human lung tissue. Klin Wochenschr 1991;69:819-24.

(136) Graziano MJ, Dorough HY. Effect of cigarette smoking on hepatic biotransformations in rats. Toxicol Appl Pharmacol 1984;75:229-39.

(137) Cody J. Mass Spectrometry. In: Levine B, editor. Principles of Forensic Toxicology. 2nd ed. Washington D.C.: AACC Press; 2003. p. 139-53.

(138) Myers AL, Williams HE, Kraner JC, Callery PS. Identification of anhydroecgonine ethyl ester in the urine of a drug overdose victim (*In Press)*. J Forensic Sci 2005.

(139) Brown RD. Cochlear N_1 depression produced by the sodium salts of ethacrynic acid and its cysteine adduct. Neuropharmacology 1973;12:967-74.

(140) Brown RD. Comparison of the cochlear toxicity of sodium ethacrynate, furosemide, and the cysteine adduct of sodium ethacrynate in cats. Toxicol Appl Pharmacol 1975;31:270-82.

(141) Brown RD, McElwee TW. The effects of intra-arterially and intravenously administered ethacrynic acid and furosemide on cochlear N_1 in cats. Toxicol Appl Pharmacol 1972;22:589-94.

(142) Fox KE, Brummett RE. Protein binding of ethacrynic acid and its cysteine derivative in relation to depression of the cochlear potential in guinea pigs. Fed Proc 1974;33(2):271.

(143) Schneider WJ, Becker EL. Acute transient hearing loss after ethacrynic acid therapy. Arch Intern Med 1966;117:715-7.

(144) Lazenby CM, Lee SJ, Harpur ES, Gescher A. Glutathione depletion in the guinea pig and its effect on the acute cochlear toxicity of ethacrynic acid. Biochem Pharmacol 1988;37(19):3743-7.

(145) Koechel DA. Ethacrynic acid and related diuretics: relationship of structure to beneficial and detrimental actions. Ann Rev Pharmacol Toxicol 1981;21:265-93.

(146) Church MW, Overbeck GW. Sensorineural hearing loss as evidenced by the auditory brainstem response following prenatal cocaine exposure in the long-evans rat. Teratology 1991;43(6):561-70.

(147) Potter SM, Zelazo PR, Stack DM, Papageorgiou AN. Adverse effects of fetal cocaine exposure on neonatal auditory information processing. Pediatrics 2000;105(3):E40.

(148) Shih L, Cone-Wesson B, Reddix B. Effects of maternal cocaine abuse on the neonatal auditory system. Int J Pediatr Otorhinolaryngol 1988;15(3):245-51.

(149) Baldwin GC, Tashkin DP, Buckley DM, Park AN, Dubinett SM, Roth MD. Marijuana and cocaine impair alveolar macrophage function and cytokine production. Am J Respir Crit Care Med 1997;156:1606-13.

(150) Thadani PV. NIDA conference report on cardiopulmonary complications of "crack" cocaine use- clinical manifestations and pathophysiology. Chest 1996;110:1072-6.

(151) Traganos F. Flow cytometry: principles and applications. I. Cancer Invest 1984;2(2):149-63.

(152) Traganos F. Flow cytometry: principles and applications. II. Cancer Invest 1984;2(3):239-58.

(153) Jacob SW, Herschler R. Pharmacology of DMSO. Cryobiology 1986;23:14-27.

(154) Tacker DH, Okorodudu AO. Evidence for injurious effect of cocaethylene in human microvascular endothelial cells. Clin Chim Acta 2004;345:69-77.

(155) Gonzalez ML, Carnicero M, de la Torre R, Ortuno J, Segura J. Influence of the injection technique on the thermal degradation of cocaine and its metabolites in gas chromatography. J Chromatogr B Biomed Sci Appl 1995;664(2):317-27.

(156) Brzezinski MR, Spink BJ, Dean RA, Berkman CE, Cashman JR, Bosron WF. Human liver carboxylesterase hCE-1: binding specificity for cocaine, heroin, and their metabolites and analogs. Drug Metab Dispos 1997;25(9):1089-96.

(157) Redinbo MR, Bencharit S, Potter PM. Human carboxylesterase 1: from drug metabolism to drug discovery. Biochem Soc Trans 2003;31(Pt 3):620-4.

Alan L. Myers, Pharm.D.

Academic Address:
Department of Basic Pharmaceutical Sciences
School of Pharmacy, PO Box 9530
West Virginia University
Morgantown, WV 26506
(304) 293-1478

Home Address:
1223 Valley View Woods
Morgantown, WV 26505
(304) 599-1711 (Home)
(304) 677-1585 (Cell)
Email: amyers2@mix.wvu.edu

EDUCATION

Ph.D., Pharmaceutical Sciences, West Virginia University. Dissertation**:** Glutathione Conjugation of a Cocaine Pyrolysis Product AEME and Related Compounds. Degree Expected August 2005.

Pharm.D., Pharmacy, University of the Sciences in Philadelphia, Philadelphia College of Pharmacy, Degree: May 1999.

RESEARCH EXPERIENCE

Doctoral Research, WVU, 08/01-present.

Synthesized glutathione and mercapturic acid conjugates of arecoline, arecaidine and arecaidine propyl ester. Synthesized cocaine pyrolysis products, AE, AEME, AEEE and conjugates. Performed structural analysis of the conjugates using LC/MS and NMR spectroscopy. Studied the mechanism of conjugation to Michael acceptors with glutathione. Assisted in the synthesis of deuterated dapsone and analyzed flurbiprofen metabolism by CYP 2C9.

Dissertation Advisor: Patrick S. Callery, Ph.D., Professor and Chair, Department of Basic Pharmaceutical Sciences, School of Pharmacy, West Virginia University

TEACHING EXPERIENCE

Teaching Assistant, WVU School of Pharmacy, 08/01-present.

- Taught various pharmaceutical care labs offered to professional pharmacy students. Organized and conducted laboratory experiments, graded lab reports and writing assignments, organized final examinations.

- Primary instructor for two clinical pharmacy labs focusing on drug-drug reactions and adverse drug reactions. Lab included introductory lecture, practical case studies and evaluation of group presentations.

- Assisted in instruction of "Chemical Properties of Drugs (PH 711)." Led several review sessions and a lecture.

PUBLICATIONS

Identification of anhydroecgonine ethyl ester in the urine of a drug overdose victim. **Alan L. Myers**, Heather E. Williams, James C. Kraner and Patrick S. Callery. *J Forensic Sci* 2005, 50(6): 1-5.

Mercapturic acid derivative of a cocaine pyrolysis product, 3-(*N*-acetylcystein-*S*-yl)anhydroecgonine methyl ester. **Alan L. Myers**, Jonathan R. Daft, Peter M. Gannett, Patrick S. Callery. *Drug Metabolism Reviews* 2004; 36(1): 223.

Synthesis of deuterated 4,4'-diaminodiphenylsulfone (Dapsone) and related analogs. Peter M. Gannett, Edward M. Johnson II, Michael A. Grimes, **Alan L. Myers,** Robert E. Deavers III and Timothy S. Tracy. *Journal of Labelled Compounds and Radiopharmaceuticals* 2003; 46: 107-14.

ABSTRACTS AND PRESENTATIONS

- 7th International ISSX (International Society for the Study of Xenobiotics) Meeting, Aug-Sep 2004. Vancouver, BC. "Mercapturic Acid Derivative of a Cocaine Pyrolysis Product, 3-(*N*-Acetylcystein-*S*-yl)anhydroecgonine methyl ester. **Alan L. Myers**, Jonathan R. Daft, Peter M. Gannett, Patrick S. Callery.

- 42nd Annual SOT (Society of Toxicology) Meeting, March 2003. Salt Lake City, UT. "Formation of a Glutathione Adduct with a Cocaine Pyrolysis Product- Anhydroecgonine Methyl Ester. **Alan L. Myers**, Steven S. Wolfe, Madhu Sanga, Timothy S. Tracy, Peter M. Gannett, Patrick S. Callery.

- 55th Annual AAFS (American Academy of Forensic Sciences) Meeting, February 2003. Chicago, IL. "Formation of a Glutathione Adduct with a Cocaine Pyrolysis Product- Anhydroecgonine Methyl Ester." **Alan L. Myers**, Steven S. Wolfe, Madhu Sanga, Timothy S. Tracy, Peter M. Gannett, Patrick S. Callery.

HONORS

- Rho Chi Professional Society (1997)- Alpha Mu Chapter of Philadelphia College of Pharmacy

- Alpha Lambda Delta Honor Society (1994)- Philadelphia College of Pharmacy

PROFESSIONAL AFFLIATIONS

- International Society for the Study of Xenobiotics (ISSX)
- American Association of Pharmaceutical Scientists (AAPS)

RESEARCH FOCUS

Organic synthesis and structure determination
Analytical Chemistry

Drug Metabolism and Toxicology
Forensic Chemistry
Drugs of Abuse

RESEARCH SKILLS

Organic Synthesis of Metabolites and Related Compounds

- Synthesized glutathione and mercapturic acid adducts of anhydroecgonine methyl ester, arecoline and ethacrynic acid
- Synthesized anhydroecgonine, anhydroecgonine methyl ester, anhydroecgonine ethyl ester and arecaidine propyl ester
- Synthesized deuterated 4,4'-diaminodiphenylsulfone
- Synthesized silyl derivatives of 5-chlorouracil and 5-fluorouracil

Structure Determination

- NMR analysis of glutathione conjugates
  - Experience with the following experiments: 1H, C13, DEPT, COSY, TOCSY, HETCOR, NOESY, CYCLENOE
  - Evaluated stereochemistry of AEME-NAC adduct
- LC-MS analysis of glutathione conjugates
  - Experience with electrospray mass spectrometry and liquid chromatography (TLC, HPLC, LP chromatography)
  - Purified AEME-NAC adduct by preparative HPLC
- LC-MS/MS of anhydroecgonine ethyl ester from urine
- GC-MS analysis of pyrimidine and cocaine derivatives

In Vitro Drug Metabolism

- Human Liver Cytosol Studies of AEME
  - Studied GST catalysis of glutathione addition to AEME and ethacrynic acid using HPLC and LC-MS
  - Monitored chemical and enzymatic GSH conjugation of DCNB in the presence of AEME, arecoline and ethacrynic acid
  - Studied inhibition of cytosolic GST activity by AEME using CDNB as a probe GST substrate
- CYP2C9 metabolism of flurbiprofen
  - Studied oxidation of flurbiprofen by HPLC

In vitro Kinetics

- Investigated reaction between Michael acceptors (ethacrynic acid, arecoline and AEME) and glutathione
  - Developed method using Ellman's Reagent and UV spectroscopy
  - Calculated 2nd order rate constants and half-life

- Developed method to monitor degradation of chemically synthesized conjugates over time

Urine Analysis

- Developed solid phase extraction (SPE) method to extract metabolites from urine
- Detected and structurally identified cocaine, cocaethylene, AEME and AEEE from the urine of known freebase cocaine smokers using LC-MS/MS

Cellular Toxicity

- Studied toxicity of cocaine pyrolysis products and styrene oxide on A549 lung fibroblast cells
  - Trypan Blue Exclusion Assay
  - Flow Cytometry

PROFESSIONAL EXPERIENCE

- Graduate Assistant/Teaching Assistant
  -- WVU from 08/2001 to present
- Pharmacy Manager
  -- Eckerd Pharmacy from 08/1999 to 07/2001
- Professional Pharmacy Clerkship Rotations
  -- PCP directed from 08/1998 to 05/1999

COMPUTER SKILLS

Experience in:

- Windows XP, NT, 98 and Microsoft Office
- ISIS and ChemWindow chemical structure drawing programs
- Sigma Plot 2001, Enzyme Kinetics Module
- Xcalibur MS software
- MassLynx MS software
- Millennium HPLC software
- Varian VNMR 6.1c software (UNIX based)

CERTIFICATIONS/LABORATORY TRAININGS

- HIPAA, West Virginia University
- Chemical Hygiene Training, West Virginia University
- Hazard Communication Training, West Virginia University

REFERENCES AVAILABLE UPON REQUEST